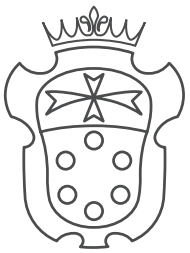

SCUOLA
NORMALE
SUPERIORE

Classe di Scienze

Corso di perfezionamento in
Matematica

XXXVII ciclo

Building hyperbolic manifolds using Coxeter polytopes

Settore Scientifico Disciplinare **MAT/03**

Candidato
dr. Edoardo Rizzi

Relatore
Prof. Stefano Riolo

Supervisione interna
Prof. Andrea Malchiodi

Anno accademico 2024–2025

Abstract

In this work we explicitly build original examples of cusped hyperbolic manifolds gluing Coxeter polytopes. In detail, we realize every closed flat 3-manifold as a cusp section of a complete, finite-volume hyperbolic 4-manifold whose symmetry group acts transitively on the set of cusps. Moreover, we show that for every such 3-manifold, a dense subset of its flat metrics can be realized as cusp sections of a cusp-transitive 4-manifold. Furthermore, we prove that there are a lot of 4-manifolds with pairwise isometric cusps, for any given cusp type. Finally, we build a non-compact, orientable, hyperbolic 4-manifold of finite volume that does not admit any spin structure.

Contents

Chapter 1

Introduction

Hyperbolic geometry has been recognized for a long time as essential in the study of low-dimensional topology. In the case of two-dimensional surfaces, every closed surface can be equipped with a metric of constant curvature, and for all but a finite set of such surfaces, this metric is hyperbolic. Three-dimensional topology is much more coplicated and was one of the most active areas of research throughout the last century. A major result in this field was Perelman's proof of Thurston's Geometrization Conjecture: every closed, orientable 3-manifold can be decomposed along spheres and tori, with each resulting piece admitting one of eight possible geometric structures, almost entirely determined by its fundamental group. Among these, hyperbolic geometry appears in the most general situation. Consequently, hyperbolic geometry emerges as the most interesting, common, complex, and rich structure. Hyperbolic 3-manifolds are also widespread in knot theory, since the complements of the majority of prime knots or links can be equipped with hyperbolic metrics of finite volume.

In higher dimensions, however, the study of hyperbolic manifolds becomes less accessible due to the growing theoretical and computational difficulties. Furthermore, there is a pronounced lack of tools to construct and study examples. A major contributing factor is the absence of any form of classification or decomposition starting from dimension four. Moreover, as the dimension increases, the importance of hyperbolic geometry becomes less clear. However, results on hyperbolic manifolds in higher dimensions can still have applications in other areas of mathematics, such as geometric group theory.

There are methods to construct arithmetic hyperbolic manifolds relatively easily, but the manifolds obtained in this way are often difficult to study. Alternatively, one can explicitly build hyperbolic manifolds by gluing Coxeter polytopes, as we do in

this work. In this case, the resulting manifolds are easier to analyze. (A hyperbolic polytope is said to be a Coxeter one if its dihedral angles are submultiples of π, see Section 2.2 for more details.) In this spirit, several related works have appeared in the literature [BFS24; BM22; Che25c; CR21; CM05; Dav85; FKS21; IMM22; KM13; KS16; Lon08; MZ23; MRS20; MRS21; RT00; RT21; Rio24; RS19]. See also the survey [Mar18]. The main difficulty of this method lies in the fact that hyperbolic Coxeter polytopes are rare. If one considers the finite volume ones, none exist in dimensions higher than 995 [Pro87], while examples are known up to dimension 19 [Vin72] and in dimension 21 [Bor87]. If one restricts to compact Coxeter polytopes, there are none in dimensions greater than 29 [Vin81], and examples exist only up to dimension 8 [FT].

1.1 Cusp-transitive manifolds

A complete, finite-volume hyperbolic manifold is *cusp transitive* if its isometry group acts transitively on the set of cusps. Very special cases are the 1-*cusped* manifolds (i.e. manifolds with a single cusp), of which infinitely many examples are well known in dimension 2 and 3, and one has been exhibited in dimension 4 for the first time in 2013 [KM13]. In higher dimension $n > 4$ we do not know whether there exists a 1-cusped hyperbolic n-manifold. In fact the existence of 1-cusped manifolds is highly non-trivial, for example there is no 1-cusped arithmetic orbifold of dimension $n \geq 30$ [Sto13]. Concerning cusp-transitive manifolds of dimension $n > 4$, we are not aware of explicit examples in the literature. By mirroring some well-known right-angled polytopes, it is easy to obtain some examples of dimension up to 8 with toric cusps.

The *type* of a cusp of a hyperbolic manifold is the diffeomorphism class of its section, which is a flat closed hypersurface. Each flat closed n-manifold is realized as a cusp type of some hyperbolic $(n+1)$-manifold [McR09] (see also [Nim98; LR02; McR04]). The latter manifold has generally several other cusps, whose type does not appear controllable with the separability methods of [Nim98; LR02; McR04; McR09]. In the orientable setting, there are obstructions for a closed flat $(4n-1)$-manifold to be the cusp type of a 1-cusped $4n$-manifold [LR00]. In this work we are interested in which closed flat manifold can be realized as the cusp type of a cusp-transitive hyperbolic manifold.

In this work we will look at the 4-dimensional case; the possible cusp types are closed flat 3-manifolds. There are 10 such manifolds [CR03]; six of them are orientable:

- E_1, the 3-torus;

- E_2, the $\frac{1}{2}$-twist manifold;
- E_3, the $\frac{1}{3}$-twist manifold;
- E_4, the $\frac{1}{4}$-twist manifold;
- E_5, the $\frac{1}{6}$-twist manifold;
- E_6, the Hantzsche–Wendt manifold;

while four are non-orientable: we will call them B_1, B_2, B_3 and B_4 (respectively denoted by $+a1$, $-a1$, $+a2$ and $-a2$ in [CR03]). These 10 manifolds can be constructed as in Figures 4.4 and 4.7 by gluing facets of polyhedral fundamental domains; the latter can be obtained, along with the associated gluing maps, by inspecting [CR03, Table 12]. Recall that E_i is a mapping torus over $S^1 \times S^1$ with monodromy of order $1, 2, 3, 4, 6$ for $i = 1, \dots, 5$, respectively, and E_6 is a rational homology sphere [Mar23, Section 12.3].

There exist 1-cusped orientable 4-manifolds with cusp type E_1 [KM13] and E_2 [KS16], while there is no 1-cusped orientable 4-manifold with cusp type E_3 or E_5 [LR00]. We refer to the discussion in [Mar18, Sections 2.5 and 2.6], for this and related issues in dimension four. Moreover, there exists a cusp-transitive 4-manifold with cusp type E_6 [FKS21]. As for the non-orientable case, there exist 1-cusped 4-manifolds with cusp type B_1 [KS15] and B_2 [RT23].

The novelty of Chapter 3 is the existence of a cusp-transitive hyperbolic 4-manifold with cusp type the $\frac{1}{4}$-twist manifold E_4. Our construction actually realizes more cusp types. Specifically we prove:

Theorem 1.1.1. *For each $i = 1, 2, 4, 6$ there exists a cusp-transitive orientable hyperbolic 4-manifold M_i with cusps of type E_i.*

Then, in Chapter 4, we improve on the technique of Chapter 3, by requiring a less explicit construction, and we prove that the remaining cusp types can also be realized; indeed, our construction actually realizes all the cusp types. Specifically we show:

Theorem 1.1.2. *For each closed flat 3-manifold N there exists a cusp-transitive hyperbolic 4-manifold M with cusps of type N.*

By Remark 4.0.1, if N is orientable, we can also take M to be orientable. The proof of this theorem is split into two parts: in Section 4.2 we discuss the case of the manifolds E_1, E_2, E_4, E_6, B_1, B_2, B_3 and B_4, while Section 4.3 is dedicated to E_3 and E_5. The 4-manifolds constructed in each section are all commensurable to each other, but they are arithmetic in the first case and non-arithmetic in the second. Hence, they fall into two commensurability classes.

Using an argument inspired by [Nim98], this result is strengthened in Section 4.4 as follows:

Theorem 4.4.1. *For every closed flat 3-manifold N, the set of flat metrics on N which can be realized as cusp sections of a cusp-transitive 4-manifold is dense in the space of all flat metrics of N.*

Moreover, with the same technique, we show an analogous result in dimension 3 (where the possible cusp types are the torus and the Klein bottle).

Finally, in Section 4.5, a variant of our method, combined with some arguments of [Bur+02; Bel+10], enables the construction of a lot of manifolds with pairwise isometric cusps:

Theorem 4.5.1. *For every closed flat 3-manifold N, there exists a positive constant c such that, for sufficiently large $V > 0$, there exist at least V^{cV} complete hyperbolic 4-manifolds with pairwise isometric cusps of type N and volume $\leq V$.*

Note that, by [Bur+02], there are at most $V^{k(n)V}$ complete hyperbolic n-manifolds without boundary of volume $\leq V$ for sufficiently large $V > 0$, where $k(n)$ depends only on the dimension n.

Our method to produce cusp-transitive hyperbolic manifolds a priori works in arbitrary dimension (but not a posteriori: there is no finite-volume hyperbolic Coxeter polytope of dimension ≥ 996 [Pro86]). The manifold M is built by orbifold covering a hyperbolic Coxeter polytope such that:

(a) it has exactly one ideal vertex;

(b) if a bounded facet and an unbounded facet intersect, then their dihedral angle is an even submultiple of π.

The construction roughly goes as follows. We glue toghether some copies of the polytope, so as to get a hyperbolic manifold with corners R satisfying the following properties. First, R is 1-cusped, and this will follow from (a). By construction the cusp will have section N, a closed, flat 3-manifold. Second, R is locally a Coxeter polytope (a so-called *reflectofold*), and this will follow from (b): when gluing two facets the dihedral angle is indeed doubled, and hence it is still an integral submultiple of π. It is homeomorphic to $N \times [0, +\infty)$, and its boundary is stratified into connected closed sets: facets, corners, edges and vertices of dimension $3, 2, 1$ and 0, respectively. Third, we need to perform the gluing in such a way that R is *developable*, that is (see for instance [CD95, Section 3]):

1. the facets are embedded (and not just immersed) hyperbolic manifolds with corners;

2. if two facets intersect, then the dihedral angles at all the corresponding corners

coincide.

These properties of R allow us to apply to R Davis' "basic construction" [Dav12], and to get a manifold M tessellated by some copies of R, with a group of symmetries G such that $M/G \cong R$. So M is cusp transitive and its cusps have section N.

We want to obtain a cover M of R, with cusps isometric to the one of R, and this will follow from the fact that M is tessellated by copies of R. Note that a generic cover of R has cusps non-homeomorphic to the one of R. The authors in [Nim98; McR09] find an orbifold with one cusp of the desired type, and then, by a separability argument, they find a manifold cover with a cusp of the same type. We do the same thing, but our construction guarantees that all the cusps of M are of the same type of the cusp of R, since the construction is more geometric. Indeed we obtain M by gluing copies of R.

We have found two hyperbolic Coxeter n-polytopes with $n \geq 4$ satisfying (a) and (b): a 4-polytope P (which we call P_0 in Chapter 3) among Im Hof's polytopes associated to Napier cycles [IH90; FT], and another 4-polytope V with 8 facets, which as far as we know does not appear in the literature. Hence, we have not been able to build manifolds of dimension greater than 4 using these techniques.

In Chapter 3, we are interested only in orientable manifolds. We find cusp-transitive manifolds of dimension four because P is 4-dimensional, and we realize only some cusp types because of the particular link type of the ideal vertex of P: a prism over a $(2, 4, 4)$-triangle. Note indeed that E_1, E_2, E_4 and E_6 can be tessellated by right parallelepipeds, and thus by such a prism.

In Chapter 4, we obtain cusp-transitive 4-manifolds with every cusp section using a different method to construct the developable reflectofold R. We again use the polytope P to obtain cusp-transitive manifolds with cusp type N, for every N different from E_3 and E_5, while we use the polytope V for the remaining cases. Indeed, the link of the ideal vertex of V is a prism K over an equilateral triangle; the fact that E_3 and E_5 are tessellated by copies of K is crucial to the construction of the corresponding cusp-transitive manifolds.

We would like to apply our construction to polytopes in dimension greater than 4, but we did not find any other polytope with the desired properties.

Ensuring (1) and (2) is the most technical point of the construction. Indeed, there is an easy way to glue some copies of P in order to get a 1-cusped reflectofold R with cusp section E_i, forse some i, but the resulting R would not be developable. Hence, in Chapter 3 we iteratively double the polytope P, obtaining a sequence $P_1, \ldots, P_m$ of polytopes which satisfy the properties (a) and (b). We continue to double until we find a gluing for a polytope P_m giving a developable R. In

Chapter 4 the construction will be less explicit and more abstract.
Question 1.1.3. Does there exist a finite-volume hyperbolic Coxeter polytope of dimension $n \geq 5$ satisfying (a) and (b)?

We would like to improve the method in a future work, with the hope of producing original examples of 1-cusped manifolds. In principle this may be done, instead of developing such an R, by closing it up gluing its facets. This is much more difficult (and sometimes impossible by some immediate obstructions), but has the advantage that more polytopes may be used, since in this case the quite restrictive property (b) is not necessarily needed.
Question 1.1.4. For which $i = 3, 4, 5, 6$ does there exist a 1-cusped hyperbolic 4-manifold whose cusp has type E_i? Can moreover such a 4-manifold be orientable when $i = 4, 6$?
Question 1.1.5. For which dimension $n \geq 5$ does there exist a 1-cusped hyperbolic n-manifold?

1.2 Non-spin manifolds

It follows from a couple of works of Deligne and Sullivan [DS75; Sul79] of the 1970s that every hyperbolic manifold M is finitely covered by a stably parallelizable manifold M'. In particular, the Stiefel–Whitney classes satisfy $w_k(M') = 0$ for all $k > 0$. Unless otherwise stated, all manifolds in this section and in Chapter 5 are smooth, connected and orientable (i.e. with $w_1 = 0$), and all hyperbolic manifolds are complete and of finite volume.

The existence of hyperbolic n-manifolds that do not admit spin structures (i.e. with $w_2 \neq 0$) has been proved in 2020: there are closed for all $n \geq 4$ [MRS20] and cusped for all $n \geq 5$ [LR20]. Recall instead that surfaces are stably parallelizable and 3-manifolds are parallelizable. Then several examples of hyperbolic manifolds with non-trivial Stiefel–Whitney classes have been produced with different techniques [Che25a; Che25b; Che25c; LR20; RS], but the existence of cusped 4-manifolds with $w_2 \neq 0$ appears open. We fill here the gap:
Theorem 1.2.1. *There exists a cusped orientable (arithmetic) hyperbolic 4-manifold M that does not admit any spin structure.*

Since M is arithmetic and even-dimensional, we can iteratively apply the embedding theorem of Kolpakov, Reid and Slavich [KRS18] as in [MRS20, Section 5], to get a sequence of totally geodesic embeddings $M = \mathbb{H}^4/\Gamma_4 \subset \mathbb{H}^5/\Gamma_5 \subset \dots$ of n-manifolds with $\Gamma_n \subset \mathrm{PSO}(1, n; \mathbb{Q})$ commensurable with $\mathrm{PO}(1, n; \mathbb{Z})$. None of them admits a spin structure because an orientable hypersurface does not, so:
Corollary 1.2.2. *For every $n \geq 4$, there exists a cusped orientable (arithmetic)*

hyperbolic n-manifold that does not admit any spin structure.

This has already been proved by Long and Reid for $n \geq 5$ [LR20] as follows: (1) there is a closed flat 4-manifold F^4 with $w_2(F^4) \neq 0$, so $F^{n-1} = F^4 \times S^1 \times \ldots \times S^1$ has $w_2(F^{n-1}) \neq 0$ for all $n \geq 5$; (2) as every closed flat manifold, F^{n-1} is diffeomorphic to a cusp section of a cusped hyperbolic manifold M^n [LR02; McR09], so as before $w_1(F^{n-1}) = 0,\ w_2(F^{n-1}) \neq 0 \implies w_2(M^n) \neq 0$.

To prove Theorem 1.2.1, we instead proceed as done in the closed case by Martelli, Slavich and the first author in [MRS20] (see also [MRS21]), explicitly constructing a hyperbolic 4-manifold M satisfying a stronger condition: its intersection form is *odd*; equivalently, there is a closed oriented surface $S \subset M$ with odd self-intersection $S \cdot S$ (the Euler number of the normal bundle). Then $w_2(M) \neq 0$ because the result of clashing $w_2(M)$ with the $\mathbb{Z}/2\mathbb{Z}$-homology class of S is $S \cdot S \mod 2$. Note that S must necessarily be closed, otherwise $S \cdot S = 0$. Moreover, S is not homologous to any immersed totally geodesic surface in M, since such surfaces have even self-intersection (see [MRS20]).

As in [MRS20; MRS21], we build M by gluing some copies of a right-angled hyperbolic polytope Q^4 in such a way that S is contained in the 2-skeleton of the tessellation. For this purpose, we need that Q^4 has a compact 2-face Q^2. The only unbounded, right-angled, hyperbolic 4-polytope of finite volume with a compact 2-face that we know is introduced in Section 5.2. It belongs to a continuous family of hyperbolic 4-polytopes discovered in 2010 by Kerckhoff–Storm [KS10], further studied in [MR18] and later used for different purposes [Rio24; RS22b; RS22a; RS19]. The polytope Q^4 has 22 facets and octahedral symmetry. Its reflection group is arithmetic, and like for the well-known ideal 24-cell, is commensurable with the integral lattice $\mathrm{PO}(1,4;\mathbb{Z})$. The manifold M belongs to this commensurability class. We thank Leone Slavich for pointing out that a conjugate of Γ_4 lies in $\mathrm{PSO}(1,4;\mathbb{Q})$, which gives Corollary 1.2.2.

Like in [Mar22; MRS20; MRS21], we use some right-angled polytopes $Q^2 \subset Q^3 \subset Q^4$ (where Q^n is a facet of Q^{n+1}) to build some auxiliary hyperbolic manifolds with right-angled corners of increasing dimension. These objects have been fruitfully used in four- and five- dimensional hyperbolic geometry in the very last years [BFS24; Che25a; Che25c; Rio24]. The surface S is piecewise geodesic and tessellated by copies of Q^2, and the cells of M intersecting S form a 4-manifold with right-angled corners X (see Figure 5.1–right).

1.3 Organization of the thesis

The work is organized as follows. In Chapter 2 we give the preliminaries about hyperbolic manifolds, Coxeter polytopes and spin structures. In Chapter 3 we build cusp-transitive orientable 4-manifolds with cusp type E_1, E_2, E_4, E_6. In particular, in Section 3.1 we describe how to obtain a cusp-transitive manifold from a 1-cusped developable reflectofold. in Section 3.2 we double the polytope P many times in order to obtain two Coxeter polytopes which we will use in Section 3.3 in order to get some 1-cusped developable reflectofolds. In Chapter 4 we build cusp-transitive 4-manifolds with all cusp sections and prove other related results. In detail, in Section 4.1 we study the polytope P and assemble 16 copies of it to create a bigger polytope Q. In Section 4.2 we show how to construct reflectofolds by gluing copies of Q according to some cubical tessellations, and consequently prove the first case of Theorem 1.1.2. In Section 4.3 we introduce the polytope V and construct reflectofolds by gluing copies of it according to certain tessellations in prisms, proving the second and final case of Theorem 1.1.2. In Section 4.4, we prove Theorem 4.4.1 and its 3-dimensional counterpart. Lastly, in Section 4.5, we prove Theorem 4.5.1. In Chapter 5 we build an orientable non-spin hyperbolic 4-manifold. More precisely, the proof of Theorem 1.2.1 is summarized in Section 5.1, the polytope is introduced in Section 5.2, and the construction is performed in Section 5.3. In Chapter 6 we collect some information about polytopes studied in Chapter 3.

Chapter 2

Preliminaries

2.1 Hyperbolic manifolds

In this subsection we want to briefly recall the topology of complete, finite-volume, hyperbolic manifolds. For the content of this section and further details, the reader can check [Mar23, Chapter 4].

Recall that for every complete hyperbolic manifold M, there exists a discrete and torsion free subgroup $\Gamma < \mathrm{Isom}(\mathbb{H}^n)$ such that $M \cong \mathbb{H}^n/\Gamma$. A subgroup Γ of $\mathrm{Isom}(\mathbb{H}^n)$ is discrete if and only if the action on $\mathbb{H}^n$ is properly discontinuous; while if it is discrete, then it is torsion free if and only if the action is free. Hence the group Γ contains only parabolic and hyperbolic elements (that by definition respectively fix exactly one and two elements in $\partial\mathbb{H}^n$), along with the identity.

Definition 2.1.1. Let x be a point in the manifold M. The injectivity radius $inj_x M = \sup\{r > 0 | \exp_x\big|_{B_0(r)} : B_0(r) \to M \text{ is a diffeomorphism onto its image}\}$.

Definition 2.1.2. Let $S \subset \mathbb{H}^n$ be a discrete subset, then

$$d(S) \coloneqq \inf\{d(x,y) | x, y \in \mathbb{H}^n\}.$$

Proposition 2.1.3. *Let $M = \mathbb{H}^n/\Gamma$ be a complete hyperbolic manifold, where $\pi : \mathbb{H}^n \to M$ is the projection, then*

$$inj_x M = \frac{1}{2} d(\pi^{-1}(x)).$$

We now define tubes and cusps.

Let $\Gamma =< \varphi >$ be the infinite cyclic group generated by a hyperbolic isometry. The manifold $M = \mathbb{H}^n/\Gamma$ is called an infinite tube. Let $N_R(I)$ be the R-neighbourhood

of the axys I of φ. An R-tube is the quotient $N_R(I)/\Gamma$. If $R > 0$ is sufficiently small, the R-neighbourhood of a simple closed geodesic in a complete hyperbolic manifold is isometric to a R-tube.

Let $\Gamma < \mathrm{Isom}(\mathbb{H}^n)$ be a discrete group of parabolic transformations fixing the same point at infinity. The manifold $M = \mathbb{H}^n/\Gamma$ is called a cusp. If we use the half-space model for $\mathbb{H}^n$ and we assume that the point fixed by the parabolic isometries is the point at infinity, then every parabolic transformation is of the type $\varphi(x,t) = (\phi(x),t)$, where $x \in \mathbb{R}^{n-1}, t \in R_+$ and ϕ is a Euclidean isometry acting freely on $\mathbb{R}^{n-1}$. Let Γ' be the group of Euclidean isometries of $\mathbb{R}^{n-1}$ that naturally descend from Γ. We have that $N = \mathbb{R}^{n-1}/\Gamma'$ is a flat $(n-1)$-manifold. Moreover, we have that the manifold M is diffeomorphic to $N \times \mathbb{R}_+$, where the metric tensor at the point (x,t) is

$$g^M_{(x,t)} = \frac{g^N_x \oplus 1}{t^2}.$$

A truncated cusp is of the form $M' = N \times [a, +\infty)$, with boundary equal to the flat manifold $M \times \{a\}$ and not totally geodesic. The volume of a truncated cusp is finite, indeede we have that

$$\mathrm{Vol}(M') = \frac{\mathrm{Vol}(\partial M')}{n-1}$$

In dimension $n = 2$ there is only one cusp up to isometry, which is diffeomorphic to $S^1 \times \mathbb{R}$, where the subgroup $\Gamma' < \mathrm{Isom}(\mathbb{R})$ is the infinite cyclic group generted by a translation.

We say that an elementary group is a non-trivial discrete subgroup of $\mathrm{Isom}(\mathbb{H}^n)$ that preserves a finite set of points in $\overline{\mathbb{H}^n}$. One can easily prove that an elementary group Γ acting freely on $\mathbb{H}^n$ is generated by a hyperbolic isometry or it is generated by parabolic isometries fixing the same point at infinity.

Let Γ be a group of isometries of M and let $\varepsilon > 0$ be a constant. We define

$$\Gamma_\varepsilon \coloneqq \{\varphi \in \Gamma | d(\varphi(x), x)\}.$$

We state now the Margulis Lemma.

Lemma 2.1.4. *In every dimension $n \geq 2$ there exist a Margulis constant $\varepsilon_n > 0$ such that for every $\Gamma < Isom(\mathbb{H}^n)$ discrete and torsion free and for every $x \in \mathbb{H}^n$, the subgroup Γ_{ε_n} is either trivial or elementary.*

We define a star-shaped set centered at $p \in \partial\mathbb{H}^n$ as a set $U \subset \mathbb{H}^n$ which intersects every half-line pointing at p in a half-line. An easy example is an horoball centered at p. A star-shaped neighbourhood of a line $I \subset \mathbb{H}^n$ is any neighbourhood V of I which intersect every line orthogonal to I in a connected set. An easy example is a R-neighbourhood of I.

These two definitions we just give pass to the quotient. We define a star-shaped cusp neighbourhood as the quotient U/Γ, where U is a Γ-invariant star-shaped set centered at $p \in \partial\mathbb{H}^n$ and Γ is a discrete group of parabolic isometries of $\mathbb{H}^n$ fixing the point p. A R-tube we defined earlier is a particularly nice example. We define a star-shaped simple closed geodesic neighbourhood as the quotient V/Γ, where V is a Γ-invariant star-shaped neighbourhood of a line $I \subset \mathbb{H}^n$ and Γ is a discrete group of hyperbolic isometries of $\mathbb{H}^n$ with axis I. A truncated cusp we defined earlier is a particularly nice example.

Let ε_n be a Margulis constant, we define the thick part $M_{[\varepsilon_n,\infty)}$ as the set of points $x \in M$ such that $inj_x M \geq \epsilon_n$, and the thin part $M_{(0,\varepsilon_n]}$ as the closure of the complementary $M \setminus M_{[\varepsilon_n,\infty)}$.

We do not define the thin part $M_{(0,\varepsilon_n]}$ as the points $x \in M$ such that $inj_x M \geq \varepsilon_n$ since we want to exclude the case where there is a closed geodesic with length exactly ε_n. With our definition, the points of this geodesic are in $M_{[\varepsilon_n,\infty)}$ and not in $M_{(0,\varepsilon_n]}$.

We now state the most important result on complete hyperbolic manifold, the thick-thin decomposition, and we give a sketch of the proof.

Theorem 2.1.5. *Let M be a complete hyperbolic n-manifold. The thin part $M_{(0,\varepsilon_n]}$ consists of a disjoint union of star-shaped neighbourhoods of cusps and of simple closed geodesics of length $< \varepsilon_n$.*

Proof. There exists a discrete and torsion free subgroup $\Gamma < \mathrm{Isom}(\mathbb{H}^n)$ such that $M = \mathbb{H}^n/\Gamma$. For every isometry $\varphi \in \Gamma$, we define the following set in $\mathbb{H}^n$

$$S_\varphi(\varepsilon) \coloneqq \{x \in \mathbb{H}^n | d(\varphi(x), x) < \varepsilon\}.$$

One can prove that the thin part of M is the quotient S/Γ, where $S = \bigcup_{\varphi \in \Gamma \setminus \{\mathrm{id}\}} S_\varphi(\varepsilon_n)$.

Let S' be a connected component of S. Thanks to the lemma 2.1.4 we can show that S' is the union of all $S_\varphi(\varepsilon_n)$, where φ varies in a maximal elementary subgroup $\Gamma' < \Gamma$ of parabolics fixing the same point p at infinity or hyperbolics fixing the same line I. The set S_0 is union of star-shaped sets centered at p or I, hence it is star-shaped.

Finally, since the group Γ preserves S and the only isometries in Γ that preserve S' are those in Γ', we have that the quotient $S/\Gamma = M_{(0,\varepsilon_n]}$ consists of star-shaped neighbourhoods of cusps and of simple closed geodesics. □

Using this decomposition, we can obtain the following results.
Proposition 2.1.6. *A complete hyperbolic manifold has finite volume if and only if the thick part is compact.*

Proof. If the thick part is not compact, it contains an infinite number of points that stay pairwise at a distance greater than ε_n. Hence the thick part contains an infinite number of disjoint embedded open balls with radius $\frac{\varepsilon_n}{2}$. Therefore, the thick part has infinite volume.

If the thick part is compact, it has finite volume. Moreover, also its boundary is compact, hence the thin part consists of finitely many star-shaped neighbourhoods of cusps and of simple closed geodesics. They are both of finite volume, since they are contained respectively in an bigger truncated cusp and in a R-tube. □

Corollary 2.1.7. *Every complete finite volume hyperbolic manifold without boundary is diffeomorphic to the interior of a compact manifold with boundary, which is the disjoint union of manifolds that admit a flat metric.*

Proof. We have just seen that the thick part is compact and the thin part is the union of finitely many star-shaped neighbourhoods of cusps and of simple closed geodesics. Each star-shaped neighbourhoods of cusps contains a smaller cusp diffeomorphic to $N \times [0, 1)$, with N that admits a flat structure. The complement in M of these cusps is compact. Each truncated cusp can be compactified by adding $N \times \{1\}$. □

2.2 Coxeter polytopes

In this section we introduce the Coxeter polytopes. In particular, we are interested in hyperbolic ones. Indeed, these polytopes are useful to build hyperbolic manifolds by gluing them together.

A polytope in $\mathbb{R}^n, \mathbb{S}^n, \mathbb{H}^n$ is a finite intersection of half-spaces and is called respectively Euclidean, spherical and hyperbolic.

The dimension of a polytope P, called $\dim P$, is the least dimension of a subspace containing P.

The boundary of a polytope is naturally stratified by dimension and consists of polytopes of dimension $k \in \{0, 1, 2, \ldots, \dim P - 1\}$, called the k-faces of P.

We call vertices, ridges and facets the 0-dimensional, $(n-2)$-dimensional and $(n-1)$-dimensional faces of the polytope, respectively.

When two facets meet at a ridge, the dihedral angle between them is well defined. Since the polytope in convex, the dihedral angle is always $< \pi$.
Definition 2.2.1. A polytope is a *Coxeter polytope* if all its dihedral angles are integral submultiples of π.
Remark 2.2.2. In a Coxeter polytope, since the dihedral angles are $< \frac{\pi}{2}$, if the bounding hyperplanes of two facets intersect, then the two facets intersect.

We refer to Vinberg's paper [Vin85] for the general theory of hyperbolic Coxeter polytopes and groups, that we will see later.

A particular case of Coxeter polytope is the one of right-angled polytope. They are polytopes where every dihedral angles is equal to $\frac{\pi}{2}$. Every face of a right-angled polytope is again a right-angled polytope.

In the hyperbolic case, the closure of a polytope may intersect the boundary at infinity $\partial\mathbb{H}^n$. If a polytope is of finite volume, then the inyersection of its closure with $\partial\mathbb{H}^n$ consists of isolated finitely many points, called ideal vertices.

2.2.1 Coxeter diagrams, groups and Gram matrices

To a hyperbolic Coxeter polytope P one associated a decorated graph, called the Coxeter diagram of P. However, we can define a Coxeter diagram indipendently from any polytope.
Definition 2.2.3. A *Coxeter diagram* is a diagram where if between two vertices there is an edge, then it is one of the following:

- an edge optionally labeled with an integer number $n \geq 4$, or ∞;
- a dashed edge, optionally labeled with a real number $x \geq 1$.

We define in the following the Coxeter diagram of a hyperbolic Coxeter polytope. The graph has a node for each bounding hyperplane of a facet, and an edge joining nodes i and j has label m_{ij} if the corresponding hyperplanes intersect with dihedral angle $\frac{\pi}{m_{ij}}$. By usual convention, the label is $m_{ij} = \infty$ when the two hyperplanes are tangent at infinity. The edge of the graph is omitted when $m_{ij} = 2$, while it is dashed when two hyperplanes are ultraparallel. In this case, we may decide to label the edge with $\cosh(d) \geq 1$, where d is the distance between the two hyperplanes.

We can define a Coxeter group associated to every Coxeter diagram, even if it does not come from a polytope.
Definition 2.2.4. Let $S = r_1, \ldots, r_k$ be the set of vertices of a Coxeter diagram D. Let m_{ij} be the label of a non-dashed edge joining r_i and r_j. If there is not an

edge between r_i and r_j, then we set $m_{ij} = 2$. If the label of the edge between r_i and r_j is ∞, or the edge is dashed, then we set $m_{ij} = \infty$. We define the *Coxeter group* W_D of D as a finitely presented group, as in the following:

$$W_D \coloneqq < r_1, \dots, r_k | r_i^2 = 1 \, \forall i = 1, \dots, k, (r_i r_j)^{m_{ij}} = 1 \, \forall i \neq j > .$$

If the diagram D comes from a polytope P, then the group W_D can be called the Coxeter group of P.

Remark 2.2.5. If a diagram D is the disjoint union of some connected diagrams $D = D_1 \sqcup \cdots \sqcup D_m$, then the group W_D will be the product of the associated groups $W_D = W_{D_1} \times \cdots \times W_{D_m}$. Moreover, if D is a diagram of a polytope P, then the polytope P is a product of polytopes $P = P_1 \times \cdots \times P_m$, where P_i is associated to D_i.

We observe that passing from the diagram D to the group W_D we loose we some information. Indeed, if two generators of W_D do not have a relation, then we do not know if they come from two vertices with an edge with label ∞ or a dashed edge with a certain label.

Proposition 2.2.6. *Let P be a hyperbolic Coxeter polytope. For every facet F_i, we denote with r_i the reflection through the supporting hyperplane of F_i. The group generated by the reflections is isomorphic to the Coxeter group of P, with an isomorphism sending each reflection r_i to the generator of the Coxeter group associated to the facet F_i.*

We can also represent the information of a Coxeter diagram with a matrix.

Definition 2.2.7. The *Gram matrix* G of a Coxeter diagram D with k vertices $r_1, \dots, r_k$ is a real $k \times k$ matrix. Let e be the edge between r_i and r_j, then the entry of G_{ij} is:

$$G_{ij} \coloneqq \begin{cases} 1 & \text{if } i = j; \\ -\cos(\pi/m_{ij}) & \text{if } e \text{ is non-dashed with label } m_{ij}; \\ -1 & \text{if } e \text{ is non-dashed with label } \infty; \\ -x & \text{if } e \text{ is dashed with label } x. \end{cases} \tag{2.1}$$

Proposition 2.2.8 ([Vin85, Theorem 2.1])**.** *If a Gram matrix of a Coxeter diagram D has signature $(n, 1, m)$, then D is the Coxeter diagram of a hyperbolic Coxeter polytope.*

2.2.2 Faces of Coxeter polytopes

In this section we will show the connection between a face of a polytope, the Coxeter diagram and the Coxeter group.

We have the following result.

Proposition 2.2.9. *Every face, excluding the ideal vertices, of codimension c of a Coxeter polytope is the intersection of exactly c facets.*

Hence, if F is a face of a polytope P, then there is a unique set of facets of P such that their intersect is equal to F. Therefore, it is well defined the subdiagram D_F of D associated to F, where D is the Coxeter diagram of P. Moreover, we have the following inclusion between the Coxeter groups.
Proposition 2.2.10. *The homomorphism $W_{D_F} \to W_D$, induced by the inclusion $D_F \subset D$, is well-defined and injective.*

Moreover, we have another result about the group W_{D_F}.
Proposition 2.2.11. *The group W_{D_F} is the stabilizer of the face F under the action of W_D on $\mathbb{H}^n/\mathbb{R}^n/\mathbb{S}^n$.*

We now state some results which are very useful in the study of the combinatorics of a Coxeter polytope.

We say that a Coxeter diagram (or group) is spherical/affine if it is associated to a spherical/Euclidean Coxeter polytope.

The spherical and affine connected Coxeter diagrams are listed [Vin85, Tables 1-2].
Proposition 2.2.12. *The faces of a Coxeter polytope P with a Coxeter diagram D are in bijection with the spherical subdiagrams of D.*
Proposition 2.2.13. *The finite vertices of a Coxeter polytope P with a Coxeter diagram D are in bijection with the spherical subdiagrams of D with as many vertices as the dimension of P. If P is compact, then the vertices correspond to maximal spherical subdiagrams.*
Proposition 2.2.14. *The ideal vertices of a Coxeter polytope with diagram D are in bijection with the maximal affine subdiagrams of D.*

2.3 Spin structures

We begin defining the Stiefel-Whitney classes. We can define them using the following theorem.
Theorem 2.3.1 ([MS74, Chapter 4])**.** *There exists a unique way to assign to every vector bundle $\pi : E \to M$ (with M connected manifold) a class $w \in H^*(M, \mathbb{Z}/2\mathbb{Z})$ with $w = 1 + w_1 + w_2 + \dots$ ($w_i \in H^i(M, \mathbb{Z}/2\mathbb{Z})$) such that:*

1. *$w_i = 0 \ \forall i > rk(E)$;*
2. *if we have $f : N \to M$, then we have $f^* w(E) = w(f^* E)$;*
3. *if $p : E' \to M$ is a vector bundle, then $w(E \oplus E') = w(E) \smile w(E')$;*

4. $w(Moebius \to S^1) = 1 + a$, where a is the generator of $H^1(S^1)$.

We now restrict the study only to 4-manifolds and we give an explicit definition for the first two classes in the case of the tangent bundle. For the content of this section and further details, the reader can check [Sco05, Chapter 4].

The Stiefel-Witney class $w_k(TM) \in H^k(M, \mathbb{Z}/2\mathbb{Z})$ measures the obstruction to finding a field of $4 - k + 1$ linearly indipendent vectors over the k-skeleton of M (we see M as a CW-complex), which is the union of the cells of dimension $\leq k$.

The class $w_1(TM) \in H^1(M, \mathbb{Z}/2\mathbb{Z})$ measures the obstruction to finding a trivialization of TM over the 1-skeleton. We can define it by its values on embedded circles in M, since $H^1(M, \mathbb{Z}/2\mathbb{Z}) \cong \mathrm{Hom}(H_1(M, \mathbb{Z}/2\mathbb{Z}), \mathbb{Z}/2\mathbb{Z})$.

$$\begin{cases} w_1(TM) \cdot C = 1 & \text{if } TM\big|_C \text{ is trivial;} \\ w_1(TM) \cdot C = 0 & \text{if } TM\big|_C \text{ is not trivial.} \end{cases} \tag{2.2}$$

Since a 4-frame over a circle is either trivial or non-orientable, we observe that the first Stiefle-Whitney class detects if a loop in M is orientation-reversing or not. Hence $w_1(TM) = 0$ if and only if M is orientable.

We now restrict to the case where M is orientable, hence $w_1(TM) = 0$. The second Stiefel-Whitney class $w_2(TM) \in H^2(M, \mathbb{Z}/2\mathbb{Z})$ measures the obstruction to finding a 3-frame over the 2-skeleton of M. Using an orientation, we have that a 3-frame can be completed to a 4-frame. Hence, if M is oriented, $w_2(TM)$ is the obstruction to finding a trivialization of TM over the 2-skeleton.

We can define $w_2(TM)$ as a cochain. Given a trivialization of TM over the 1-skeleton of M, we can define a cellular cochain θ by assigning $1 \in \mathbb{Z}/2\mathbb{Z}$ to any 2-cell across which the chosen trivialization cannot be extended. We assign $0 \in \mathbb{Z}/2\mathbb{Z}$ to the other 2-cells. Hence, this cochain will be trivial if and only if the trivialization of TM over the 1-skeleton extends over the 2-skeleton. If we go back and change the trivialization over the 1-skeleton, the resulting cochain will be modified by addition of a coboundary. Moreover, our cochain is a cocycle. Hence we have defined a class in $H^2(M, \mathbb{Z}/2\mathbb{Z})$ which is $w_2(TM)$ and is trivial if and only if the trivialization of TM over the 1-skeleton extends over the 2-skeleton.

Let D be a disk in the 2-skeleton of M, then a trivialization of TM over the 1-skeleton induces a map $\phi : \partial D \to SO(4)$ and the trivialization of TM extends to D if and only if the map ϕ extends to D. The latter is true when the map ϕ is null in $\pi_1(SO(4)) \cong \mathbb{Z}/2\mathbb{Z}$. Recall that a generator of $\pi_1(SO(4))$ is any path of rotations of angles increasing from 0 to 2π; if we the angle keeps increasing to 4π,

then the resulting loop is null-homotopic in $SO(4)$. In our case, is usefull to think of $SO(4)$ as the space of orienting orthonormal frames in $\mathbb{R}^4$.

A manifold with $w_1(TM) = w_2(TM) = 0$ is said to be a spin manifold. A spin manifold admits at least a spin structure. A spin structure on a manifold M is a choice of trivialization of TM over the 1-skeleton that can be extended over the 2-skeleton, considered up to homotopies.

We now describe an action of $H^1(M, \mathbb{Z}/2\mathbb{Z})$ on the set of spin structures, which allows for a better understanding of spin structures. Let s be a spin structure on M, hence it is a trivialization of TM over the 1-skeleton that can be extended over the 2-skeleton. We take a class $\alpha \in H^1(M, \mathbb{Z}/2\mathbb{Z})$ and we represent it via a 3-submanifold N_α (which may not be orientable). We move the latter in a way that it is transverse to every cell of M. We now define a new spin structure $\alpha \cdot s$: for every edge e in the 1-skeleton, we modify the 4-frame by an addiction of a $2k$-twist for every intersection between e and N_α. We now prove that the trivialization $\alpha \cdot s$ extends over the 2-skeleton. Let D be a 2-cell in the 2-skeleton of M, then $Y_\alpha \cap D$ is a disjoint union of circle (in the interior of D) and properly embedded arcs, hence the number of intersection between ∂D and N_α is the double of the number of arcs, hence it is even. Thus, the trivialization over ∂D is modified by an addiction of a certain number of 4π-twist, hence the map $\partial D \to SO(4)$ is still zero in $\pi_1(SO(4))$.

We have just defined an action of $H^1(M, \mathbb{Z}/2\mathbb{Z})$ on the spin structures of M. One can also prove that this action is free and transitive. Hence, once fixed a spin structure on M, the action gives a bijection between $H^1(M, \mathbb{Z}/2\mathbb{Z})$ and the set of all spin structures on M. In particular, if M is simply connected, there exists exactly one spin structure.

If a 4-manifold M is spin, then there exists a trivialization of TM over the 3-skeleton. Indeed, let B be a 3-cell of the 3-skeleton of M, then the trivialization of TM over ∂B gives us a map $\psi : \partial B \to SO(4)$. Since we have that $\pi_2(SO(4) = 0$, the map ψ extends to B. Hence, the trivialization of TM extends to all the 3-skeleton. Since the 4-skeleton can be chosen contractile, there exists a point $p \in M$ such that TM is trivial on $M \setminus \{p\}$. The manifolds with the latter condition are called almost-parallelizable.

In general, in a manifold M of any dimension, we have the following implications:

M is parallelizable $\implies$ M is stably parallelizable $\implies$ M is almost parallelizable $\implies$ $w_i(M) = 0 \ \forall i \geq 1 \implies$ M is spin $\implies$ M is orientable.

A manifold M is stably parallelizable if the vector bundle $TM \oplus \epsilon^k$ is trivial for some k, where e^k is the trivial fiber bundle over M with fiber $\mathbb{R}^k$.

A compact, orientable surface is stably parallelizable, while a compact, orientable 3-manifold is parallelizable. As we have seen, an orientable 4-manifold is spin if and only if is almost parallelizable.

We now want to give another definition for the spin structure.

Recall that a vector bundle of rank k on a manifold M is a map $\pi : E \to M$, where E is a manifold with $\dim E = \dim M + k$, there is an open covering $\{U_\alpha\}$ and there is a set of diffeomorphisms $\{\phi_\alpha : \pi^{-1}(U_\alpha) \to U_\alpha \times \mathbb{R}^k\}$, with $\pi_1 \circ \phi_\alpha = \pi$, where π_1 is the projection to the first factor, and so that, if $U_\alpha \cap U_\beta \neq \emptyset$, then $\phi_\alpha \circ \phi_\beta^{-1}(x, w) = (x, g_{\alpha,\beta}(x) \cdot w)$, for some $g_{\alpha,\beta} : U_\alpha \cap U_\beta \to GL(k)$.

One can also define the fiber bundle E over M just giving an open covering $\{U_\alpha\}$ and the maps $\{g_{\alpha,\beta}\}$: we obtain E gluing pieces of $U_\alpha \times \mathbb{R}^k$ by identifying, if $U_\alpha \cap U_\beta \neq \emptyset$, $(x, w_\alpha) \in U_\alpha \times \mathbb{R}^k$ with $(x, w_\beta) \in U_\beta \times \mathbb{R}^k$ when $w_\alpha = g_{\alpha,\beta}(x) \cdot w_\beta$. Moreover, these maps have to verify some conditions:

$$g_{\alpha,\alpha}(x) = \mathrm{id} \qquad g_{\alpha,\beta}(x) \cdot g_{\beta,\alpha}(x) = \mathrm{id} \qquad g_{\alpha,\gamma}(x) = g_{\alpha,\beta}(x) \cdot g_{\beta,\gamma}(x).$$

These three conditions can be contracted in just one condition, the cocycle condition:

$$g_{\alpha,\beta}(x) \cdot g_{\beta,\gamma}(x) \cdot g_{\gamma,\alpha}(x) = \mathrm{id}.$$

We say that any collection $\{U_\alpha, g_{\alpha,\beta}\}$ satisfying the cocycle condiction is a cocycle.

Two cocycles $\{g_{\alpha,\beta}\}$ and $\{g'_{\alpha,\beta}\}$ are isomorphic if there exists some functions $\{f_\alpha : U_\alpha \to GL(k)\}$ such that $g'_{\alpha,\beta}(x) = f_\alpha \cdot g'_{\alpha,\beta} \cdot f_\beta(x)^{-1}$.

Given a cocycle $\{g_{\alpha,\beta} : U_\alpha \cap U :_\beta \to GL(k)\}$ and a subgroup $G < GL(k)$, if we can find a G-valued cocycle $\{g'_{\alpha,\beta} : U_\alpha \cap U_\beta \to GL(k)\}$ that is isomorphic to the first cocycle, we say that we have reduced the structure group of the cocycle to G.

For example, if we have a vector bundle E over M and we put a Riemannian metric on M, we reduce the structure group of E to $O(k)$. Moreover, if we put an orientation on M, we reduce the structure group of E to $SO(k)$.

We are now ready to define a spin structure on an orientable 4-manifold M. We put a Riemannian metric and an orientation on M, hence the tangent bundle TM can be described by an $SO(4)$-valued cocycle.

We consider the universal cover Spin(4) of $SO(4)$. Since we have that $\pi_1(SO(4)) = \mathbb{Z}/2\mathbb{Z}$, this cover is a double cover.

A spin structure on M is a lift of the $SO(4)$-valued cocycle of TM to a Spin(4)-valued cocycle, considered up to isomorphism. Given a map $g_{\alpha,\beta} : U_\alpha \cap U_\beta \to SO(4)$ and

the projection $p : \mathrm{Spin}(4) \to SO(4)$, we can obtain a lifting $\overline{g_{\alpha,\beta}} : U_\alpha \cap U_\beta \to \mathrm{Spin}(4)$, since we can choose $\{U_\alpha\}$ such that $U_\alpha \cap U_\beta$ is contractible. The problem is that the cocycle condition may be not verified, indeed we have that

$$\overline{g_{\alpha,\beta}}(x) \cdot \overline{g_{\beta,\gamma}}(x) \cdot \overline{g_{\gamma,\alpha}}(x) = \pm \mathrm{id}.$$

Hence, we say that the manifold M admits a spin structure if we can find a $SO(4)$-cocycle $\{U_\alpha, g_{\alpha,\beta}\}$ that can be lifted to a $\mathrm{Spin}(4)$-cocycle where the cocycle condition is verified, hence where the minus sign never appears in the equality above.

We do not prove here the equivalence of the definitions of spin structure, since the proof is rather technical. For the detailed proof, the reader can check [Sco05, Chapter 4].

Chapter 3

Some cusp-transitive hyperbolic 4-manifolds

This chapter is based on the published paper [Riz25]. We build orientable cusp-transitive 4-manifolds with cusp type E_i for $i = 1, 2, 4, 6$ by gluing copies of a Coxeter polytope. We collect in Chapter 6 certain information about some polytopes of this chapter.

3.1 Cusp-transitive manifolds from 1-cusped reflectofolds

In this section we describe a general method to build a cusp-transitive, hyperbolic manifold from a 1-cusped reflectofold.

Definition 3.1.1. We say that a complete hyperbolic manifold R with boundary is a *reflectofold* if R is locally a hyperbolic Coxeter polytope.[1]

Let R be a reflectofold. The stratification of each local model P of R into k-dimensional faces, $k = 0, \dots, n$, naturally induces a stratification of R into maximal, connected, totally geodesic submanifolds (with boundary), called *k-faces*. The $(n-1)$-faces and the $(n-2)$-faces of R will be called *facets* and *corners*, respectively.

[1]Though we will not strictly need to deal with the orbifold theory, let us notice that a reflectofold R is isometric to a hyperbolic orbifold (sometimes called in the literature *Coxeter orbifold*). In other words, we have $R \cong \mathbb{H}^n/\Gamma$ for some discrete subgroup $\Gamma < \mathrm{Isom}(\mathbb{H}^n)$. To avoid confusion with the terminology, let us notice the following. Even if in the category of manifolds with boundary sometimes $\partial R \neq \emptyset$ and R is orientable, if seen in the orbifold category such an R is non-orientable and without boundary. Unless otherwise stated, we will consider R as a manifold with boundary.

The *dihedral angle* of a corner is the dihedral angle of the corresponding ridge of a local model.

Definition 3.1.2. A reflectofold is *developable* if the following hold:

(EF) *Embedded faces*: For each corner C there are two distinct facets F and F' such that $C \subset F \cap F'$.

(AC) *Angle consistency*: If two distinct facets F and F' intersect, then the dihedral angles of all the corners in $F \cap F'$ coincide.

Given a developable reflectofold R, we denote by G_R the Coxeter group defined by the following presentation. For each facet f of R there is the generator f and the relator f^2. Moreover, there is the relator $(fg)^k$ for every pair of facets f and g which intersect with dihedral angle $\frac{\pi}{k}$.

Let us now apply Davis' "basic construction" to R and G_R [Dav12]. We define a space $\widetilde{R}$ as follows. We take $\{gR\}_{g\in G_R}$, a set copies of R. For every generator f of G_R, we glue the copies gR and fgR identifying the two facets corresponding to f via the map induced by the identity.

Proposition 3.1.3. *Let R be a developable reflectofold. Then R is isometric to the quotient of a hyperbolic manifold M tessellated by copies of R, by a finite group G of isometries.*

By *tessellated by copies of R* we mean that M can be decomposed into some copies of R in such a way that the intersection of any two copies is a union of faces.

Proof. We begin proving that $\widetilde{R}$ is a hyperbolic manifold.

Internally to the copies of R the space $\widetilde{R}$ is locally isometric to $\mathbb{H}^n$. We have to check what happens near the boundary of the copies of R. In particular, we have to check that, given a k-face f of a copy gR, the link of f in $\widetilde{R}$ is isometric to the round sphere $\mathbb{S}^{n-k-1}$.

The link of a k-face F of R is a spherical Coxeter $(n-k-1)$-simplex S. It is well known [Dav12, Section 4.1] that the abstract Coxeter group G_S associated to S embeds in G_R, it is generated by the corresponding subset of the generators of G_R and the relators between them are the ones from the presentation of G_R. Hence the link of the k-face F in $\widetilde{R}$ is the basic construction associated to S and G_S, and is isometric to $\mathbb{S}^{n-k-1}$. We have proved that $\widetilde{R}$ is a hyperbolic manifold. It is complete by construction.

Since Coxeter groups are virtually torsion free [Dav12, Corollary D.1.4], we can take a normal subgroup $G'_R \triangleleft G_R$ of finite index and with no torsion. The group G_R acts on $\widetilde{R}$ by isometry preserving the tassellation of $\widetilde{R}$ in copies of R, and $\widetilde{R}/G_R \cong R$.

Since G'_R is torsion free it acts freely on $\widetilde{R}$. Hence $M \coloneqq \widetilde{R}/G'_R$ is a hyperbolic manifold. We set $G \coloneqq G_R/G'_R$. Since $\widetilde{R}/G_R \cong R$, we have $M/G \cong R$. □

Recall now the definition of cusp transitivity from the introduction. We immediately get:

Corollary 3.1.4. *Let R be an orientable, finite-volume, developable reflectofold. If R has compact boundary and exactly one cusp C, then there exists an orientable, cusp-transitive, hyperbolic manifold M with cusps isometric to C.*

Proof. The manifold M of Proposition 3.1.3 is cusp transitive and its cusps are isometric to C because R is 1-cusped and $M/G \cong R$. If M is non-orientable, it can be replaced by its orientable double cover $\widetilde{M}$. Indeed, for every cusp D of M, the cover $\widetilde{M}$ has two cusps isometric to D (since R is orientable). Moreover, $\widetilde{M}$ is cusp-transitive. Indeed, we can send every cusp to another one using the involution i of $\widetilde{M}$ such that $\widetilde{M}/\langle i\rangle \cong M$ and the liftings of the isometries of M which realize the cusp-transivity of M (we can lift them since an isometry sends an orientable tubolar neighborhood of a loop to an orientable tubolar neighborhood of a loop). □

Hence, in order to prove Theorem 1.1.1, we will build an orientable, finite-volume, 1-cusped, developable reflectofold with compact boundary, whose cusp has type E_i, for $i = 1, 2, 4, 6$.

3.2 The polytopes

In this section we build some Coxeter polytopes satisfying (a) and (b). We will use them in Section 3.3 to build some 1-cusped developable reflectofolds.

In Section 3.2.1 we introduce Im Hof's Coxeter polytope P_0. Then, in Section 3.2.2 we describe a way to obtain a sequence $P_0, P_1, \dots, P_8$ of Coxeter polytopes satisfying (a) and (b), by iteratively doubling P_0, and we describe how to study them. In Section 3.2.4 we build the sequence of polytopes, and we obtain the information on the polytopes using the results of Section 3.2.2.

3.2.1 The polytope P_0

In this section we introduce a Coxeter polytope from [IH90].

Consider the following Coxeter diagram D:

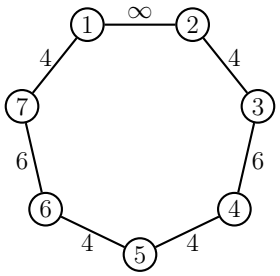

Proposition 3.2.1. *The graph D above is the Coxeter diagram of a finite-volume hyperbolic Coxeter 4-polytope P_0 which satisfies* (a) *and* (b)*. The horospherical link of the unique ideal vertex of P_0 is a Euclidean right prism over a triangle with inner angles $\frac{\pi}{2}$, $\frac{\pi}{4}$, $\frac{\pi}{4}$, and its Coxeter diagram is the subdiagram of D spanned by the vertices $1, 2, 4, 5, 6$.*

Proof. We already know from [IH90] that P_0 has finite volume. By [Vin85], the ideal vertices correspond to the maximal affine subdiagrams of the Coxeter diagram. In D we have exactly one of this kind (see [Vin85, Table 2]), spanned by the vertices $1, 2, 4, 5, 6$. □

3.2.2 The sequence of polytopes

The purpose of this section is to fix some notation, and to describe how to build and study some new Coxeter polytopes satisfying (a) and (b) by doubling iteratively P_0 along some facets.

Definition 3.2.2. We say that a facet F of a polyotpe P is *admissible* if, whenever it intersects another facet K of P, then the dihedral angle between F and K is equal to $\frac{\pi}{2k}$ for some $k \in \mathbb{N}$.

We notice that every facet of P_0 is admissible. Indeed the numbers labelling the Coxeter diagram D are even.

Given a hyperbolic n-polytope P and a facet F of P, we denote by $r_F \colon \mathbb{H}^n \to \mathbb{H}^n$ the reflection through the unique hyperplane that contains F. In Section 3.2.4, we will construct a sequence of Coxeter polytopes in $\mathbb{H}^n$ satisfying (a) and (b):

$$P_0, P_1, P_2, P_3, P_4, P_5, P_6, P_7, P_8,$$

where $P_{n+1} = P_n \cup r_{F_n}(P_n)$, for some admissible, non-compact facet F_n of P_n. We say that P_{n+1} is the *double of P_n along F_n*. Before the actual definition of P_n, we now fix some notation and deduce some information on such a sequence of polytopes in general.

Remark 3.2.3. Since P_0 is a Coxeter polytope and the facet F_n of P_n will be chosen to be admissible, also $P_1, \dots, P_8$ will be Coxeter polytopes.

Let V be the only ideal vertex of P_0 (recall Proposition 3.2.1). Notice that P_n has exactly one ideal vertex for all n, and it is always V. Indeed, we always double along a non-compact facet.

Let L_n be the link of the ideal vertex V of P_n. It is a 3-dimensional Euclidean polytope well-defined up to scaling.

Remark 3.2.4. There is a natural bijection between the set of non-compact facets of P_n and the set of the facets of L_n. Indeed, if we take a "small" orosphere O centered at V, then $O \cap P_n$ can be identified to L_n and every facet of L_n can be identified with the intersection of O with a non-compact facet of P_n. Vice versa, every non-compact facet F of P_n meets O, and $O \cap F$ is a facet of L_n. Indeed, P_n has exactly one vertex at infinity.

Notation 3.2.5. We will call the facets of L_0 with the same name of the facets of P_0.

Note that L_{n+1} is the double of L_n along its facet F_n.

The construction of P_n induces a tessellation of P_n in copies of P_0. In particular, we also have a tessellation of the facets of P_n in copies of facets of P_0. We say that a facet is *of type* i if it is tessellated into copies of the facet $\boldsymbol{i}$ of P_0.

Definition 3.2.6. Let A be a facet of P_n. Let $A_1, \dots, A_k$ be the facets that meet A and α_i be the dihedral angle at $A \cap A_i$. We define $I_n(A) := \{(A_1, \alpha_1), (A_2, \alpha_2), \dots, (A_k, \alpha_k)\}$.

Remark 3.2.7. If $(A, \frac{\pi}{2}) \in I_n(F_n)$, then in $P_{n+1} = P_n \cup r_{F_n}(P_n)$ we have that $A \cup r_{F_n}(A)$ is a unique facet. Otherwise, if $(A, \frac{\pi}{2}) \notin I_n(F_n)$ then A and $r_{F_n}(A)$ are two distinct facets of P_{n+1}.

Notation 3.2.8. From now on, we will call a facet with the same name of the hyperplane that cointains it. Hence, if $(A, \frac{\pi}{2}) \in I_n(F_n)$, we have that $A \cup r_{F_n}(A)$ is a facet of P_{n+1} that we call A by a little abuse.

We now begin the first step of our construction.

Definition 3.2.9. We define $P_1 = P_0 \cup r_5(P_0)$.

The facets of P_1 are: $\mathbf{1}, \mathbf{2}, \mathbf{3}, \mathbf{4}, r_5(\mathbf{4}), \mathbf{6}, r_5(\mathbf{6}), \mathbf{7}$. Indeed, we can deduce the list using Remark 3.2.7 and the fact that $(\mathbf{1}, \frac{\pi}{2}), (\mathbf{2}, \frac{\pi}{2}), (\mathbf{3}, \frac{\pi}{2}), (\mathbf{7}, \frac{\pi}{2}) \in I_0(\mathbf{5})$, while $(\mathbf{4}, \frac{\pi}{2}), (\mathbf{6}, \frac{\pi}{2}) \notin I_0(\mathbf{5})$.

For a shorter notation we denote $r_5(\mathbf{4})$ by $\mathbf{4}_5$, and so on. Hence, with this convention, the facets are: $\mathbf{1}, \mathbf{2}, \mathbf{3}, \mathbf{4}, \mathbf{4}_5, \mathbf{6}, \mathbf{6}_5, \mathbf{7}$. In this case the facets $\mathbf{4}$ and $\mathbf{4}_5$ are facets of type 4, while $\mathbf{6}$ and $\mathbf{6}_5$ are facets of type 6, and $\mathbf{7}$ is a facet of type 7.

By Proposition 3.2.1 we know the Coxeter diagram for L_0. Hence, the links L_0 and L_1 of the ideal vertex V of P_0 and P_1 are the ones in Figure 3.1.

Since P_1 is tessellated by two copies of P_0, we have a tessellation of every facet of

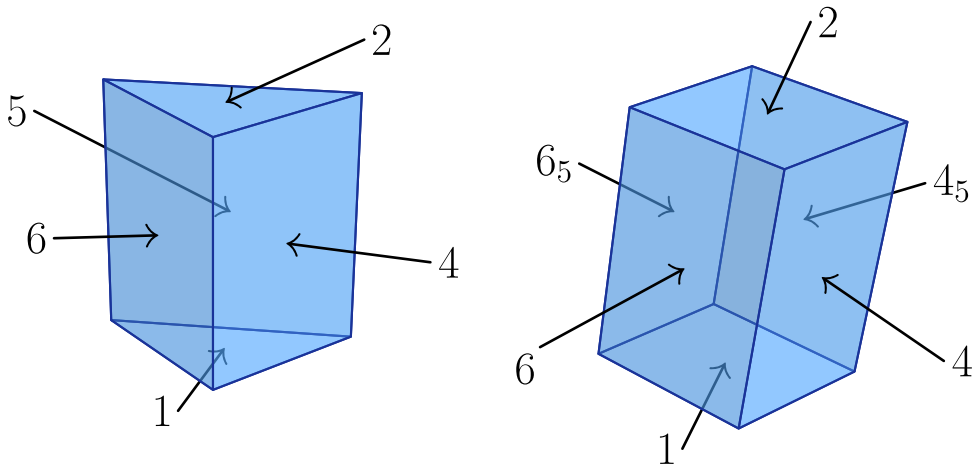

Figure 3.1: The link L_0 (left) and the link L_1 (right).

P_1 in one or two copies of a facet of P_0, and similarly for L_1 with L_0.

We collect some information on P_0 and P_1 via some pictures representing the facets of L_0 and L_1, respectively. The facets of L_0 and L_1 are represented in Figure 3.2. The meaning of these pictures is the following. Recall that L_1 is a right parallelepiped, so its facets are 6 rectangles. Each of these rectangles is tessellated by one or two copies of a facet of L_0. In the picture, each of such rectangles is tiled by some tiles (squares or triangles). Each tile also corresponds to a tile of the tessellation of a facet of P_1. In the picture, each tile contains the labels of the compact facets of P_1 that intersect the corresponding tile in P_1. To avoid writing the same label in two adjacent tiles, we put the label on the edge dividing them, like for instance the labels 3 and 7 of the facet **1**. Moreover, outside of the tiles we have written the labels of some non-compact facets of P_1. The label of a non-compact facet N is drawn near the edge of a tile if the corresponding tile in P_1 (a copy of a facet of P_0 in P_1) intersects N.

Remark 3.2.10. Since the link of the ideal vertex V of P_1 is a parallelepiped, we could take the small covers of the cube [FKS21, Section 3] to obtain three of the four desired reflectofolds (the ones with cusp section the 3-torus, the $\frac{1}{2}$-twist manifold and the Hantzsche-Wendt manifold). The problem is that these reflectofolds are not developable. Hence we will iteratively double the polytope until we find a polytope P such that we can glue P in order to obtain a 1-cusped, developable reflectofold with the desired cusp section.

For the other steps of the construction we will keep track of the following information on P_n:

(I1) the list of the facets;

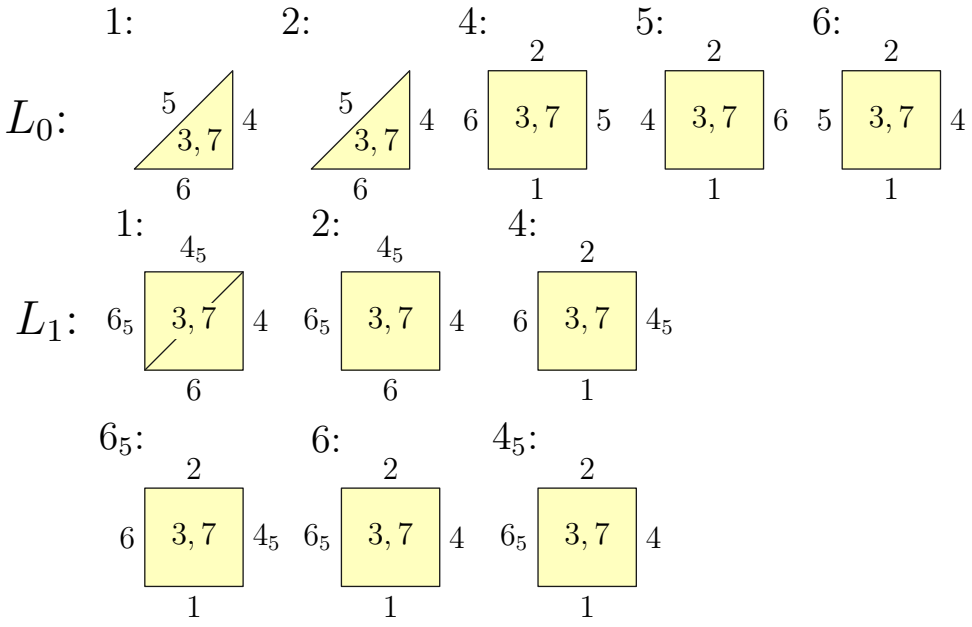

Figure 3.2: The facets of L_0 (top) and the facets of L_1 (bottom).

(I2) the adjacency graphs of the facets of type 3 and 7;

(I3) the picture of the facets of L_n tessellated and labelled with the previous convention.

Notation 3.2.11. We extend the notation given for Step 1 for the facets of P_1 to the facets of P_n. For example, we will see in Section 3.2.4 that $(r_4 \circ r_{r_5(4)} \circ r_2)(\mathbf{3})$ is a facet of P_4, and it will be denoted as $\mathbf{3}_{4,4_5,2}$. The convention will be similar for the other facets.

We will represent the adjacency graphs of the facets of type 3 and of type 7 of P_n separately, as follows. There is a vertex for each type-3 (respectively type-7) facet, and we connect two vertices with an edge with label k if the two facets meet with dihedral angle $\frac{\pi}{k}$ (including the case with $k = 2$). There is no edge joining two vertices of the graph if the two facets are at positive distance (they cannot be tangent at infinity since they are compact).

We will represent each adjacency graph via the associated adjacency matrix: in the entry corresponding to the vertices A and B we put 1 if $A = B$, we put 0 if there is no edge between them, and k if there is an edge with label k between them. For more clarity we omit the 0 in the entries.

Proposition 3.2.12. *If two facets of type i and j of P_n meet, with $i \neq j$, then the*

dihedral angle between them is the same of the one between the facets $\boldsymbol{i}$ *and* $\boldsymbol{j}$ *of* P_0*. In particular the facets* $\boldsymbol{i}$ *and* $\boldsymbol{j}$ *of* P_0 *meet.*

Proof. The polytope P_n is tessellated by some copies of P_0 and a facet of type k is tessellated by some copies of the facet $\boldsymbol{k}$ of P_0. Hence the facet A of type i and the facet B of type j of P_n meet in a copy of P_0. We deduce that the facets $\boldsymbol{i}$ and $\boldsymbol{j}$ of P_0 meet and the dihedral angle between them is the same of the dihedral angle between A and B. □

Remark 3.2.13. If $n \geq 1$, then the link L_n is a right parallelepiped. Indeed, L_1 is a right parallelepiped, at every step we double P_n along a non-compact facet, and P_n has exactly one ideal vertex. In particular, for every couple of non-compact facets of P_n that meet, the corresponding dihedral angle is $\frac{\pi}{2}$.

Corollary 3.2.14. *If* $n \geq 1$*, every facet of* P_n *that is not of type* 3 *or* 7 *is non-compact and admissible.*

Proof. Since 3 and 7 are the only compact facets of P_0, every facet of a different type from 3 and 7 in P_n is non-compact.

We show that every non-compact facet is admissible. Let A be a non-compact type-i facet of P_n. Let B be another facet of P_n that meets A. If B is non-compact, then by Remark 3.2.13 the dihedral angle between them is $\frac{\pi}{2}$. If B is compact, then A and B have different type. Hence, by Proposition 3.2.12 the dihedral angle between them is $\frac{\pi}{2k}$ for some k, since this is true for every couple of facets of P_0 that meet. □

3.2.3 The information on the polytopes

In this section we will state three propositions that will allow to recover the needed information (I1), (I2), (I3) on P_{n+1} starting from that of P_n, for $n \geq 1$.

Recall that P_{n+1} will be the double of P_n along a non-compact, admissible facet called F_n.

Proposition 3.2.15. *If* $n \geq 1$*, the information (I1) on* P_{n+1} *is obtained from the one on* P_n *as follows.*

For every facet $G \neq F_n$ *in the list (I1) of* P_n*:*

- *If the label* G *is in the picture of* F_n *in (I3) of* P_n*:*
  - *if* G *is of the same type as* F_n*, then add* G *to the list (I1) of* P_{n+1}*;*

- *if G and F_n are respectively of type i and j with $i \neq j$ and in the Coxeter diagram of P_0 there is not an edge between the vertices i and j, then add G to the list (I1) of P_{n+1};*
- *otherwise add G and $r_{F_n}(G)$ to the list (I1) of P_{n+1}.*

- *otherwise add G and $r_{F_n}(G)$ to the list (I1) of P_{n+1}.*

Proof. We divide the proof in the same cases of the statement.

- The label G is in the picture of F_n if and only if the facet G meets F_n in P_n.
  - If G is of the same type of F_n, then the two facets are both non-compact, hence by Remark 3.2.13 the dihedral angle between them is $\frac{\pi}{2}$. Hence $G \cup r_{F_n}(G)$ is a facet of P_{n+1}, that we call G. Hence we add G to the list.
  - If G and F_n are of type i and j, respectively, with $i \neq j$, then by Proposition 3.2.12 the dihedral angle between the two facets is the same dihedral angle between the facets $\boldsymbol{i}$ and $\boldsymbol{j}$ of P_0. There is no edge between the vertices i and j if and only if the dihedral angle between the facets $\boldsymbol{i}$ and $\boldsymbol{j}$ of P_0 is $\frac{\pi}{2}$. In this case $G \cup r_{F_n}(G)$ is a facet of P_{n+1}, that we call G. Hence we add G to the list.
  - Otherwise, if F_n and G are of type i and j, respectively, with $i \neq j$, and there is an edge between the vertices i and j, then by Proposition 3.2.12 the dihedral angle between G and F_n is $\frac{\pi}{k}$, with $k \neq 2$; hence we have two facets of P_{n+1} named G and $r_{F_n}(G)$. Hence we add G and $r_{F_n}(G)$ to the list.
- Otherwise, if the label G is not in the picture in (I3) of P_n, then the facets G and F_n of P_n do not meet. Hence we have two facets of P_{n+1} named G and $r_{F_n}(G)$.

In this way we have listed all the facets of P_{n+1}. Indeed the union of all the listed facets is equal to the union of all facets of P_n and of $r_{F_n}(P_n)$, minus the facet F_n. □

Notation 3.2.16. In the following, if two vertices F and G of a graph are joined by an edge with label k, we denote this edge by $(F, G; k)$.

Proposition 3.2.17. *If $n \geq 1$, the information (I2) on P_{n+1} is obtained from the one on P_n as follows.*

The vertices of the two graphs of type 3 and 7 are the facets of type 3 and 7 in (I1) of P_{n+1}, respectively. The edges of the graphs are obtained as follows.

- *If in (I2) of P_n we have (F,G;k) then:*

- *If in (I1) of P_{n+1} we have $F, r_{F_n}(F), G, r_{F_n}(G)$, then in (I2) of P_{n+1} we add the edges $(F, G; k)$ and $(r_{F_n}(F), r_{F_n}(G); k)$;*
- *If in (I1) of P_{n+1} we have $F, r_{F_n}(F), G$ and not $r_{F_n(G)}$, then in (I2) of P_{n+1} we add the edges $(F, G; k)$ and $(r_{F_n}(F), G; k)$;*
- *If in (I1) we have F, G and not $r_{F_n}(F), r_{F_n}(G)$, then in (I2) of P_{n+1} we add $(F, G; k)$.*

- *Let F be a type-3 (or type-7) facet of P_{n+1}. If in (I1) of P_{n+1} we have F and $r_{F_n}(F)$, the label F is in the picture of the facet F_n of L_n in (I3) of P_n, the facet F is of type i, the facet F_n is of type j and the label of the edge between i and j in the Coxter diagram of P_0 is $2k$, then in (I2) of P_{n+1} we add $(F, r_{F_n}(F); k)$.*

Proof. We divide the proof in the same cases of the statement.

The vertices of the two graphs are the facets of type 3 and 7 in the list of facets (I1) of P_{n+1} by definition.

- If in (I2) of P_n we have $(F, G; k)$, then it means that the dihedral angle between the facets F and G of P_n is $\frac{\pi}{k}$. The proof of each of the three subcases of the thesis is obvious, once noted that $r_{F_n}(G)$ is not in (I1) of P_{n+1} if and only if $(G, \frac{\pi}{2}) \in I_n(F_n)$, and this holds if and only if $G \cup r_{F_n}(G)$ is a facet of P_{n+1} that we call G.
- Since the label F is in the picture of F_n in (I3) of P_n, the facet F meets F_n in P_n. Since in the Coxeter diagram of P_0 the edge between i and j has label $2k > 2$, by Proposition 3.2.12, the dihedral angle between F and F_n is $\frac{\pi}{2k}$. Hence the dihedral angle between F and $r_{F_n}(F)$ in P_{n+1} is $\frac{\pi}{k}$. Hence we add the edge $(F, r_{F_n}(F); k)$ to the graph.

By construction of P_{n+1}, there is no other edge to be added to the two graphs. □

Proposition 3.2.18. *If $n \geq 1$, the information (I3) on P_{n+1} is obtained from the one on P_n as follows.*

Let $G \neq F_n$ be a facet of L_n.

- *If the picture of G does not contain the label F_n, then in P_{n+1} add the pictures of the facets G and $r_{F_n}(G)$. For the picture of G of P_{n+1} we copy the one of P_n. For the picture of $r_{F_n}(G)$ of P_{n+1} we copy the picture of G of P_n and, for every facet F such that $r_{F_n}(F)$ is in (I1) of P_{n+1}, we replace the label F with $r_{F_n}(F)$. (An example is shown in Figure 3.3.)*

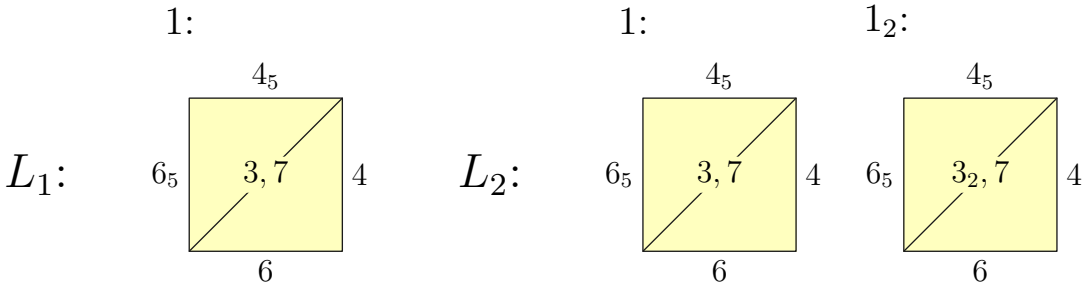

Figure 3.3: The facet 1 of L_1 (left) and the facets 1 and 1_2 of L_2 (right).

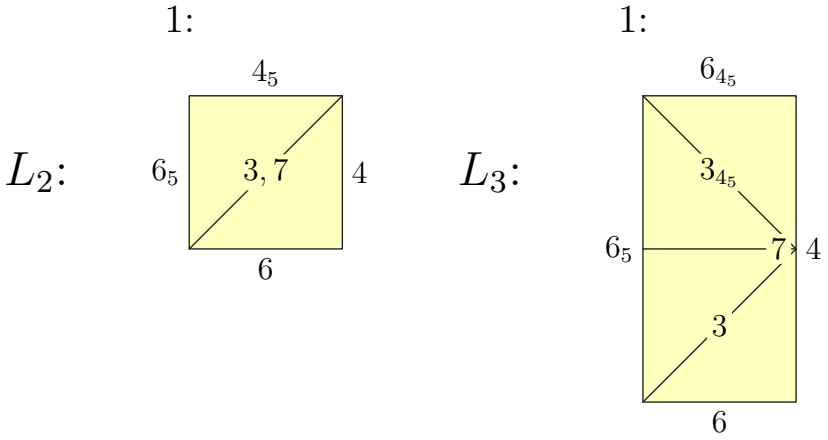

Figure 3.4: The facet 1 of L_2 (left) and the facet 1 of L_3 (right).

- *If the picture of G has the label F_n near one edge, then in P_{n+1} we add a picture of G that is the double of the picture of G of P_n along the edge with label F_n, without reporting any label. Outside of the picture, near the edge that was present also in P_n we put the same label, say K. Near the two edges that we doubled, we put the same label as before of doubling. Near the last edge, we put $r_{F_n}(K)$. The picture is tessellated in two copies C_1 and C_2 of the picture G of P_n. In the copy C_1 corresponding to the one in P_n we copy the labels inside the picture of G in L_n. In the other copy C_2, we put the same labels, in a way that the resulting labels are symmetric with respect to the edge along which we doubled the picture, and now, for every label K in C_2, if $r_{F_n}(K)$ is in (I1) of P_{n+1}, we replace K with $r_{F_n}(K)$. (An example is shown in Figure 3.4.)*

Proof. We divide the proof in the same cases of the statement, as for the previous two propositions.

- If the picture of G does not contain the label F_n, the facets G and F_n do not meet in P_n, hence in P_{n+1} we have the facets G and $r_{F_n}(G)$. Clearly $I_n(G) = I_{n+1}(G)$ and, given a tile K of the tessellation of G, we also have $I_n(K) = I_{n+1}(K)$ (with a little abuse, since K is not a facet). Moreover, $r_{F_n}(G)$ is a copy of G in $r_{F_n}(P_n)$. Hence the picture of $r_{F_n}(G)$ is the same of the picture of G, but if the label M is present in G and there is a facet $r_{F_n}(M)$ in P_{n+1}, then in $r_{F_n}(G)$ we replace the label M with $r_{F_n}(M)$.
- If G has the label F_n near one edge, it means that the facets G and F_n meet in P_n. Since they are both non-compact, by Remark 3.2.13 the corresponding dihedral angle is $\frac{\pi}{2}$. Hence in P_{n+1} there is a facet $G^{n+1} = G^n \cup r_{F_n}(G^n)$ (we are using the same notation of the proof of Proposition 3.2.12). The picture of the facet G of L_{n+1} is obtained doubling the picture of G of L_n along the edge with label F_n.

□

3.2.4 The construction

We are now ready to build our sequence of polytopes.

Recall that we want $P_{n+1} = P_n \cup r_{F_n}(P_n)$, where F_n is a non-compact and admissible facet of P_n. For every n we are going to choose as F_n a facet of different type from 3 and 7. Such a facet is non-compact and admissible in P_0 since the only compact facets are **3** and **7**, and every facet of P_0 is admissible. For every $n \geq 1$ such a facet is non-compact and admissible by Corollary 3.2.14.

Definition 3.2.19. We define the following polytopes: $P_1 = P_0 \cup r_5(P_0)$, $P_2 = P_1 \cup r_2(P_1)$, $P_3 = P_2 \cup r_{4_5}(P_2)$, $P_4 = P_3 \cup r_4(P_3)$, $P_5 = P_4 \cup r_1(P_4)$, $P_6 = P_5 \cup r_6(P_5)$, $P_7 = P_6 \cup r_{6_5}(P_6)$, $P_8 = P_7 \cup r_{1_2}(P_7)$.

We have already shown in Section 3.2.2 the information on P_1 and we report them in the following.

(I1) Facets of P_1: $1, 2, 3, 4, 4_5, 6, 6_5, 7$.

(I2) Adjacency matrices of facets of type 3 and 7 are in Table 6.2. They are clearly two 1×1 matrices, both with the entry 1. (Recall that on the left side of the matrices we put the names of the facets.)

(I3) The pictures of the facets of L_1 are in Figure 3.2.

Proposition 3.2.20. *The information (I1) on P_n, for $n = 0, \ldots, 8$, is the following.*

P_0 : $1, 2, 3, 4, 5, 6, 7$*;*

P_1 : $1, 2, 3, 4, 4_5, 6, 6_5, 7$*;*

P_2 : $1, 1_2, 3, 3_2, 4, 4_5, 6, 6_5, 7$;

P_3 : $1, 1_2, 3, 3_{4_5}, 3_2, 3_{4_5,2}, 4, 6, 6_{4_5}, 6_5, 7$

P_4 : $1, 1_2, 3, 3_4, 3_{4_5}, 3_{4,4_5}, 3_2, 3_{4,2}, 3_{4_5,2}, 3_{4,4_5,2}, 4, 6, 6_{4_5}, 6_5, 6_{4,5}, 7$;

P_5 : $1_2, 1_{1,2}, 3, 3_4, 3_{4_5}, 3_{4,4_5}, 3_2, 3_{1,2}, 3_{4,2}, 3_{1,4,2}, 3_{4_5,2}, 3_{1,4_5,2}, 3_{4,4_5,2}, 3_{1,4,4_5,2}, 6, 6_{4_5}, 6_5, 6_{4,5}, 7, 7_1$;

P_6 : $1_2, 1_{1,2}, 3, 3_4, 3_{4_5}, 3_{6,4_5}, 3_{4,4_5}, 3_{6,4,4_5}, 3_2, 3_{1,2}, 3_{4,2}, 3_{1,4,2}, 3_{4_5,2}, 3_{6,4_5,2}, 3_{1,4_5,2}, 3_{6,1,4_5,2}, 3_{4,4_5,2}, 3_{6,4,4_5,2}, 3_{1,4,4_5,2}, 3_{6,1,4,4_5,2}, 6_{4_5}, 6_{6,4_5}, 6_5, 6_{4,5}, 7, 7_6, 7_1, 7_{6,1}$;

P_7 : $1_2, 1_{1,2}, 3, 3_4, 3_{6_5,4}, 3_{4_5}, 3_{6,4_5}, 3_{4,4_5}, 3_{6_5,4,4_5}, 3_{6,4,4_5}, 3_{6_5,6,4,4_5}, 3_2, 3_{1,2}, 3_{4,2}, 3_{6_5,4,2}, 3_{1,4,2}, 3_{6_5,1,4,2}, 3_{4_5,2}, 3_{6,4_5,2}, 3_{1,4_5,2}, 3_{6,1,4_5,2}, 3_{4,4_5,2}, 3_{6_5,4,4_5,2}, 3_{6,4,4_5,2}, 3_{6_5,6,4,4_5,2}, 3_{1,4,4_5,2}, 3_{6_5,1,4,4_5,2}, 3_{6,1,4,4_5,2}, 3_{6_5,6,1,4,4_5,2}, 6_{4_5}, 6_{6,4_5}, 6_{4,5}, 6_{6_5,4,5}, 7, 7_{6_5}, 7_6, 7_{6_5,6}, 7_1, 7_{6_5,1}, 7_{6,1}, 7_{6_5,6,1}$;

P_8 : $1_{1,2}, 1_{1_2,1,2}, 3, 3_{1_2}, 3_4, 3_{1_2,4}, 3_{6_5,4}, 3_{1_2,6_5,4}, 3_{4_5}, 3_{1_2,4_5}, 3_{6,4_5}, 3_{1_2,6,4_5}, 3_{4,4_5}, 3_{1_2,4,4_5}, 3_{6_5,4,4_5}, 3_{1_2,6_5,4,4_5}, 3_{6,4,4_5}, 3_{1_2,6,4,4_5}, 3_{6_5,6,4,4_5}, 3_{1_2,6_5,6,4,4_5}, 3_2, 3_{1,2}, 3_{1_2,1,2}, 3_{4,2}, 3_{6_5,4,2}, 3_{1,4,2}, 3_{1_2,1,4,2}, 3_{6_5,1,4,2}, 3_{1_2,6_5,1,4,2}, 3_{4_5,2}, 3_{6,4_5,2}, 3_{1,4_5,2}, 3_{1_2,1,4_5,2}, 3_{6,1,4_5,2}, 3_{1_2,6,1,4_5,2}, 3_{4,4_5,2}, 3_{6_5,4,4_5,2}, 3_{6,4,4_5,2}, 3_{6_5,6,4,4_5,2}, 3_{1,4,4_5,2}, 3_{1_2,1,4,4_5,2}, 3_{6_5,1,4,4_5,2}, 3_{1_2,6_5,1,4,4_5,2}, 3_{6,1,4,4_5,2}, 3_{1_2,6,1,4,4_5,2}, 3_{6_5,6,1,4,4_5,2}, 3_{1_2,6_5,6,1,4,4_5,2}, 6_{4_5}, 6_{6,4_5}, 6_{4,5}, 6_{6_5,4,5}, 7, 7_{1_2}, 7_{6_5}, 7_{1_2,6_5}, 7_6, 7_{1_2,6}, 7_{6_5,6}, 7_{1_2,6_5,6}, 7_1, 7_{1_2,1}, 7_{6_5,1}, 7_{1_2,6_5,1}, 7_{6,1}, 7_{1_2,6,1}, 7_{6_5,6,1}, 7_{1_2,6_5,6,1}$.

Proof. The information on P_0 can be easily recovered from the definition of P_0 and we have already shown the information on P_1.

We recover the information on P_{n+1}, for $n \geq 1$, from the information on P_n and the Coxeter diagram on P_0, using Proposition 3.2.15.

We now describe in detail how to recover the information on P_2. The reader is invited to check the information on the other polytopes in the same way.

The label 1 is not in the picture of the facet 2 in (I3) of P_1, hence we add 1 and 1_2 to the list of facets (I1) of P_2.

The label 3 is in the picture of the facet 2 in (I3) of P_1. Moreover the facets **2** and **3** are of different type and there is an edge between the corresponding vertices in the Coxeter diagram of P_0 (see the diagram in Section 3.2.1). Hence we add 3 and 3_2 to the list of facets of P_2.

The label 4 is in the picture of the facet 2 in (I3) of P_1. Moreover the facets **2** and **3** are of different type and there is not an edge between the corresponding vertices in the Coxeter diagram of P_0. Hence we add 4 to the list of facets of P_2. The same holds for the remaining facets $(\mathbf{4}_5, \mathbf{6}, \mathbf{6}_5, \mathbf{7})$ distinct to **2** of P_1.

We obtained that the list of facets of P_2 is $1, 1_2, 3, 3_2, 4, 4_5, 6, 6_5, 7$. □

Proposition 3.2.21. *The information (I2) on P_n, for $n = 0, \dots, 8$ is in Tables 6.1, …, 6.9.*

Proof. As for the previous proposition, we only describe in detail how to recover the information on P_2 using Proposition 3.2.17.

The vertices of the two adjacency graphs of P_2 are the facets of type 3 or 7 in (I1) of P_2: $3, 3_2$ and 7. The two graphs in (I2) of P_1 have no edge. We have 3 and 3_2 in (I1) of P_2, the label 3 is in the picture of the facet **2** in (I3) of P_1, the facet **3** is of type 3, the facet **2** is of type 2 and the label of the edge between 3 and 2 in the Coxeter diagram of P_0 is 4. Hence we add an edge with label 2 between the vertices 3 and 3_2.

We obtained that the two adjacency matrices of P_2 are the ones in Table 6.3. □

Proposition 3.2.22. *The information (I3) on P_n, for $n = 0, \dots, 8$, is in Figure 3.2 and in Figures 6.1, …, 6.14.*

Proof. As for the previous two propositions, we only describe in detail how to recover the information on P_2 using Proposition 3.2.18.

The picture in (I3) of P_1 of the facet **1** of L_1 does not contain the label 2. Hence we add the the first two pictures of Figure 6.1. The pictures in (I3) of P_1 of the facets $\mathbf{4}, \mathbf{4}_5, \mathbf{6}, \mathbf{6}_5$ of L_1 contain the label 2. Hence we add the latter four pictures of Figure 6.1. □

3.3 The reflectofolds

In this section we glue the facets of the polytopes P_7 and P_8 in order to obtain some 1-cusped developable reflectofolds. In Section 3.3.1 we perform the gluing. Then, in Section 3.3.2 we study the facets and the corners of the constructed spaces, in order to show, in Section 3.3.3, that they are 1-cusped developable reflectofolds.

3.3.1 Defining the reflectofolds

The link L_7 of the ideal vertex of P_7 is a right parallelepiped. If we glue L_7 as described in Figure 3.5, in each of the three cases we obtain a flat 3-manifold: the 3-torus, the $\frac{1}{2}$-twist manifold and the $\frac{1}{4}$-twist manifold, respectively [Mar23, Figure 12.2].

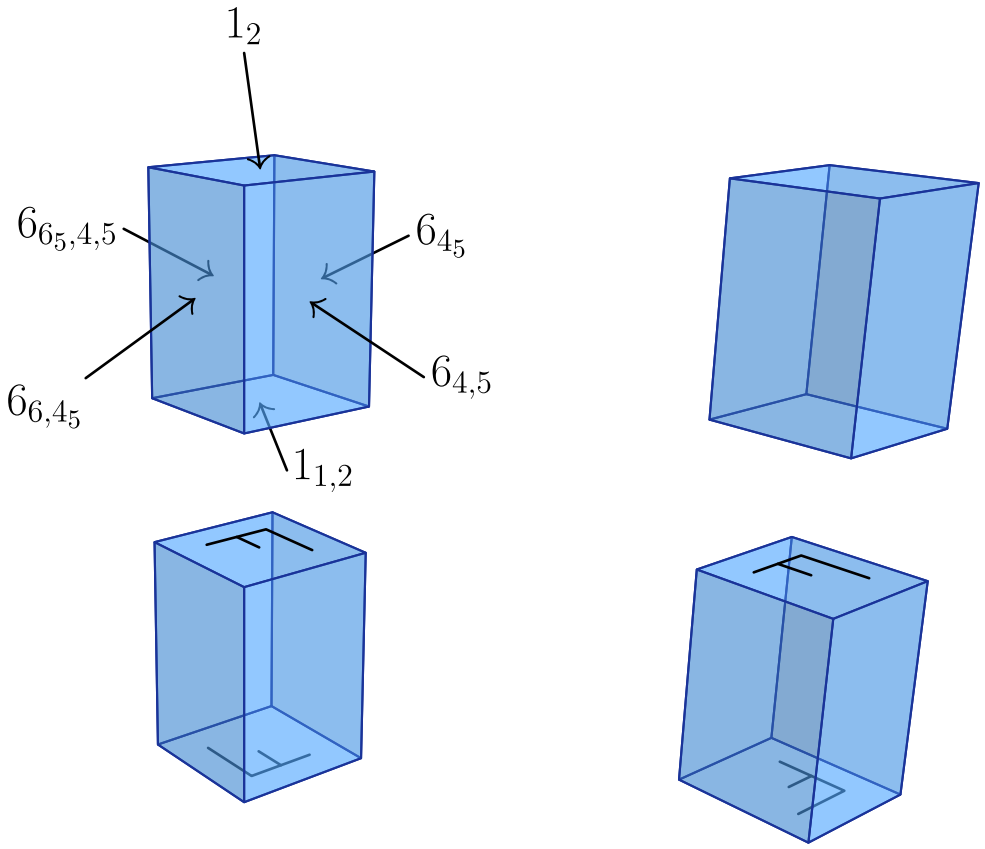

Figure 3.5: The link L_7 (top-left), the 3-torus (top-right), the $\frac{1}{2}$-twist manifold (bottom-left), the $\frac{1}{4}$-twist manifold (bottom-right). In the last three pictures, if two opposite facets do not have a letter inside, we glue them with a translation, otherwise we glue them as indicated with the letters.

We now show that, for each of the three manifolds, we can glue P_7 using isometries between the facets in a way that this induces a gluing of L_7 as described.

Let R_T be the space obtained from P_7 by gluing the facet 6_{4_5} with $6_{6,4_5}$ using the isometry $r_6|_{6_{4_5}}$, the facet $6_{4,5}$ with $6_{6_5,4,5}$ using the isometry $r_{6_5}|_{6_{4,5}}$, and the facet 1_2 with $1_{1,2}$ using the isometry $r_1|_{1_2}$. We have indeed $r_6(6_{4_5}) = 6_{6,4_5}$, $r_{6_5}(6_{4,5}) = 6_{6_5,4,5}$ and $r_1(1_2) = 1_{1,2}$. This can be seen from Figure 3.6 for L_7, and therefore it also holds for P_7 since each map is a reflection through a copy of a facet of P_0.

In the next cases the argument is analog to the one of R_T.

Definition 3.3.1. The space R_T is obtained from P_7 by gluing the facets via the following isometries:

$$r_6\big|_{6_{4_5}} : 6_{4_5} \to 6_{6,4_5}, \quad r_{6_5}\big|_{6_{4,5}} : 6_{4,5} \to 6_{6_5,4,5}, \quad r_1\big|_{1_2} : 1_2 \to 1_{1,2}.$$

Let $R_{\frac{1}{2}}$ be the space obtained from P_7 by gluing the facets via the following isometries:

$$r_6\big|_{6_{4_5}} : 6_{4_5} \to 6_{6,4_5} \quad r_{6_5}\big|_{6_{4,5}} : 6_{4,5} \to 6_{6_5,4,5}, \quad r_1 \circ r_6 \circ r_{6_5}\big|_{1_2} : 1_2 \to 1_{1,2}.$$

Let $R_{\frac{1}{4}}$ be the space obtained from P_7 by gluing the facets via the following isometries:

$$r_6\big|_{6_{4_5}} : 6_{4_5} \to 6_{6,4_5} \quad r_{6_5}\big|_{6_{4,5}} : 6_{4,5} \to 6_{6_5,4,5}, \quad r_1 \circ r_6 \circ r_5\big|_{1_2} : 1_2 \to 1_{1,2}.$$

We see from Figure 3.6 that each gluing induces a gluing of L_7 as in Figure 3.5, thus producing the 3-torus, the $\frac{1}{2}$-twist manifold and the $\frac{1}{4}$-twist manifold, respectively.

The link L_8 of the ideal vertex of P_8 is a right parallelepiped. If we glue L_8 as described in Figure 3.7, we obtain a flat 3-manifold, the Hantzsche-Wendt manifold [Mar23, Figure 12.2]. We now show that we can glue P_8 using isometries between the facets in a way that this induces the gluing of L_8 described in Figure 3.7.

We notice that the facet $6_{4,5}$ is divided in two parts, $6^U_{4,5}$ and $6^D_{4,5}$, as in Figure 3.7. Similarly, we define $6^U_{6_5,4,5}$ and $6^D_{6_5,4,5}$.

Definition 3.3.2. Let R_{HW} be the space obtained from P_8 by gluing the facets via the following isometries:

$$r_{1_2}\big|_{1_{1,2}} : 1_{1,2} \to 1_{1_2,1,2}, \quad r_{1_2} \circ r_{6_5} \circ r_6\big|_{6_{4_5}} : 6_{4_5} \to 6_{6,4_5},$$

$$r_6 \circ (r_1 \circ r_2)^2\big|_{6^U_{4,5}} : 6^U_{4,5} \to 6^D_{4,5}, \quad r_6 \circ (r_1 \circ r_2)^2\big|_{6^U_{6_5,4,5}} : 6^U_{6_5,4,5} \to 6^D_{6_5,4,5}$$

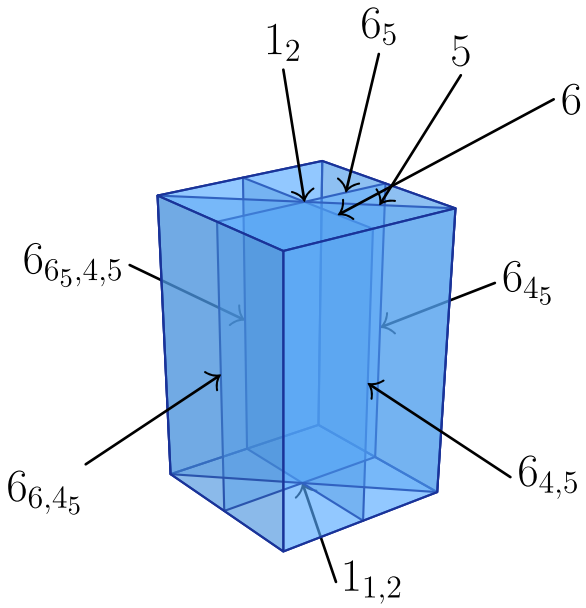

Figure 3.6: The link L_7 and the fixed planes of the reflections used to define $R_T, R_{\frac{1}{2}}, R_{\frac{1}{4}}$.

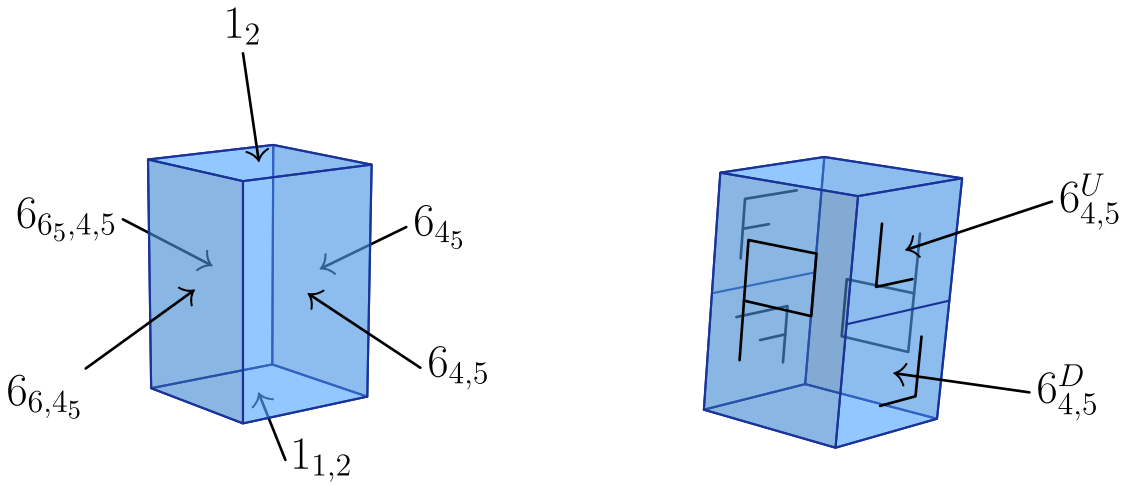

Figure 3.7: The link L_8 (left) and the Hantzsche-Wendt manifold (right), with the same notation of Figure 3.5. Moreover, we see how the facet $6_{4,5}$ is divided in the two parts $6^U_{4,5}$ and $6^D_{4,5}$. Similarly the facet $6_{6_5,4,5}$ is divided in the two parts $6^U_{6_5,4,5}$ and $6^D_{6_5,4,5}$

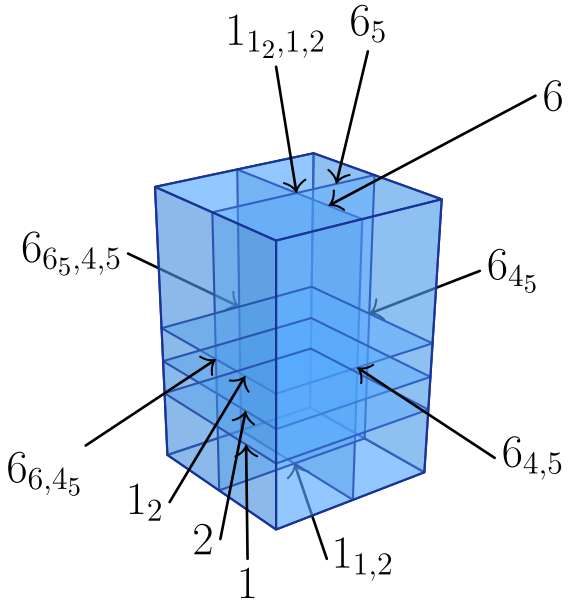

Figure 3.8: The link L_8 with the fixed planes of the reflections used to define R_{HW}.

We see from Figure 3.8 that this gluing induces the gluing of L_8 described in Figure 3.7.

Remark 3.3.3. Let f be one of the gluing maps used above for the polytope P_7. Then f is the restriction of a symmetry of P_7 that preserves its tessellation in copies of P_0. Indeed, we see from Figure 3.6 that $f(L_7) = L_7$, hence it easily follows that $f(P_7) = P_7$. Moreover, f is a composition of reflections along copies of facets of P_0. Hence it is a symmetry of P_7 and preserves the tessellation.

If f is a gluing map for the polytope P_8, the statement is slightly different. Indeed, if we consider the natural tessellation of $\mathbb{R}^3$ in copies of L_8, then f is induced by a symmetry of $\mathbb{R}^3$ that preserves its tesselletion in copies of L_0. The argument is analog to the previous case.

Let R be any of R_T, $R_{\frac{1}{2}}$, $R_{\frac{1}{4}}$, R_{HW}. The purpose of the following sections will be to prove this theorem.

Theorem 3.3.4. *The space R is an orientable, finite-volume, 1-cusped, developable reflectofold with compact, non-empty boundary. Moreover, the cusp of $R_T, R_{\frac{1}{2}}, R_{\frac{1}{4}}, R_{HW}$ has section the 3-torus, the $\frac{1}{2}$-twist manifold, the $\frac{1}{4}$-twist manifold, the Hantzsche-Wendt manifold, respectively.*

The proof of Theorem 1.1.1 will immediately follow from Theorem 3.3.4 and Corollary 3.1.4.

3.3.2 The facets and the corners

The purpose of this section is to study the facets and the corners of R. This will help us to prove Theorem 3.3.4 in the next section.

Let P be any of P_7 and P_8, and $p\colon P \to R$ denote the quotient map.
Lemma 3.3.5. *A facet of R is:*

- *either the image through p of a facet of type 7,*
- *or the image through p of a union of facets of type 3.*

We call the first facets of R *of type* 7 and the other facets *of type* 3.

Proof. Since we glued all the facets of different type from 3 and 7, the union of the facets of R is the image through p of the union of the facets of P of type 3 and 7.

If in P a facet of type 3 and a facet along which we glue meet, they do so with a dihedral angle of $\frac{\pi}{2}$. This is true by Proposition 3.2.12, since we glue facets that are of type 1 and 6 and in P_0 the facets **1** and **6** are orthogonal to **3**. Let A and B be two facets of P that are identified in R via the gluing. By Remark 3.3.3, if F and G are facets of P of type 3 or 7 such that $p(F \cap A) = p(G \cap B) \neq \emptyset$, then F and G are of the same type.

Let S_A and S_B be the sets of facets of P of type 3 that meet A and B, respectively. Then given $F \in S_A$, there exists $G \in S_B$ such that $p(F \cap A) = p(G \cap B)$. Then $p(F)$ and $p(G)$ are contained in the same facet of R (since we have already seen that the dihedral angle in P between F and A, and G and B, is $\frac{\pi}{2}$). Since the image through p of a facet is contained in a facet of R, we have shown that a facet of R is the image through p of a union of facets of the same type: either 7 or 3. It thus only remains to show that in the type-7 case such a facet is the image of exactly one facet of P.

If in P a facet of type 7 and a facet along which we glue meet, they do so with a dihedral angle different from $\frac{\pi}{2}$. Indeed this is true by Proposition 3.2.12, since we glue facets that are of type 1 and 6 and in P_0 the facets **1** and **6** are not orthogonal to **7**.

Hence for every type-7 facet M of P, we obtain that $p(M)$ is a facet of R. □

It will be easy to check that R satisfies (AC) and (EF) once we have found the corner graphs of type 3 or 7 of R.
Definition 3.3.6. For $i = 3, 7$, the *type-i corner graph* G_i of R is the graph whose vertices are the type-i facets of R and between two vertices A and B there is an edge for every corner in $A \cap B$. Moreover, we put a label $k \in \mathbb{N}$ on an edge if the

dihedral angle associated to the corresponding corner is $\frac{\pi}{k}$. If the angle is not in the form $\frac{\pi}{k}$ (this will never be the case), then we put the underlined angle as a label.

By Lemma 3.3.5 we already know the vertices of the type-7 corner graph of R.

We call a ridge of P *of type* (i,j) if it is the intersection of a facet of type i and a facet of type j. We call a corner of R *of type* (i,j) if it is contained in the intersection of two facets, one of type i and one of type j.

Lemma 3.3.7. *A corner of R is:*

- *either of type* $(3,3)$*, and in this case it is the image through p of a union of some type-*$(3,3)$ *ridges;*
- *either of type* $(7,7)$*, and in this case it is:*
  - *either the image through p of a type-*$(7,7)$ *ridge of P;*
  - *or the image through p of a type-*$(7,i)$ *ridge of P, with $i = 1, 6$;*
- *or of type* $(3,7)$*, and in this case it is the image through p of a type-*$(3,7)$ *ridge of P.*

Proof. Since the facets of R are of type 3 or 7, there are three kinds of corners in R: type $(3,3)$, $(7,7)$, and $(3,7)$.

By Proposition 3.2.12, if a facet of type 3 and a facet of type 1 or 6 of P meet, the dihedral angle between them is $\frac{\pi}{2}$. Hence the image through p of a type-$(3,i)$ ridge of P, with $i = 1, 6$, is contained in the relative interior of a type-3 facet. Hence the union of the type-$(3,3)$ corners of R is the image through p of the union of the type-$(3,3)$ ridges of P.

The image through p of a type-$(3,3)$ ridge is contained in a corner, hence every type-$(3,3)$ corner is the image through p of the union of some type-$(3,3)$ ridges.

Since by Lemma 3.3.5 the image through p of a facet of type 7 of P is a facet of type 7 of R, the image of a type-$(7,7)$, or type-$(3,7)$, ridge is a corner of R. Moreover, the image of a type-$(7,i)$ ridge, with $i = 1, 6$, is a type-$(7,7)$ corner. □

Let $3_X, 3_Y$ be two type-3 facets of P. Let us define the following equivalence relation: we set $3_X \sim 3_Y$ if $p(3_X)$ and $p(3_Y)$ are contained in the same facet of R. Moreover, the type-3 facets of R are in natural bijection with the equivalence classes. Indeed, $\overline{3_X} = \{3_{X_1}, \dots, 3_{X_k}\}$ is an equivalence class if and only if $\bigcup_{i=1}^{k} p(3_{X_i})$ is a facet of R.

Since by Lemma 3.3.5 the map p gives a correspondence between the type-7 facets of P and the type-7 facets of R, we will call the type-7 facets of R with the same

$\overline{3_{4,4_5,2}}$	$3_{4,4_5,2}$	$3_{6,4,4_5,2}$	$3_{6_5,6,4,4_5,2}$	$3_{6_5,4,4_5,2}$	$3_{1,4,4_5,2}$	$3_{6,1,4,4_5,2}$	$3_{6_5,1,4,4_5,2}$	$3_{6_5,6,1,4,4_5,2}$
$\overline{3_{4,2}}$	$3_{4,2}$	$3_{6_5,4,2}$	$3_{1,4,2}$	$3_{6_5,1,4,2}$				
$\overline{3_4}$	3_4	$3_{6_5,4}$						
$\overline{3_{4_5}}$	3_{4_5}	$3_{6,4_5}$						
$\overline{3_2}$	3_2	$3_{1,2}$						
$\overline{3_{4,4_5}}$	$3_{4,4_5}$	$3_{6,4,4_5}$	$3_{6_5,4,4_5}$	$3_{6_5,6,4,4_5}$				
$\overline{3_{4_5,2}}$	$3_{4_5,2}$	$3_{6,4_5,2}$	$3_{1,4_5,2}$	$3_{6,1,4_5,2}$				
$\overline{3}$	3							

Table 3.1: The equivalence classes of the type-3 facets of R_T and $R_{\frac{1}{2}}$. We write the equivalence classes in the left column, while the elements of the classes appear on the right.

$\overline{3_{4,4_5,2}}$	$3_{4,4_5,2}$	$3_{6,4,4_5,2}$	$3_{6_5,6,4,4_5,2}$	$3_{6_5,4,4_5,2}$	$3_{1,4,4_5,2}$	$3_{6,1,4,4_5,2}$	$3_{6_5,1,4,4_5,2}$	$3_{6_5,6,1,4,4_5,2}$
$\overline{3_{4,2}}$	$3_{4,2}$	$3_{6_5,4,2}$	$3_{1,4_5,2}$	$3_{6,1,4_5,2}$				
$\overline{3_4}$	3_4	$3_{6_5,4}$						
$\overline{3_{4_5}}$	3_{4_5}	$3_{6,4_5}$						
$\overline{3_2}$	3_2	$3_{1,2}$						
$\overline{3_{4,4_5}}$	$3_{4,4_5}$	$3_{6,4,4_5}$	$3_{6_5,4,4_5}$	$3_{6_5,6,4,4_5}$				
$\overline{3_{4_5,2}}$	$3_{4_5,2}$	$3_{6,4_5,2}$	$3_{1,4,2}$	$3_{6_5,1,4,2}$				
$\overline{3}$	3							

Table 3.2: The equivalence classes of the type-3 facets of $R_{\frac{1}{4}}$.

name of the ones of P. Instead we will call the type-3 facets of R with the same name of the equivalence classes.

Lemma 3.3.8. *The equivalence classes of R_T are described in Table 3.1. The type-$(7,7)$ corners of R_T that are the images through p of the type-$(7,i)$ ridges, with $i = 1, 6$, of the polytope P_7 are listed in Table 3.4.*

Proof. We divide the proof by analyzing each gluing of the polytope P_7 separately.

- $6_{4,5}$ and $6_{6_5,4,5}$: We refer to Figure 6.8 and 3.14 for the information (I3) on these two facets and the way to glue them. The latter figure is not necessary, since we can deduce its content from Figures 3.5, but it helps the reader to check the results.

$\overline{3_{4,4_5,2}}$	$3_{4,4_5,2}$	$3_{6_5,1,4,4_5,2}$	$3_{1_2,6_5,1,4,4_5,2}$	$3_{6_5,6,4,4_5,2}$	$3_{6,1,4,4_5,2}$	$3_{1_2,6,1,4,4_5,2}$
$\overline{3_{1,4_5,2}}$	$3_{1,4_5,2}$	$3_{1_2,1,4_5,2}$	$3_{6,1,4_5,2}$	$3_{1_2,6,1,4_5,2}$		
$\overline{3_{1,4,4_5,2}}$	$3_{1,4,4_5,2}$	$3_{1_2,1,4,4_5,2}$	$3_{6,4,4_5,2}$	$3_{6_5,6,1,4,4_5,2}$	$3_{6_5,4,4_5,2}$	$3_{1_2,6_5,6,1,4,4_5,2}$
$\overline{3_{1,2}}$	$3_{1,2}$	$3_{1_2,1,2}$				
$\overline{3_{4,2}}$	$3_{4,2}$	$3_{1,4,2}$	$3_{1_2,1,4,2}$			
$\overline{3_{4,4_5}}$	$3_{4,4_5}$	$3_{1_2,6,4,4_5}$	$3_{6_5,4,4_5}$	$3_{1_2,6_5,6,4,4_5}$		
$\overline{3_4}$	3_4	$3_{1_2,4}$				
$\overline{3_{6,4,4_5}}$	$3_{6,4,4_5}$	$3_{1_2,4,4_5}$	$3_{1_2,6_5,4,4_5}$	$3_{6_5,6,4,4_5}$		
$\overline{3_{6_5,4}}$	$3_{6_5,4}$	$3_{1_2,6_5,4}$				
$\overline{3_{6,4_5}}$	$3_{6,4_5}$	$3_{1_2,4_5}$				
$\overline{3_{4_5,2}}$	$3_{4_5,2}$	$3_{6,4_5,2}$				
$\overline{3_{4_5}}$	3_{4_5}	$3_{1_2,6,4_5}$				
$\overline{3_{6_5,4,2}}$	$3_{6_5,4,2}$	$3_{1_2,6_5,1,4,2}$	$3_{6_5,1,4,2}$			
$\overline{3}$	3					
$\overline{3_{1_2}}$	3_{1_2}					
$\overline{3_2}$	3_2					

Table 3.3: The equivalence classes of the type-3 facets of R_{HW}.

$7 \cap_3 7_{6_5}$	$7_1 \cap_3 7_{6_5,1}$	$7_6 \cap_3 7_{6_5,6}$	$7_{6,1} \cap_3 7_{6_5,6,1}$	$7 \cap_3 7_6$	$7_1 \cap_3 7_{6,1}$
$7_{6_5} \cap_3 7_{6_5,6}$	$7_{6_5,1} \cap_3 7_{6_5,6,1}$	$7 \cap_2 7_1$	$7_6 \cap_2 7_{6,1}$	$7_{6_5} \cap_2 7_{6_5,1}$	$7_{6_5,6} \cap_2 7_{6_5,6,1}$

Table 3.4: The type-$(7,7)$ corners of R_T that are the images through p of the type-$(7,i)$ ridges, with $i = 1, 6$, of the polytope P_7. We write $7_X \cap_k 7_Y$ to indicate a corner between the facets 7_X and 7_Y with angle $\frac{\pi}{k}$.

$7 \cap_3 7_{6_5}$	$7_1 \cap_3 7_{6_5,1}$	$7_6 \cap_3 7_{6_5,6}$	$7_{6,1} \cap_3 7_{6_5,6,1}$	$7 \cap_3 7_6$	$7_1 \cap_3 7_{6,1}$
$7_{6_5} \cap_3 7_{6_5,6}$	$7_{6_5,1} \cap_3 7_{6_5,6,1}$	$7 \cap_2 7_{6_5,6,1}$	$7_1 \cap_2 7_{6_5,6}$	$7_{6_5} \cap_2 7_{6,1}$	$7_{6_5,1} \cap_2 7_6$

Table 3.5: The type-$(7,7)$ corners of $R_{\frac{1}{2}}$ that are the images through p of the type-$(7,i)$ ridges, with $i = 1, 6$, of the polytope P_7.

$7 \cap_3 7_{6_5}$	$7_1 \cap_3 7_{6_5,1}$	$7_6 \cap_3 7_{6_5,6}$	$7_{6,1} \cap_3 7_{6_5,6,1}$	$7 \cap_3 7_6$	$7_1 \cap_3 7_{6,1}$
$7_{6_5} \cap_3 7_{6_5,6}$	$7_{6_5,1} \cap_3 7_{6_5,6,1}$	$7 \cap_2 7_{6,1}$	$7_6 \cap_2 7_{6_5,6,1}$	$7_{6_5} \cap_2 7_1$	$7_{6_5,6} \cap_2 7_{6_5,1}$

Table 3.6: The type-$(7,7)$ corners of $R_{\frac{1}{4}}$ that are the images through p of the type-$(7,i)$ ridges, with $i = 1, 6$, of the polytope P_7.

$7 \cap_3 7_{1_2,6,1}$	$7_{1_2,1} \cap_3 7_6$	$7_1 \cap_3 7_{1_2,6}$	$7_{1_2} \cap_3 7_{6,1}$	$7_{6_5} \cap_3 7_{1_2,6_5,6,1}$
$7_{1_2,6_5,1} \cap_3 7_{6_5,6}$	$7_{1_2,6_5,6} \cap_3 7_{6_5,1}$	$7_{1_2,6_5} \cap_3 7_{6_5,6,1}$	$7_{1_2,6_5,1} \cap_3 7_{6,1}$	$7_{1_2,1} \cap_3 7_{6_5,6,1}$
$7_{1_2,6_5} \cap_3 7_6$	$7_{1_2} \cap_3 7_{6_5,6}$	$7_{6_5} \cap_3 7_{1_2,6}$	$7 \cap_3 7_{1_2,6_5,6}$	$7_{6_5,1} \cap_3 7_{1_2,6,1}$
$7_1 \cap_3 7_{1_2,6_5,6,1}$	$7_{6_5,1} \cap_2 7_{1_2,6_5,1}$	$7_1 \cap_2 7_{1_2,1}$	$7_{6_5,6,1} \cap_2 7_{1_2,6_5,6,1}$	$7_{6,1} \cap_2 7_{1_2,6,1}$

Table 3.7: The type-$(7,7)$ corners of R_{HW} that are the images through p of the type-$(7,i)$ ridges, with $i = 1, 6$, of the polytope P_8.

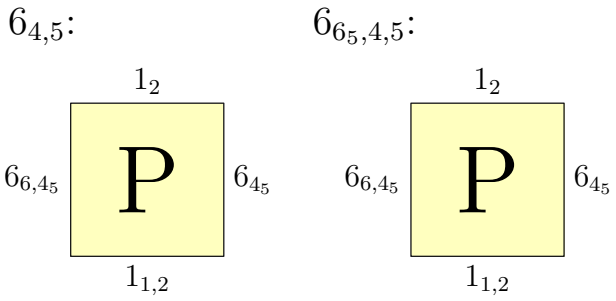

Figure 3.9: The way to glue the facets $6_{4,5}$ and $6_{6_5,4,5}$ of L_7.

Hence we see that:

$$3_{6,4,4_5,2} \sim 3_{6_5,6,4,4_5,2}; \quad 3_{4,2} \sim 3_{6_5,4,2}; \quad 3_{4,4_5,2} \sim 3_{6_5,4,4_5,2};$$
$$3_{6,4,4_5} \sim 3_{6_5,6,4,4_5}; \quad 3_4 \sim 3_{6_5,4}; \quad 3_{4,4_5} \sim 3_{6_5,4,4_5};$$
$$3_{6,1,4,4_5,2} \sim 3_{6_5,6,1,4,4_5,2}; \quad 3_{1,4,2} \sim 3_{6_5,1,4,2}; \quad 3_{1,4,4_5,2} \sim 3_{6_5,1,4,4_5,2}.$$

Moreover, both $6_{4,5}$ and $6_{6_5,4,5}$ meet 4 facets of type 7, with a dihedral angle of $\frac{\pi}{6}$ by Proposition 3.2.12 (since in P_0 the dihedral angle between 6 and 7 is $\frac{\pi}{6}$). Hence, in R, from the picture we notice that there are the following corners with angle $\frac{2\pi}{6} = \frac{\pi}{3}$.

$$7 \cap_3 7_{6_5}; \quad 7_1 \cap_3 7_{6_5,1}; \quad 7_6 \cap_3 7_{6_5,6}; \quad 7_{6,1} \cap_3 7_{6_5,6,1}.$$

- 6_{4_5} and $6_{6,4_5}$: We refer to Figures 6.9 and 3.15. The same argument as before leads to the following:

$$3_{4,4_5,2} \sim 3_{6,4,4_5,2}; \quad 3_{4_5,2} \sim 3_{6,4_5,2}; \quad 3_{6_5,4,4_5,2} \sim 3_{6_5,6,4,4_5,2};$$
$$3_{4,4_5} \sim 3_{6,4,4_5}; \quad 3_{1,4,4_5,2} \sim 3_{6,1,4,4_5,2}; \quad 3_{1,4_5,2} \sim 3_{6,1,4_5,2};$$
$$3_{6_5,1,4,4_5,2} \sim 3_{6_5,6,1,4,4_5,2}; \quad 3_{4_5} \sim 3_{6,4_5}; \quad 3_{6_5,4,4_5} \sim 3_{6_5,6,4,4_5}.$$

Moreover we have:

$$7 \cap_3 7_6; \quad 7_1 \cap_3 7_{6,1}; \quad 7_{6_5} \cap_3 7_{6_5,6}; \quad 7_{6_5,1} \cap_3 7_{6_5,6,1}.$$

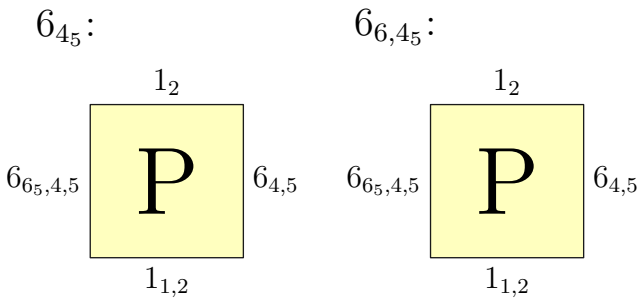

Figure 3.10: The way to glue the facets 6_{4_5} and $6_{6,4_5}$ of L_7.

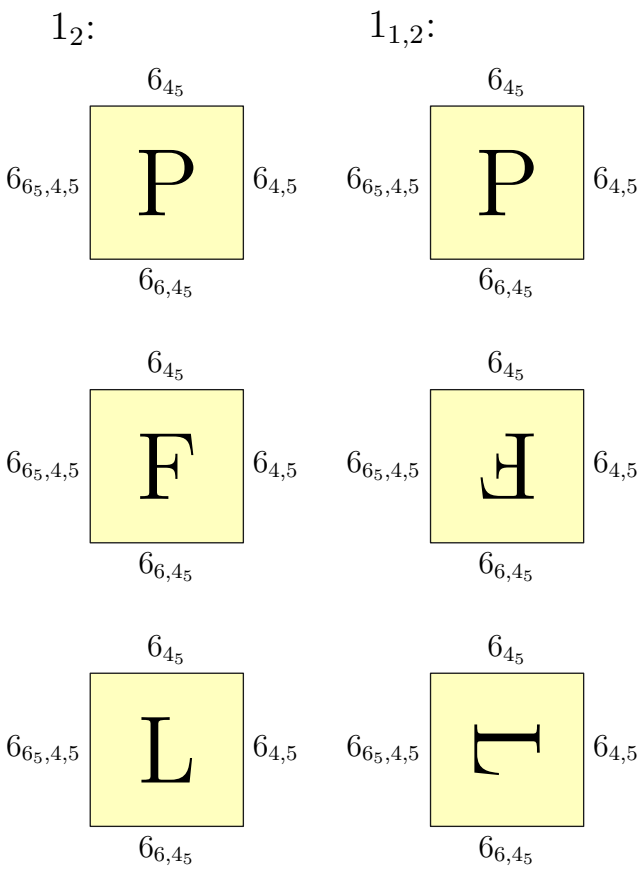

Figure 3.11: The way to glue the facets 1_2 and $1_{1,2}$ of L_7 for the 3-torus case (top), the $\frac{1}{2}$-twist manifold case (center) and the $\frac{1}{4}$-twist manifold case (bottom).

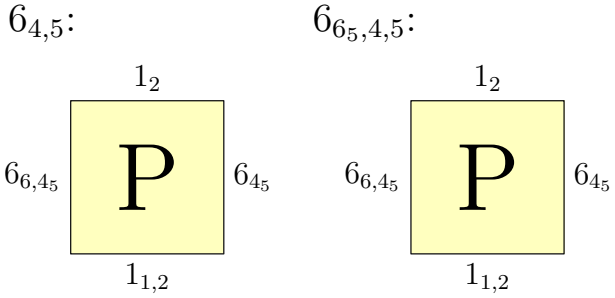

Figure 3.12: The way to glue the facets $6_{4,5}$ and $6_{6_5,4,5}$ of L_7.

- 1_2 and $1_{1,2}$: We refer to Figures 6.7 and 3.11.

$$\begin{array}{rrr} 3_{6_5,4,4_5,2} \sim 3_{6_5,1,4,4_5,2}; & 3_{4_5,2} \sim 3_{1,4_5,2}; & 3_{4,4_5,2} \sim 3_{1,4,4_5,2}; \\ 3_{6_5,4,2} \sim 3_{6_5,1,4,2}; & 3_2 \sim 3_{1,2}; & 3_{4,2} \sim 3_{1,4,2}; \\ 3_{6_5,6,4,4_5,2} \sim 3_{6_5,6,1,4,4_5,2}; & 3_{6,4_5,2} \sim 3_{6,1,4_5,2}; & 3_{6,4,4_5,2} \sim 3_{6,1,4,4_5,2}. \end{array}$$

  Moreover we have:

$$7 \cap_2 7_1; \qquad 7_6 \cap_2 7_{6,1}; \qquad 7_{6_5} \cap_2 7_{6_5,1}; \qquad 7_{6_5,6} \cap_2 7_{6_5,6,1}.$$

Putting together the results of the three gluings, we have the thesis.

□

Lemma 3.3.9. *The equivalence classes of $R_{\frac{1}{2}}$ are described in Table 3.1. The type-$(7,7)$ corners of $R_{\frac{1}{2}}$ that are the images through p of the type-$(7,i)$ ridges, with $i = 1, 6$, of the polytope P_7 are listed in Table 3.5.*

Proof. We divide the proof by analyzing each gluing of the polytope P_7 separately.

- $6_{4,5}$ and $6_{6_5,4,5}$: We refer to Figure 6.8 and 3.14 for the information (I3) on these two facets and the way to glue them. The latter figure is not necessary, since we can deduce its content from Figures 3.5, but it helps the reader to check the results.

  Hence we see that:

$$\begin{array}{rrr} 3_{6,4,4_5,2} \sim 3_{6_5,6,4,4_5,2}; & 3_{4,2} \sim 3_{6_5,4,2}; & 3_{4,4_5,2} \sim 3_{6_5,4,4_5,2}; \\ 3_{6,4,4_5} \sim 3_{6_5,6,4,4_5}; & 3_4 \sim 3_{6_5,4}; & 3_{4,4_5} \sim 3_{6_5,4,4_5}; \\ 3_{6,1,4,4_5,2} \sim 3_{6_5,6,1,4,4_5,2}; & 3_{1,4,2} \sim 3_{6_5,1,4,2}; & 3_{1,4,4_5,2} \sim 3_{6_5,1,4,4_5,2}. \end{array}$$

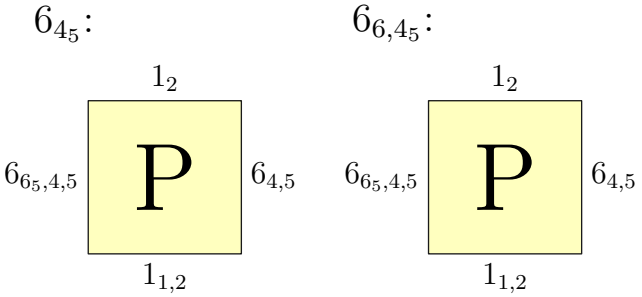

Figure 3.13: The way to glue the facets 6_{4_5} and $6_{6,4_5}$ of L_7.

Moreover, both $6_{4,5}$ and $6_{6_5,4,5}$ meet 4 facets of type 7, with a dihedral angle of $\frac{\pi}{6}$ by Proposition 3.2.12 (since in P_0 the dihedral angle between 6 and 7 is $\frac{\pi}{6}$). Hence, in R, from the picture we notice that there are the following corners with angle $\frac{2\pi}{6} = \frac{\pi}{3}$.

$$7 \cap_3 7_{6_5}; \qquad 7_1 \cap_3 7_{6_5,1}; \qquad 7_6 \cap_3 7_{6_5,6}; \qquad 7_{6,1} \cap_3 7_{6_5,6,1}.$$

- 6_{4_5} and $6_{6,4_5}$: We refer to Figures 6.9 and 3.15. The same argument as before leads to the following:

$$\begin{aligned} 3_{4,4_5,2} &\sim 3_{6,4,4_5,2}; & 3_{4_5,2} &\sim 3_{6,4_5,2}; & 3_{6_5,4,4_5,2} &\sim 3_{6_5,6,4,4_5,2}; \\ 3_{4,4_5} &\sim 3_{6,4,4_5}; & 3_{1,4,4_5,2} &\sim 3_{6,1,4,4_5,2}; & 3_{1,4_5,2} &\sim 3_{6,1,4_5,2}; \\ 3_{6_5,1,4,4_5,2} &\sim 3_{6_5,6,1,4,4_5,2}; & 3_{4_5} &\sim 3_{6,4_5}; & 3_{6_5,4,4_5} &\sim 3_{6_5,6,4,4_5}. \end{aligned}$$

Moreover we have:

$$7 \cap_3 7_6; \qquad 7_1 \cap_3 7_{6,1}; \qquad 7_{6_5} \cap_3 7_{6_5,6}; \qquad 7_{6_5,1} \cap_3 7_{6_5,6,1}.$$

- 1_2 and $1_{1,2}$: We refer to Figures 6.7 and 3.11.

$$\begin{aligned} 3_{6_5,4,4_5,2} &\sim 3_{6,1,4,4_5,2}; & 3_{4_5,2} &\sim 3_{6,1,4_5,2}; & 3_{4,4_5,2} &\sim 3_{6_5,6,1,4,4_5,2}; \\ 3_{6_5,4,2} &\sim 3_{1,4,2}; & 3_2 &\sim 3_{1,2}; & 3_{4,2} &\sim 3_{6_5,1,4,2}; \\ 3_{6_5,6,4,4_5,2} &\sim 3_{1,4,4_5,2}; & 3_{6,4_5,2} &\sim 3_{1,4_5,2}; & 3_{6,4,4_5,2} &\sim 3_{6_5,1,4,4_5,2}. \end{aligned}$$

Moreover we have:

$$7 \cap_2 7_{6_5,6,1}; \qquad 7_1 \cap_2 7_{6_5,6}; \qquad 7_{6_5} \cap_2 7_{6,1}; \qquad 7_{6_5,1} \cap_2 7_6.$$

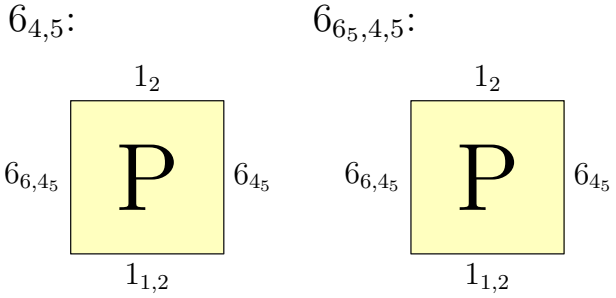

Figure 3.14: The way to glue the facets $6_{4,5}$ and $6_{6_5,4,5}$ of L_7.

□

Lemma 3.3.10. *The equivalence classes of $R_{\frac{1}{4}}$ are described in Table 3.2. The type-$(7,7)$ corners of $R_{\frac{1}{4}}$ that are the images through p of the type-$(7,i)$ ridges, with $i = 1, 6$, of the polytope P_7 are listed in Table 3.6.*

Proof. We divide the proof by analyzing each gluing of the polytope P_7 separately.

- $6_{4,5}$ and $6_{6_5,4,5}$: We refer to Figure 6.8 and 3.14 for the information (I3) on these two facets and the way to glue them. The latter figure is not necessary, since we can deduce its content from Figures 3.5, but it helps the reader to check the results.

  Hence we see that:

  $$\begin{array}{lll} 3_{6,4,4_5,2} \sim 3_{6_5,6,4,4_5,2}; & 3_{4,2} \sim 3_{6_5,4,2}; & 3_{4,4_5,2} \sim 3_{6_5,4,4_5,2}; \\ 3_{6,4,4_5} \sim 3_{6_5,6,4,4_5}; & 3_4 \sim 3_{6_5,4}; & 3_{4,4_5} \sim 3_{6_5,4,4_5}; \\ 3_{6,1,4,4_5,2} \sim 3_{6_5,6,1,4,4_5,2}; & 3_{1,4,2} \sim 3_{6_5,1,4,2}; & 3_{1,4,4_5,2} \sim 3_{6_5,1,4,4_5,2}. \end{array}$$

  Moreover, both $6_{4,5}$ and $6_{6_5,4,5}$ meet 4 facets of type 7, with a dihedral angle of $\frac{\pi}{6}$ by Proposition 3.2.12 (since in P_0 the dihedral angle between 6 and 7 is $\frac{\pi}{6}$). Hence, in R, from the picture we notice that there are the following corners with angle $\frac{2\pi}{6} = \frac{\pi}{3}$.

  $$7 \cap_3 7_{6_5}; \qquad 7_1 \cap_3 7_{6_5,1}; \qquad 7_6 \cap_3 7_{6_5,6}; \qquad 7_{6,1} \cap_3 7_{6_5,6,1}.$$

- 6_{4_5} and $6_{6,4_5}$: We refer to Figures 6.9 and 3.15. The same argument as before leads to the following:

  $$\begin{array}{lll} 3_{4,4_5,2} \sim 3_{6,4,4_5,2}; & 3_{4_5,2} \sim 3_{6,4_5,2}; & 3_{6_5,4,4_5,2} \sim 3_{6_5,6,4,4_5,2}; \\ 3_{4,4_5} \sim 3_{6,4,4_5}; & 3_{1,4,4_5,2} \sim 3_{6,1,4,4_5,2}; & 3_{1,4_5,2} \sim 3_{6,1,4_5,2}; \\ 3_{6_5,1,4,4_5,2} \sim 3_{6_5,6,1,4,4_5,2}; & 3_{4_5} \sim 3_{6,4_5}; & 3_{6_5,4,4_5} \sim 3_{6_5,6,4,4_5}. \end{array}$$

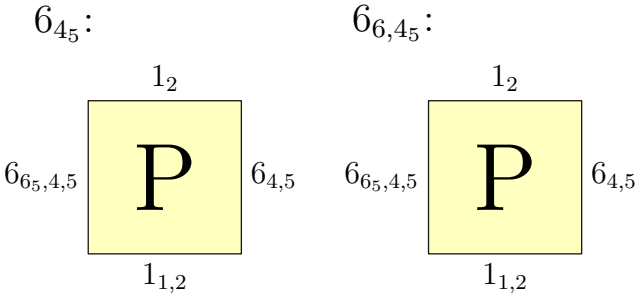

Figure 3.15: The way to glue the facets 6_{4_5} and $6_{6,4_5}$ of L_7.

Moreover we have:

$$7 \cap_3 7_6; \qquad 7_1 \cap_3 7_{6,1}; \qquad 7_{6_5} \cap_3 7_{6_5,6}; \qquad 7_{6_5,1} \cap_3 7_{6_5,6,1}.$$

- 1_2 and $1_{1,2}$: We refer to Figures 6.7 and 3.11.

$$\begin{array}{lll} 3_{6_5,4,4_5,2} \sim 3_{1,4,4_5,2}; & 3_{4_5,2} \sim 3_{1,4,2}; & 3_{4,4_5,2} \sim 3_{6,1,4,4_5,2}; \\ 3_{6_5,4,2} \sim 3_{1,4_5,2}; & 3_2 \sim 3_{1,2}; & 3_{4,2} \sim 3_{6,1,4_5,2}; \\ 3_{6_5,6,4,4_5,2} \sim 3_{6_5,1,4,4_5,2}; & 3_{6,4_5,2} \sim 3_{6_5,1,4,2}; & 3_{6,4,4_5,2} \sim 3_{6_5,6,1,4,4_5,2}. \end{array}$$

Moreover we have:

$$7 \cap_2 7_{6,1}; \qquad 7_6 \cap_2 7_{6_5,6,1}; \qquad 7_{6_5} \cap_2 7_1; \qquad 7_{6_5,6} \cap_2 7_{6_5,1}.$$

□

Lemma 3.3.11. *The equivalence classes of R_{HW} are described in Table 3.3. The type-$(7,7)$ corners of R_{HW} that are the images through p of the type-$(7,i)$ ridges, with $i = 1, 6$, of the polytope P_8 are listed in Table 3.7.*

Proof. We divide the proof by analyzing each gluing of the polytope P_8 separately.

- $6_{4,5}$: We refer to Figure 6.11 and 3.16.

$$\begin{array}{lll} 3_{1_2,6,1,4,4_5,2} \sim 3_{4,4_5,2}; & 3_{1_2,1,4,2} \sim 3_{4,2}; & 3_{1_2,1,4,4_5,2} \sim 3_{6,4,4_5,2}; \\ 3_{1_2,6,4,4_5} \sim 3_{4,4_5}; & 3_{1_2,4} \sim 3_4; & 3_{1_2,4,4_5} \sim 3_{6,4,4_5}; \\ 3_{6,4,4_5,2} \sim 3_{1,4,4_5,2}; & 3_{4,2} \sim 3_{1,4,2}; & 3_{4,4_5,2} \sim 3_{6,1,4,4_5,2}. \end{array}$$

Moreover we have:

$$7_{1_2,6,1} \cap_3 7; \qquad 7_{1_2,1} \cap_3 7_6; \qquad 7_{1_2,6} \cap_3 7_1; \qquad 7_{1_2} \cap_3 7_{6,1}.$$

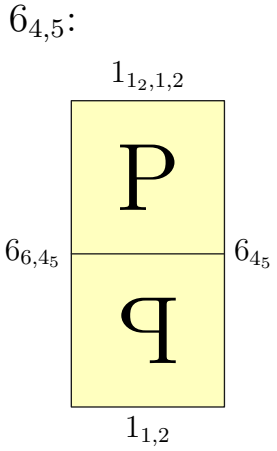

Figure 3.16: The way to glue the facet $6_{4,5}$ of L_8.

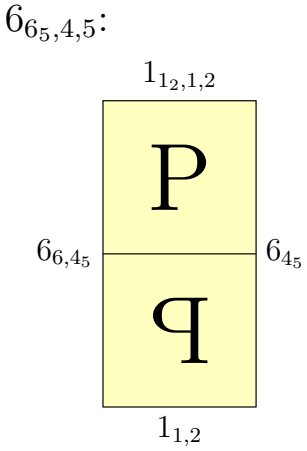

Figure 3.17: The way to glue the facet $6_{6_5,4,5}$ of L_8.

- $\underline{6_{6_5,4,5}}$: We refer to Figure 6.12 and 3.17.

$$3_{1_2,6_5,6,1,4,4_5,2} \sim 3_{6_5,4,4_5,2}; \qquad 3_{1_2,6_5,1,4,2} \sim 3_{6_5,4,2};$$
$$3_{1_2,6_5,6,4,4_5} \sim 3_{6_5,4,4_5}; \qquad 3_{1_2,6_5,4} \sim 3_{6_5,4};$$
$$3_{6_5,6,4,4_5,2} \sim 3_{6_5,1,4,4_5,2}; \qquad 3_{6_5,4,2} \sim 3_{6_5,1,4,2};$$
$$3_{1_2,6_5,1,4,4_5,2} \sim 3_{6_5,6,4,4_5,2}; \qquad 3_{1_2,6_5,4,4_5} \sim 3_{6_5,6,4,4_5};$$
$$3_{6_5,4,4_5,2} \sim 3_{6_5,6,1,4,4_5,2}.$$

  Moreover we have:

$$7_{1_2,6_5,6,1} \cap_3 7_{6_5}; \qquad 7_{1_2,6_5,1} \cap_3 7_{6_5,6}; \qquad 7_{1_2,6_5,6} \cap_3 7_{6_5,1}; \qquad 7_{1_2,6_5} \cap_3 7_{6_5,6,1}.$$

- $\underline{6_{4_5}}$ and $\underline{6_{6,4_5}}$: We refer to Figure 6.13, 6.14 and 3.18.

$$3_{1_2,6_5,1,4,4_5,2} \sim 3_{6,1,4,4_5,2}; \qquad 3_{1_2,1,4_5,2} \sim 3_{6,1,4_5,2};$$
$$3_{1_2,6_5,4,4_5} \sim 3_{6,4,4_5}; \qquad 3_{1_2,4_5} \sim 3_{6,4_5};$$
$$3_{6_5,4,4_5,2} \sim 3_{6,4,4_5,2}; \qquad 3_{4_5,2} \sim 3_{6,4_5,2};$$
$$3_{6_5,4,4_5} \sim 3_{1_2,6,4,4_5}; \qquad 3_{4_5} \sim 3_{1_2,6,4_5};$$
$$3_{6_5,1,4,4_5,2} \sim 3_{1_2,6,1,4,4_5,2}; \qquad 3_{1,4_5,2} \sim 3_{1_2,6,1,4_5,2};$$
$$3_{1_2,1,4,4_5,2} \sim 3_{6_5,6,1,4,4_5,2}; \qquad 3_{1_2,4,4_5} \sim 3_{6_5,6,4,4_5};$$
$$3_{4,4_5,2} \sim 3_{6_5,6,4,4_5,2}; \qquad 3_{4,4_5} \sim 3_{1_2,6_5,6,4,4_5};$$
$$3_{1,4,4_5,2} \sim 3_{1_2,6_5,6,1,4,4_5,2}.$$

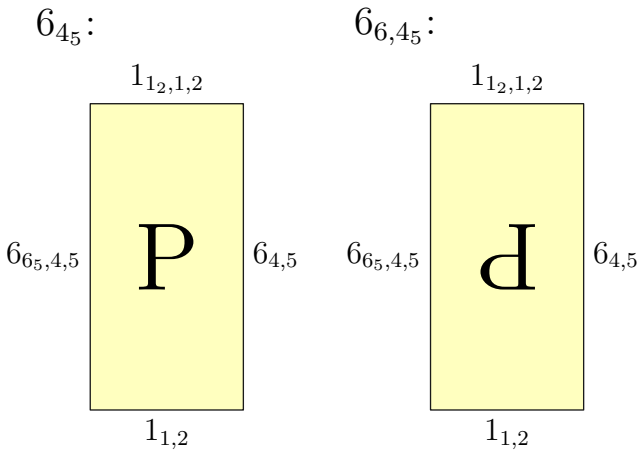

Figure 3.18: The way to glue the facets 6_{4_5} and $6_{6,4_5}$ of L_8.

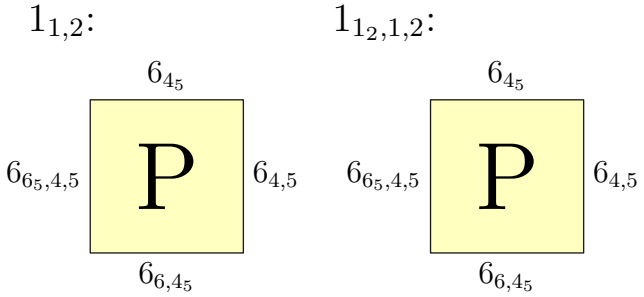

Figure 3.19: The way to glue the facets $1_{1,2}$ and $1_{1_2,1,2}$ of L_8.

Moreover we have:

$$7_{1_2,6_5,1} \cap_3 7_{6,1}; \quad 7_{1_2,1} \cap_3 7_{6_5,6,1}; \quad 7_{1_2,6_5} \cap_3 7_6; \quad 7_{1_2} \cap_3 7_{6_5,6}$$
$$7_{6_5} \cap_3 7_{1_2,6}; \quad 7 \cap_3 7_{1_2,6_5,6}; \quad 7_{6_5,1} \cap_3 7_{1_2,6,1}; \quad 7_1 \cap_3 7_{1_2,6_5,6,1}.$$

- $1_{1,2}$ and $1_{1_2,1,2}$: We refer to Figure 6.10 and 3.19.

$$3_{6_5,1,4,4_5,2} \sim 3_{1_2,6_5,1,4,4_5,2}; \quad 3_{1,4_5,2} \sim 3_{1_2,1,4_5,2};$$
$$3_{6_5,1,4,2} \sim 3_{1_2,6_5,1,4,2}; \quad 3_{1,2} \sim 3_{1_2,1,2};$$
$$3_{6_5,6,1,4,4_5,2} \sim 3_{1_2,6_5,6,1,4,4_5,2}; \quad 3_{6,1,4_5,2} \sim 3_{1_2,6,1,4_5,2};$$
$$3_{1,4,4_5,2} \sim 3_{1_2,1,4,4_5,2}; \quad 3_{1,4,2} \sim 3_{1_2,1,4,2};$$
$$3_{6,1,4,4_5,2} \sim 3_{1_2,6,1,4,4_5,2}.$$

Moreover we have:

$$7_{6_5,1} \cap_2 7_{1_2,6_5,1}; \quad 7_1 \cap_2 7_{1_2,1}; \quad 7_{6_5,6,1} \cap_2 7_{1_2,6_5,6,1}; \quad 7_{6,1} \cap_2 7_{1_2,6,1}.$$

□

3.3.3 The space R is a 1-cusped developable reflectofold.

We conclude here the proof of Theorem 3.3.4.

Recall Definition 3.3.6 of the corner graphs G_3 and G_7. We can now recover enough information about them.

Definition 3.3.12. Let $\widetilde{G_3}$ be the graph obtained by identifying the vertices of the adjacency graph of facets of type 3 of P by the relation $\sim$. Let $\widetilde{G_7}$ be the graph obtained by taking the adjacency graph of facets of type 7 of P and adding a labelled edge $(F, G; k)$, for every $F \cap_k G$ in Lemmas 3.3.8, 3.3.9, 3.3.10 and 3.3.11.

Proposition 3.3.13. *The corner graph G_3 is a subgraph of $\widetilde{G_3}$. More specifically, the vertices of the two graphs are the same, while if two vertices of $\widetilde{G_3}$ have m edges connecting them with label l, in G_3 we have n edges with label l between the corresponding vertices, with $1 \leq n \leq m$.*

Proof. The vertices of $\widetilde{G_3}$ coincide with the ones of G_3 by Lemmas 3.3.8, 3.3.9, 3.3.10 and 3.3.11.

Let $\overline{3_X} = \{3_{X_1}, \dots, 3_{X_k}\}$ and $\overline{3_Y} = \{3_{Y_1}, \dots, 3_{Y_k}\}$ be two equivalence classes of type-3 facets of P. By construction, for every ridge between two facets 3_{X_i} and 3_{Y_j} with dihedral angle $\frac{\pi}{k}$, there is an edge in $\widetilde{G_3}$ between the vertices $\overline{3_X}$ and $\overline{3_Y}$ with label k.

By Lemma 3.3.7 a type-$(3,3)$ corner of R is the image through p of a union of some type-$(3,3)$ ridges of P. Hence if the image through p of the union of r ridges is a single corner between the facets $\overline{3_X}$ and $\overline{3_Y}$ in R, then in G_3 we have one edge between $\overline{3_X}$ and $\overline{3_Y}$; while in $\widetilde{G_3}$ we have r edges between them. It is easy to check that these r edges have the same label associated (by checking the adiacency graph of P in Table 6.8 and 6.9, and the results of Lemmas 3.3.8, 3.3.9, 3.3.10 and 3.3.11). □

Proposition 3.3.14. *The corner graph G_7 is equal to $\widetilde{G_7}$.*

Proof. The vertices of $\widetilde{G_7}$ coincide with the ones of G_7 by Lemma 3.3.5. By Lemma 3.3.7 the edges of G_7 are the ones of $\widetilde{G_7}$. □

It is easy to verify (by checking the adjacency matrices of P in Table 6.8 and 6.9, and the results of Lemmas 3.3.8, 3.3.9, 3.3.10 and 3.3.11) that $\widetilde{G_3}$ and $\widetilde{G_7}$ have no loop (an edge connecting one vertex to itself) and if two vertices have more then

3	1	2	3		3			
3_2	2	1		3		3		
3_{4_5}	3		1	2			3	
$3_{4_5,2}$		3	2	1				3
3_4	3				1	2	3	
$3_{4,2}$		3			2	1		3
$3_{4,4_5}$			3		3		1	2
$3_{4,4_5,2}$				3		3	2	1

7	1	2	3		3			
7_1	2	1		3		3		
7_6	3		1	2			3	
$7_{6,1}$		3	2	1				3
7_{6_5}	3				1	2	3	
$7_{6_5,1}$		3			2	1		3
$7_{6_5,6}$			3		3		1	2
$7_{6_5,6,1}$				3		3	2	1

Table 3.8: Type-3 and type-7 adjacency matrices of R_T.

3	1	2	3		3			
3_2	2	1		3		3		
3_{4_5}	3		1	2			3	
$3_{4_5,2}$		3	2	1				3
3_4	3				1	2	3	
$3_{4,2}$		3			2	1		3
$3_{4,4_5}$			3		3		1	2
$3_{4,4_5,2}$				3		3	2	1

7	1	2	3		3			2
7_1	2	1		3		3	2	
7_6	3		1	2		2	3	
$7_{6,1}$		3	2	1	2			3
7_{6_5}	3			2	1	2	3	
$7_{6_5,1}$		3	2		2	1		3
$7_{6_5,6}$		2	3		3		1	2
$7_{6_5,6,1}$	2			3		3	2	1

Table 3.9: Type-3 and type-7 adjacency matrices of $R_{\frac{1}{2}}$.

one edge connecting them, all these edges have the same label. Hence it makes sense to define the adjacency matrices of R.

Definition 3.3.15. For $i = 3, 7$, the *type-i adjacency matrix* of R is the matrix where in the entry corresponding to the type-i facet A and B we put 1 if $A = B$, we put 0 if $A \cap B = \emptyset$, we put k if the dihedral angle at the corners of $A \cap B$ is $\frac{\pi}{k}$ and we put $\underline{\alpha}$ if the dihedral angle at the corners of $A \cap B$ is $\alpha \neq \frac{\pi}{k}$, for every k.

One could also obtain the adjacency matrix of R, but we are only interested in the type-3 and type-7 ones, which are the submatrices corresponding to the facets of type 3 and of type 7, respectively.

Proposition 3.3.16. *For $i = 3, 7$, the type-i adjacency matrix of R is in Tables 3.8, 3.9, 3.10 and 3.11.*

Proof. By Proposition 3.3.13 and 3.3.14, if $\widetilde{G_i}$ has at least one edge with label l between the vertices A and B, then in the matrix the entry between A and B is l. If in $\widetilde{G_i}$ there is no edge between A and B, then there is a 0 in the corresponding entry. □

Proposition 3.3.17. *The space R is a finite-volume reflectofold.*

3	1	2	3		3			
3_2	2	1		3		3		
3_{4_5}	3		1	2		2	3	
$3_{4_5,2}$		3	2	1	2			3
3_4	3			2	1	2	3	
$3_{4,2}$		3	2		2	1		3
$3_{4,4_5}$			3		3		1	2
$3_{4,4_5,2}$				3		3	2	1

7	1	2	3	2	3			
7_1	2	1		3	2	3		
7_6	3		1	2			3	2
$7_{6,1}$	2	3	2	1				3
7_{6_5}	3	2			1	2	3	
$7_{6_5,1}$		3			2	1	2	3
$7_{6_5,6}$			3		3	2	1	2
$7_{6_5,6,1}$			2	3		3	2	1

Table 3.10: Type-3 and type-7 adjacency matrices of $R_{\frac{1}{4}}$.

Proof. The dihedral angles at the type-$(3,3)$ and type-$(7,7)$ corners of R are all of the form $\frac{\pi}{k}$ since in Tables 3.8, 3.9, 3.10 and 3.11 there are not underlined labels. Every type-$(3,7)$ ridge of P has dihedral angle $\frac{\pi}{2}$ by Proposition 3.2.12 (since the dihedral angle between **3** and **7** in P_0 is $\frac{\pi}{2}$). Hence, by Lemma 3.3.7, also every type-$(3,7)$ corner of R has dihedral angle $\frac{\pi}{2}$. By Lemma 3.3.7, this runs out all the corners of R.

We show that R is locally a Coxeter polytope. The faces of P induce a natural stratification of R in closed strata. We have that R is locally modeled on $\mathbb{H}^n$ near the non-compact strata and far from the compact strata, since its end is isometric to a cusp (with section a flat, closed manifold) by construction. We have that R is locally a Coxeter polytope near the compact strata since we have proved that the angle corresponding to the corners are in the form $\frac{\pi}{k}$.

Moreover, R is complete by construction, since we glued using reflections through copies of the facets of P_0. Hence R is a reflectofold. Finally, the polytope P is tessellated into a finite number of copies of P_0, which has finite volume, hence also R has finite volume. □

Proposition 3.3.18. *The reflectofold R is 1-cusped, has compact, non-empty boundary and is orientable. Moreover, the cusp of $R_T, R_{\frac{1}{2}}, R_{\frac{1}{4}}, R_{HW}$ has section, the 3-torus, the $\frac{1}{2}$-twist manifold, the $\frac{1}{4}$-twist manifold, the Hantzsche-Wendt manifold, respectively.*

Proof. The boundary of R is the image of the union of the facets of P that we do not glue. Since these facets are of type 3 or 7, that are compact, the boundary of R is compact (and non-empty).

Since by construction we glued P in a way that this induces a gluing of the link L_7 (of the only ideal vertex) to form the 3-torus, the $\frac{1}{2}$-twist manifold, the $\frac{1}{4}$-twist manifold, the space R has exaclty one cusp with the requested section.

3	1	2	3		2		3			3	3					
3_2	2	1		2		3		3				3				
3_4	3		1	3		2			3		3					
3_{1_2}		2	3	1	2		3			3	3					
$3_{1,2}$	2			2	1	3						3		3		
$3_{4,2}$		3	2		3	1					2		3			3
3_{4_5}	3			3			1	2	3					2		
$3_{4_5,2}$		3					2	1		2					3	3
$3_{4,4_5}$			3				3		1		3				2	2
$3_{6,4_5}$	3			3				2		1			3	2		
$3_{6_5,4}$	3		3	3		2			3		1	2				
$3_{6_5,4,2}$		3			3						2	1			3	3
$3_{6,4,4_5}$						3				3			1		2	2
$3_{1,4_5,2}$					3		2			2				1	3	3
$3_{4.4_5,2}$								3	2			3	2	3	1	3
$3_{1,4,4_5,2}$						3		3	2			3	2	3	3	1

7	1	2	3		3				2			3			3	
7_1	2	1		3		3				2	3					3
7_6	3		1	2			3			3	2		3			
$7_{6,1}$		3	2	1				3	3			2		3		
7_{6_5}	3				1	2	3				3		2			3
$7_{6_5,1}$		3			2	1		3				3		2	3	
$7_{6_5,6}$			3		3		1	2	3					3	2	
$7_{6_5,6,1}$				3		3	2	1		3			3			2
7_{1_2}	2			3			3		1	2	3		3			
$7_{1_2,1}$		2	3					3	2	1		3		3		
$7_{1_2,6}$		3	2		3				3		1	2			3	
$7_{1_2,6,1}$	3			2		3				3	2	1				3
$7_{1_2,6_5}$			3		2			3	3				1	2	3	
$7_{1_2,6_5,1}$				3		2	3			3			2	1		3
$7_{1_2,6_5,6}$	3					3	2				3		3		1	2
$7_{1_2,6_5,6,1}$		3			3			2				3		3	2	1

Table 3.11: Type-3 and type-7 adjacency matrices of R_{HW}.

Finally, the space R is orientable, since it is homeomorphic to $E \times [0,1)$, where E is the cusp section, which is orientable. □

Proposition 3.3.19. *The reflectofold R is developable.*

Proof. Since the graph $\widetilde{G_i}$ has no loops, also the corner graph G_i has no loops, for $i = 3, 7$, by Proposition 3.3.13 and Proposition 3.3.14. Hence R satisfies (EF).

Moreover, R satisfies (AC):

- If two facets F and G both of type 3 (or 7) intersect, then the dihedral angles of all the corners in $F \cap G$ coincide; indeed, as already stated, in $\widetilde{G_3}$ (or $\widetilde{G_7}$), and hence in G_3 (or G_7), if two vertices have more then one edge connecting them, all these edges have the same label.
- Every type-$(3,7)$ ridge of P has dihedral angle $\frac{\pi}{2}$ by Proposition 3.2.12 (since the dihedral angle between **3** and **7** in P_0 is $\frac{\pi}{2}$). Hence, by Lemma 3.3.7, also every type-$(3,7)$ corner of R has dihedral angle $\frac{\pi}{2}$.

□

Putting together Proposition 3.3.18, Proposition 3.3.17 and Proposition 3.3.19, we have proved Theorem 3.3.4. Putting together Theorem 3.3.4 and Corollary 3.1.4, we have proved Theorem 1.1.1.

Chapter 4

Cusp-transitive 4-manifolds with every cusp section

This chapter is based on the paper [CR]. We streighten the result of Chapter 3 by building a cusp-transitive 4-manifold with cusp type N, for every N closed, flat 3-manifold. The construction will be less explicit and more astract than the one in Chapter 3. Moreover, we will prove some other results. Indeed, we will prove that for every closed flat 3-manifold N, the set of flat metrics on N which can be realized as cusp sections of a cusp-transitive 4-manifold is dense in the space of all flat metrics of N. Furthermore, we will prove the same result but with one dimension less. Finally, we will prove that there are a lot of manifolds with pairwise isometric cusps. More specifically, for every closed, flat 3-manifold N, there exists a constant $c > 0$ such that, for sufficiently large $V > 0$, there exist at least V^{cV} complete hyperbolic 4-manifolds with pairwise isometric cusps of type N and volume $\leq V$. Observe that the latter manifolds are not necessarily cusp transitive.

In this chapter we will use the same terminology of Chapter 3 about (developable) reflectofolds. We will use them to build the desired cusp-transitive manifolds as before. The only difference is that in this chapter we do not require reflectofolds to be complete; however, the cusp-transitive manifolds constructed will still be complete since they are obtained by gluing polytopes, and have complete cusp sections (see [Rat19, Theorem 11.1.6]).
Remark 4.0.1. If the cusp section of the cusp-transitive manifold M thus constructed is orientable, we can also construct an orientable cusp-transitive manifold with the same cusp section, namely the orientable double cover of M, as in Section 3.1.

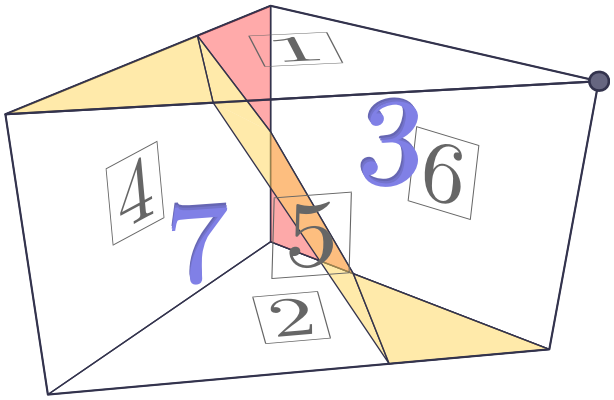

Figure 4.1: The projection of P onto the link L of its ideal vertex. The five faces of L and the two interior regions are labeled with the corresponding facets of P: five non-compact $(\mathbf{1}, \mathbf{2}, \mathbf{4}, \mathbf{5}, \mathbf{6})$ and two compact $(\mathbf{3}, \mathbf{7})$.

4.1 Some polytopes

In this section we will introduce and construct the polytopes that we are going to use in Section 4.2.

4.1.1 Visualizing polytopes with one ideal vertex

We consider the polytope P_0 of Section 3.2.1 and we will refer to it as P in this chapter. Recall that P is a finite-volume hyperbolic Coxeter 4-polytope, which satisfies (a) and (b). Moreover, it is arithmetic; indeed, one can verify it using the program CoxIter [Gug15; Gug].

In order to better understand the geometry of the 4-dimensional polytope P, it may prove useful to *project* the compact boundary facets onto the horospherical link of the ideal vertex as follows.

Place the polytope P in the half-space model of $\mathbb{H}^4$ with the ideal vertex at infinity, so that the non-compact facets of P become vertical, and let $\pi : \mathbb{H}^4 \to \mathbb{R}^3$ be the orthogonal projection onto a horizontal hyperplane, such as a horosphere or the ideal boundary. The image of P under π is the three-dimensional link L of the ideal vertex, and the non-compact facets are mapped to its boundary.

We can compute the face lattice of P by enumerating all spherical subdiagrams of D, and therefore determine the shape of the two regions associated to the facets **3** and **7** (Figure 4.1) by applying the following result.

Proposition 4.1.1. *Let Z be an n-polytope in $\mathbb{H}^n$ with one ideal vertex v. Let Λ be the link of v. The images of the compact facets of Z under the projection onto a*

horosphere centered at v partition Λ into a polyhedral complex, whose face lattice is combinatorially isomorphic to the lattice of compact faces of Z.

Proof. We consider the half-space model where v is at infinity. We say that a k-subspace of the half-space model is *vertical* if its ideal boundary contains v.

Let F be a compact k-face of Z. Then, in the half-space model, F is supported on a k-hemisphere H. Let Σ be the unique vertical $(k+1)$-space containing H. The face F is bounded by the supporting $(k-1)$-spaces of its facets $F_1, \dots, F_m$. Each F_i lies on a unique vertical k-space S_i. As such, F is the intersection of H and some hyperbolic half-$(k+1)$-spaces bounded by the S_i and contained in Σ. Let P_F be the Euclidean k-polytope obtained by intersecting the projections of these half-spaces on the horosphere; then we have $F = (P_F \times (0, +\infty)) \cap H$. Hence, the projection is a homeomorphism between F and P_F, which preserves facets. Since Z has only one ideal vertex, every compact face of Z is contained in a compact facet. Hence, by induction on the codimension of faces, the projection preserves the face lattice of the compact boundary of Z. □

Note that dihedral angles between facets of P are defined along ridges (codimension-2 faces), which appear in Figure 4.1 either as 2-faces (if the angle involves a compact facet) or as edges of L (if the angle is between two non-compact facets). We mark the former by coloring certain 2-faces of the projection, with the following rule. Every 2-face corresponds to a ridge between either two compact facets or a compact facet and a non-compact one. In the first case, we assign the dihedral angle to the 2-face, while in the second case, we assign the doubled dihedral angle. We use yellow for $\pi/2$, red for $\pi/3$, and we leave the 2-face transparent for π.

This rule keeps track of the fact that, if we glue two copies of P along a non-compact facet F, the angle along any ridge it shares with a compact facet gets doubled. For instance, the dihedral angle between facets **1** and **7** is $\pi/4$; when doubling P along **1**, the angle becomes $\pi/2$, so we color in yellow the corresponding triangle in Figure 4.1.

Moreover, after doubling, some ridges end up with an angle of π, meaning that the compact facet is coplanar with its mirrored copy. Leaving the 2-face transparent has the advantage of visually representing when compact facets merge together in an arbitrary gluing of copies of P.

4.1.2 The construction of the polytope Q

In this section we will take 16 copies of P and we will glue them in order to form a bigger polytope Q.

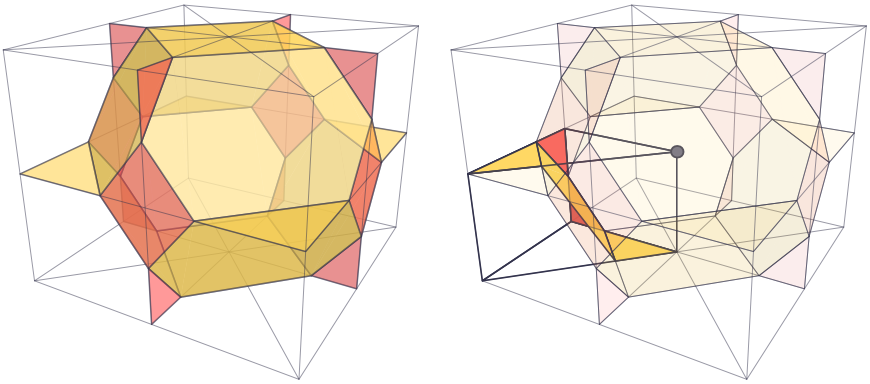

Figure 4.2: On the left, the projection of Q onto the link C. The truncated octahedron corresponds to a facet made of 16 copies of the facet **3** of P. The other 8 regions appear when copies of the facet **7** merge together two at a time. On the right, we emphasize one copy of L inside C.

Consider the subdiagram of D spanned by the vertices $1, 5, 6$. This induces a subgroup $G \simeq \mathbb{Z}_2 \times D_4$, of cardinality 16, which is the stabilizer of a non-compact edge of P. This edge projects to the marked vertex in Figure 4.1.

We can define a new polytope Q by taking the orbit of P under G. Equivalently, we glue 16 copies of P along their non-compact facets $\mathbf{1}, \mathbf{5}, \mathbf{6}$ using the identity map. By construction, Q has exactly one ideal vertex, whose link is a right prism C with a square base, obtained by placing 16 copies of L around the marked vertex (Figure 4.2).

The facets **3** merge together into a single facet of Q (which we will also call **3**), which projects to an irregular truncated octahedron in C, with 8 hexagonal and 6 quadrilateral facets. The latter correspond to ridges of Q where the facet **3** meets the non-compact facets: the dihedral angles are $\pi/6$ for the vertical quadrilaterals and $\pi/4$ for the horizontal ones.

The height, width and depth of C are in a ratio of $\cos(\pi/4) : \cos(\pi/6) : \cos(\pi/6) = \sqrt{2} : \sqrt{3} : \sqrt{3}$. Indeed, suppose that C is the cuboid $[-x_1, x_1] \times [-x_2, x_2] \times [-x_3, x_3]$. Then, in the conformal half-space model, each non-compact facet of Q is contained in the product of a facet of C and $(0, +\infty)$. The facet **3** is supported on a hemisphere, which is centered at $(0, 0, 0, 0)$ by symmetry. It is not hard to see that, if this hemisphere has radius r, then the acute angles with the supporting hyperplanes of the non-compact facets of Q are $\theta_i := \arccos(x_i/r)$. Hence, the cosines of the θ_i are in the same ratios as the x_i.

Because of this, all symmetries of C must preserve or exchange the two horizontal faces. There are 16 such symmetries, and they are generated by reflections in

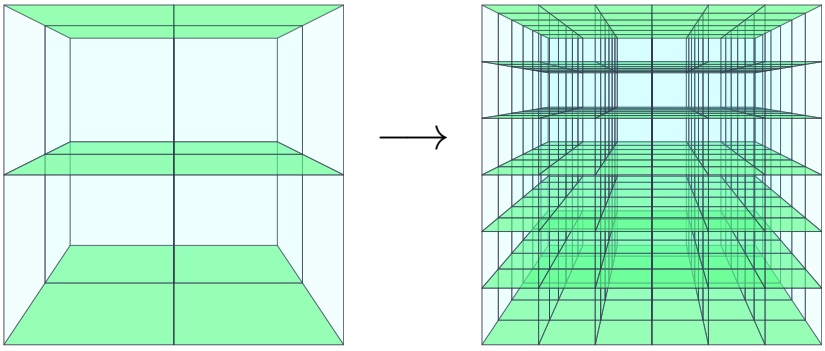

Figure 4.3: Subdividing a layered tessellation. Special faces are colored green.

the facets $\mathbf{1}, \mathbf{5}, \mathbf{6}$ of L, so they extend to symmetries of Q and they form a group isomorphic to G. This group can also be defined *a priori* as the group of symmetries of a *combinatorial* cube preserving or exchanging a certain pair of opposite facets.
Remark 4.1.2. The polytope C naturally tessellates $\mathbb{R}^3$ by translations. This gives a tessellation into truncated octahedra in the following way: some are centered and contained in the copies of C, as in Figure 4.2, while the others are centered at the vertices of the tessellation; one-eighth of a truncated octahedron can be seen near each vertex of C in Figure 4.2. The two types of truncated octahedra are actually congruent, because of the symmetry of D that exchanges 3 and 7. Indeed, passing to the dual tessellation by copies of C exchanges the two types of truncated octahedra.

4.2 Layered tessellations of 3-manifolds

In this section we will prove that if a flat 3-manifold N admits a tessellation in cubes with some properties, then there is a cusp-transitive hyperbolic 4-manifold with cusp type N.
Definition 4.2.1 (Layered tessellation)**.** Let T be a tessellation of a flat 3-manifold N into Euclidean cubes, with some chosen *special* 2-cells. We say that T is *layered* if each cube has two opposite special facets, and whenever two cubes C_1, C_2 share a facet F, the reflection through F sends the special facets of C_1 to those of C_2, and vice versa.

The above condition causes the special facets to fall into several embedded geodesic surfaces tessellated by squares, in a discrete analog of a foliation.
Remark 4.2.2. We will only make use of the combinatorial properties of layered tessellations; hence, we may define generalizations, such as layered tessellations by rectangular cuboids, in the same way.

Remark 4.2.3. A layered tessellation can be *subdivided* by replacing every cube with a block of $n \times n \times n$ cubes, $n \geq 1$, in which we mark as special all facets parallel to the two original special facets (see Figure 4.3).

Definition 4.2.4. We say that a layered tessellation is *proper* if the following dual conditions hold:

- every cube is distinct from its six neighbors, which are pairwise distinct;
- every vertex is distinct from its six neighbors, which are pairwise distinct.

Lemma 4.2.5. *Every layered tessellation can be subdivided into a proper one.*

Proof. First, we realize each cube of the tessellation as a cube with side length 1. This gives a flat Riemannian metric on a compact 3-manifold, which has an injectivity radius $r > 0$. We then subdivide the tessellation as in Remark 4.2.3, in such a way that the side length of the little cubes is less than r. The resulting tessellation is proper because, for every cube, the centers of it and its neighbors are contained in an embedded ball, and a similar argument applies to the vertices. □

Theorem 4.2.6. *Let N be a closed 3-manifold that admits a layered tessellation. Then there exists an arithmetic cusp-transitive hyperbolic 4-manifold with cusp type N.*

Proof. By Proposition 3.1.3, it suffices to prove that there exists a 1-cusped developable reflectofold with cusp type N, obtained by gluing copies of Q.

By Lemma 4.2.5, we may assume that the tessellation is proper.

We have that N is obtained by gluing some copies of C along their facets, where the gluing maps are restrictions of isometries of G: this gluing is induced by the layered tessellation, where the special facets correspond to the horizontal facets of C. Since there is a natural correspondence between facets of C and non-compact facets of Q, and every isometry in G extends to Q accordingly, we can glue copies of Q in the same pattern. This gives a 1-cusped reflectofold with cusp type N.

It remains to prove that N is developable. The facets of N are hyperbolic truncated octahedra, which arise from the merging of 16 facets **3** or **7**; we will call them *of types* **3** and **7** respectively. The former are centered at the centers of the cubes, while the latter are centered at the vertices of the tessellation.

If a facet of type **3** were adjacent to itself, it would be so along a quadrilateral corner, and so it would also occupy a neighboring cube. However, the two cubes must be distinct by properness of the tessellation. A similar argument involving vertices works for facets of type **7**.

As for angle consistency, if two facets of different type intersect, they do so in a hexagonal corner with a dihedral angle of $\pi/2$. If a facet intersects another of the same type, say **3**, it must do so at a single quadrilateral corner, since the neighbors of a given cube are pairwise distinct by properness; angle consistency follows trivially. A dual argument deals with the case of two facets of type **7**.

The 4-manifold thus constructed is arithmetic since it covers the arithmetic orbifold P. □

Corollary 4.2.7. *Let N be one of the manifolds $E_1, E_2, E_4, E_6, B_1, B_2, B_3, B_4$. Then there exists a cusp-transitive arithmetic hyperbolic 4-manifold with cusp type N.*

Proof. As shown in Figure 4.4, the manifold N admits a layered tessellation, so the result follows from Theorem 4.2.6. □

4.3 The remaining manifolds

In this section we will construct cusp-transitive manifolds having the $\frac{1}{3}$-twist and $\frac{1}{6}$-twist manifolds as cusp sections.

4.3.1 The polytope V

Let D_2 be the following Coxeter diagram:

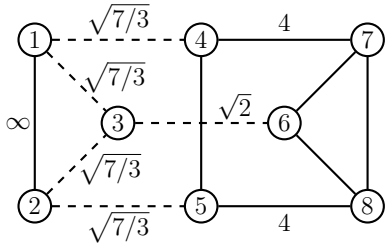

The diagram D_2 is obviously connected, and we can check that its Gram matrix has signature $(4, 1, 3)$ with non-positive off-diagonal entries; hence, by Vinberg's theorem [Vin85, Theorem 2.1], it defines a hyperbolic Coxeter 4-polytope V. Using CoxIter [Gug15; Gug], we find that V has finite volume and is non-arithmetic. Moreover, like the polytope P, it satisfies (a) and (b): there is exactly one ideal vertex, corresponding to the unique maximal affine subdiagram of D_2 [Vin85], which is spanned by $1, 2, 6, 7, 8$. Its link K is a Euclidean right prism over an equilateral triangle (Figure 4.5, obtained by using Proposition 4.1.1, and colored with the rule of Section 4.1.1).

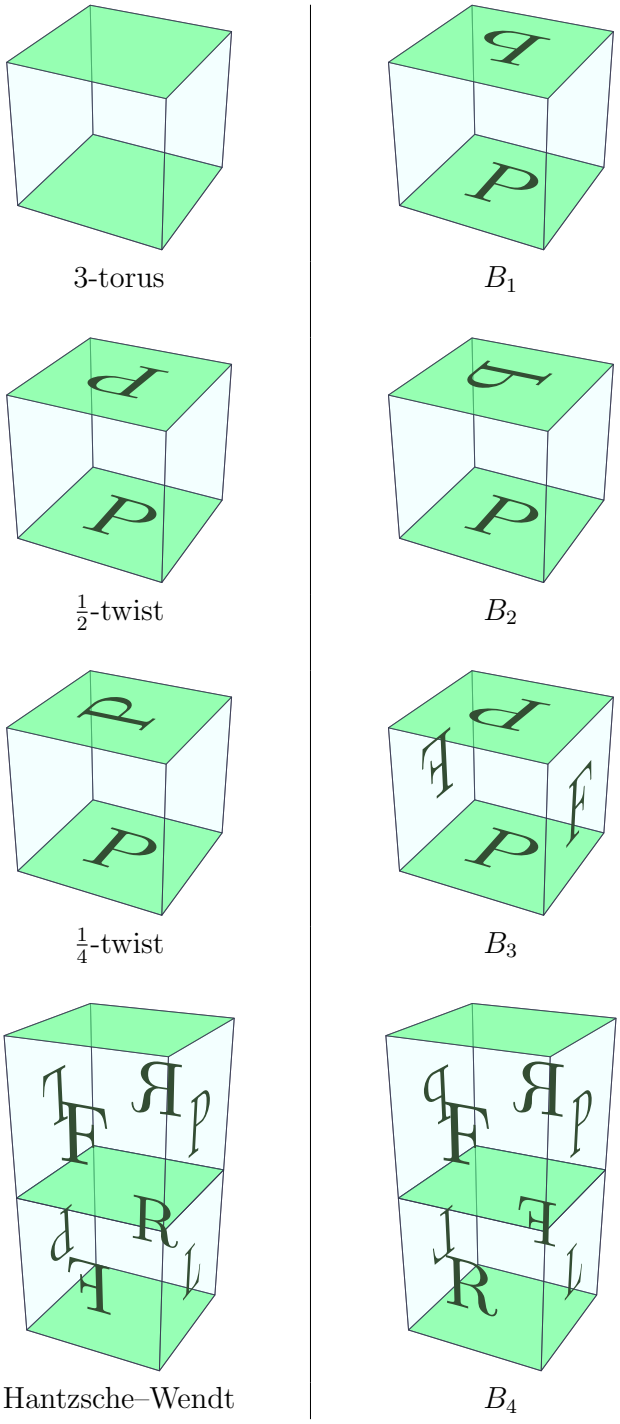

Figure 4.4: Layered tessellations for eight closed flat 3-manifolds. Labeled facets are glued according to their labels, while unlabeled facets are glued to the opposite facets by translation. The fundamental domains and gluing maps can be deduced from the algebraic descriptions of [CR03, Table 12].

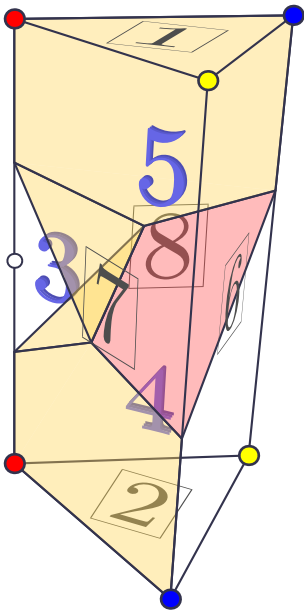

Figure 4.5: The projection of V onto the link K of its ideal vertex, with labels indicating the five non-compact facets $(\mathbf{1}, \mathbf{2}, \mathbf{6}, \mathbf{7}, \mathbf{8})$ and three compact facets $(\mathbf{3}, \mathbf{4}, \mathbf{5})$.

From the diagram D_2, we can see that the polytope V has a symmetry σ that exchanges the facets **1** and **2**, **4** and **5**, **7** and **8**. This induces a half-turn rotation of K swapping each vertex with the other one of the same color in Figure 4.5. This rotation is the only nontrivial color-preserving combinatorial automorphism of K.

4.3.2 Marked tessellations of 3-manifolds

Mirroring the previous sections, we will prove that if a flat 3-manifold N admits a tessellation in prisms over equilateral triangles with some properties, then there is a cusp-transitive hyperbolic 4-manifold with cusp type N.

Definition 4.3.1 (Marked tessellation)**.** Let T be a tessellation of a flat 3-manifold N into right prisms over equilateral triangles, such that the vertices are colored red, yellow or blue. We say that T is *marked* if the vertices of each prism are colored as in Figure 4.5 (up to combinatorial isomorphism), and whenever two prisms share a facet F, they are symmetrical with respect to F, including their vertex colorings.

Remark 4.3.2. Given a marked tessellation T and two natural numbers a, b, we can *subdivide* each prism as follows. First, note that an equilateral triangle can be subdivided into a^2 triangles (whose sides are a times smaller), by cutting it with three sets of equally spaced lines parallel to the sides; similarly, a prism can be subdivided into a^2 thin prisms. Each of those can then be cut, parallel to the bases,

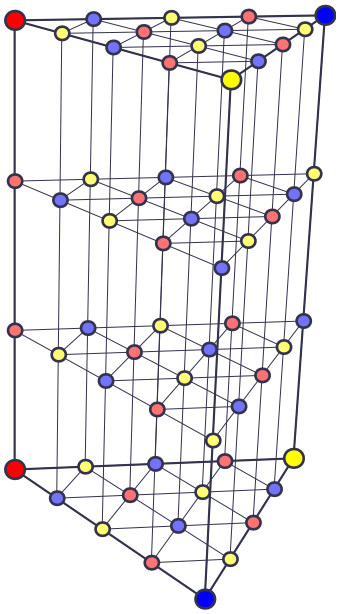

Figure 4.6: Subdividing a marked tessellation ($a = 4$, $b = 3$). The pattern on the bottom face of the prism works whenever $a - 1$ is a multiple of 3.

into b equal prisms. The new tessellation T' can be marked provided that b is odd and that $a - 1$ is a multiple of 3 (see Figure 4.6 for the case $a = 4$, $b = 3$). Indeed, for each prism t of T, we now have $b + 1$ layers of vertices of T'. It is not hard to see that, whenever $a \equiv 1 \pmod 3$, there is a unique way to 3-color the bottom layer consistently with the lower three vertices of t. Each subsequent layer will be the same as the one below it, but with yellow and blue swapped. If b is odd, then the top and bottom layers are the same with yellow and blue swapped, ensuring consistency with the coloring of t.

Remark 4.3.3. When gluing copies of V along non-compact facets, the compact facets merge into two kinds of new facets, which we can visualize with the help of the projection in Figure 4.5. The first kind arises from 6 copies of the facet **3** around the white dot, while the second comes from 12 copies of the facet **4** or **5** around the corresponding yellow dot. Both kinds of facets are bounded.

Theorem 4.3.4. *Let N be a closed 3-manifold that admits a marked tessellation. Then there exists a non-arithmetic cusp-transitive hyperbolic 4-manifold with cusp type N.*

Proof. The proof is similar in many aspects to that of Theorem 4.2.6, so we will only go over the main points. Again, by Proposition 3.1.3, it suffices to prove that there exists a 1-cusped developable reflectofold with cusp type N, obtained by gluing copies of V.

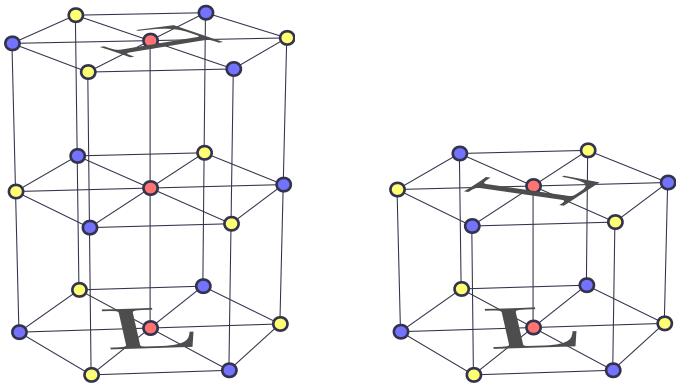

$\frac{1}{3}$-twist $\frac{1}{6}$-twist

Figure 4.7: Marked tessellations for E_3 and E_5. Labeled facets are glued according to their labels, while unlabeled facets are glued to the opposite facets by translation. The fundamental domains and gluing maps can be deduced from the algebraic descriptions of [CR03, Table 12].

A marked tessellation of N induces a way to glue copies of V along their non-compact facets; a key fact is that every color-preserving combinatorial automorphism of K is induced by a symmetry of V. This gives a 1-cusped reflectofold with cusp type N.

In order to ensure (EF) and (AC), it suffices that each facet of the reflectofold, together with its adjacent facets, is inside an embedded ball. Indeed, this ensures that every facet is embedded and that the intersection of two adjacent facets is a single corner. Since the facets are bounded by Remark 4.3.3, this can be done by an argument involving the injectivity radius and a sufficiently fine subdivision of the marked tessellation; the reflectofold constructed from the subdivided tessellation is developable.

The 4-manifold thus constructed is non-arithmetic since it covers the non-arithmetic orbifold $V/\langle\sigma\rangle$, where σ is the order-2 isometry of V defined in Section 4.3.1. □

Corollary 4.3.5. *Let N be one of the manifolds E_3, E_5. Then there exists a cusp-transitive hyperbolic 4-manifold with cusp type N.*

Proof. The manifolds E_3 and E_5 have marked tessellations, as shown in Figure 4.7; the result follows from Theorem 4.3.4. □

4.4 Density

In this section we will strengthen the previous results by investigating the possible Euclidean structures that can be realized by the cusp sections of a cusp-transitive 4-manifold, and we show how the same techniques can be used in the 3-dimensional case. We have the following result:

Theorem 4.4.1. *For every closed flat 3-manifold N, the set of flat metrics on N which can be realized as cusp sections of a cusp-transitive 4-manifold is dense in the space of all flat metrics of N.*

Proof. The argument is inspired by the proof of [Nim98, Theorem 2]. We divide the proof into two cases: the manifolds $E_1, E_2, E_4, E_6, B_1, B_2, B_3, B_4$ (tessellated by cubes) and the manifolds E_3, E_5 (tessellated by triangular prisms).

We start with the first case. Any flat metric on N is induced by a subgroup $\Gamma < \mathrm{Isom}(\mathbb{R}^3)$. Generators for Γ are found in [Nim98, Table 1] in the form (A, t_u), where $A \in \mathrm{O}(3)$ and t_u is a translation by the vector u, denoting the map $v \mapsto u + Av$.

The group Γ can be conjugated as in [Nim98, pp. 128–129] so that all the matrices A_i are certain fixed signed permutation matrices, which preserve the x axis, and preserve or exchange the y and z axes. In this *normalized form*, the translation vectors have some zero entries, while the k-uple of the other *free* entries can take any value in an open set of $\mathbb{R}^k$, containing $(\mathbb{R} \setminus \{0\})^k$. A dense subset of these forms can be obtained by considering only vectors of the form $v_i \coloneqq (\sqrt{2}a_i, \sqrt{3}b_i, \sqrt{3}c_i)$, where a_i, b_i, c_i are in $\mathbb{Q} \setminus \{0\}$ or $\{0\}$, depending on whether the corresponding entry of v_i is free or not. Let Γ' be a group with parameters in this dense subset; we shall prove that the metric resulting from Γ' can be realized by a layered tessellation by copies of C (see Remark 4.2.2).

The group Γ' preserves a lattice of the form

$$\left\{ \frac{1}{d}(\sqrt{2}m, \sqrt{3}n, \sqrt{3}p) \mid m, n, p \in \mathbb{Z} \right\},$$

where d is a common denominator of all the a_i, b_i, c_i. Furthermore, it preserves a layered tessellation of $\mathbb{R}^3$ by copies of C (having side lengths $\sqrt{2}/d$ and $\sqrt{3}/d$) with the special facets orthogonal to the x axis; this is because the x axis is preserved by the A_i. This tessellation descends to the quotient $\mathbb{R}^3/\Gamma'$. The result follows as in Theorem 4.2.6.

As for the second case, we refer to [CR03, Section 4]. The space of flat metrics on N has two parameters: in the hexagonal prism fundamental domains of Figure 4.7, they can be taken as the side length and height of the prisms. When subdividing a

marked tessellation in the proof of Theorem 4.3.4, we can choose two parameters a and b provided that b is odd, $a-1$ is a multiple of 3, and they are sufficiently large. The effect of these parameters is to multiply the side length and height of the fundamental domains by a and b respectively. Since we can realize the tessellation with arbitrarily small copies of K, by choosing a and b in an appropriate way, we can approximate any values of the two parameters of the metric of N. The result follows as in Theorem 4.3.4. □

4.4.1 Dimension 3

We consider the following diagram D_3, found in [Che69]:

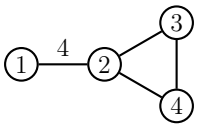

The corresponding Coxeter polytope Y is a finite-volume hyperbolic tetrahedron with one ideal vertex, corresponding to the subdiagram spanned by 2, 3, 4; its link is an equilateral triangle. The polytope has the properties (a) and (b).

Theorem 4.4.2. *For every closed flat 2-manifold S (i.e. the torus and the Klein bottle), the set of flat metrics on S which can be realized as cusp sections of a cusp-transitive 3-manifold is dense in the space of all flat metrics of S.*

Proof. We begin by gluing six copies of Y around the edge between the facets **3** and **4**. The resulting polytope Z has one ideal vertex, whose link is a regular hexagon, and one compact facet, which meets the other six facets at an angle of $\pi/4$.

If S has a tessellation by regular hexagons, such that every hexagon is embedded, then we can glue copies of Z along their non-compact facets in the same pattern. The resulting manifold with corners R is a developable reflectofold: its dihedral angles are all equal to $2 \cdot \pi/4 = \pi/2$, also implying (AC), and its facets are embedded hyperbolic hexagons (EF). Moreover, the section of its unique cusp is isometric to S up to global rescaling. As usual, by Proposition 3.1.3, we can construct a cusp-transitive manifold which covers R, with cusps isometric to S.

It remains to show that, up to arbitrarily small perturbations, every flat metric on the torus or the Klein bottle admits a tessellation by regular hexagons.

First, consider a parallelogram fundamental domain D_T for the torus, and overlay it onto a tessellation of small regular hexagons. We can perturb D_T by moving three vertices to the nearest hexagon center, and the fourth in such a way as to make a parallelogram; the fourth vertex will also fall into the center of a hexagon. This gives our desired tessellation.

As for the Klein bottle, the generic fundamental domain D_K is a rectangle, with two opposite sides s_1,s_2 identified with a twist. We overlay D_K onto a tessellation of small regular hexagons with some sides parallel to s_1,s_2. We can perturb D_K by translation or scaling along either axis, obtaining a rectangle with all vertices at the centers of hexagons. Note that the tessellation is symmetrical with respect to the line joining the midpoints of the perturbed s_1 and s_2. Hence, we have a tessellation of the Klein bottle. □

4.5 Lots of manifolds

In this section we prove the following theorem.

Theorem 4.5.1. *For every closed flat 3-manifold N, there exists a positive constant c such that, for sufficiently large $V > 0$, there exist at least V^{cV} complete hyperbolic 4-manifolds with pairwise isometric cusps of type N and volume $\leq V$.*

Proof. Let R be a reflectofold constructed as in the proof of Theorem 4.2.6 or 4.3.4 (according to N). Let D be the Coxeter diagram with one vertex for each facet of R, where if two facets meet with dihedral angle of π/k (resp. do not intersect), the corresponding vertices are joined by an edge labeled k (resp. a dashed edge).

If R is constructed from a sufficiently fine subdivision of a tessellation, then the diagram D is connected. Indeed, two non-adjacent facets are connected by a dashed edge, while for any two adjacent facets F, F' there exists a third one not adjacent to them (in the projection onto the link, it can be found in a large embedded ball centered on, say, F). As a consequence, we can also assume that D has a dashed edge.

Let G be the Coxeter group associated to D. It is neither affine nor spherical, since D has a dashed edge (compare [Vin85, Tables 1-2]). By [MV00, Corollary 2], G has a finite-index subgroup H with a quotient isomorphic to the free group F_2. Since H is a subgroup of a Coxeter group, it has a torsion-free subgroup H' such that $d \coloneqq [G : H'] < +\infty$. The image of H' in F_2 is free of rank at least 2, so H' also has a quotient isomorphic to F_2. Recall that F_2 has at least $r \cdot r!$ subgroups of index $\leq r$ [Hal49]. Hence, by pulling back to H', we obtain at least $r \cdot r!$ torsion-free subgroups of G of index $\leq dr$. These correspond to manifold covers of R with degree $\leq dr$, which have pairwise isometric cusps of type N by construction. As at the beginning of this chapter, we can show that these manifolds are complete; indeed, they are obtained by gluing polytopes, and have complete cusp sections (see [Rat19, Theorem 11.1.6]).

Let v be the volume of R and let $V \coloneqq vdr$. Then our manifolds have volume $\leq V$. Using Stirling's approximation, we have the following estimate (for some $k, k', c > 0$

and for r large):

$$\begin{aligned}\log(r \cdot r!) &= \log r + \log r! \\ &= \log r + r \log r - r + O(\log r) \\ &\geq kr \log r \\ &= k' \frac{V}{vd} \log \frac{V}{vd} \\ &\geq cV \log V \\ &= \log(V^{cV}).\end{aligned}$$

Hence, we have at least V^{cV} torsion-free subgroups of G. The associated manifolds (of volume $\leq V$) are not necessarily distinct; however, the same estimate holds on the number of isometry classes, with a smaller constant c. Indeed, if G is non-arithmetic, we conclude with the same argument of [Bur+02, "The lower bound"] using Margulis' theorem on the commensurator [Mar91, Theorem 1, p. 2], while if G is arithmetic, we conclude as in [Bel+10, Section 5.2] using the Kazhdan–Margulis theorem. □

Remark 4.5.2. Note that, since we take subgroups of G which are not necessarily normal, the group G does not act on the associated covers. Hence, we do not necessarily get cusp-transitive manifolds.

Chapter 5

A cusped hyperbolic 4-manifold without spin structures

This chapter is based on the paper [RR25]. We build a non-compact, orientable, hyperbolic four-manifold of finite volume that does not admit any spin structure. As in the other chapters, this is achieved by glueing copies of a Coxeter polytope.

5.1 Summary

As already explained in Section 1.2, like in [MRS20; MRS21] for the compact case, our goal is to prove the following:

Theorem 5.1.1. *There exists a cusped, oriented, arithmetic, hyperbolic* 4*-manifold* M *that contains an oriented surface* S *with self-intersection* $S \cdot S = 1$*.*

A *(hyperbolic) manifold with (right-angled) corners* is a complete hyperbolic manifold with boundary X, locally modeled on an orthant of $\mathbb{H}^n$. The connected submanifolds with boundary that naturally stratify ∂X are called *faces*. We call *facets* and *corners* the $(n-1)$-dimensional and $(n-2)$-dimensional faces, respectively. Each face is naturally the image under a local isometry of a manifold with corners. These local isometries are all embeddings precisely when every corner is the intersection of two facets.

An n-manifold with corners and embedded facets X is contained in a hyperbolic n-manifold M without boundary, obtained in a standard way by iteratively doubling and re-doubling X along its facets (see Section 5.3.5). So, to prove Theorem 5.1.1, we are reduced to building a cusped 4-manifold with corners X with embedded faces and a surface $S \subset X$ such that $S \cdot S = 1$.

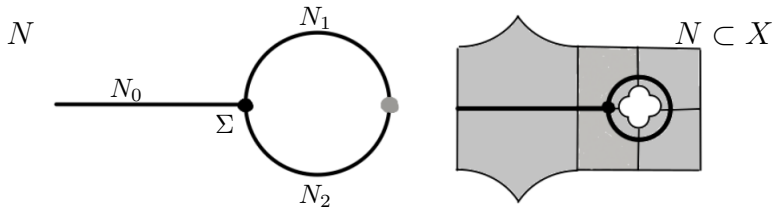

Figure 5.1: On the left, a schematic picture of the three-dimensional thickening $N = N_0 \cup N_1 \cup N_2$ of the piecewise geodesic surface $S = S_0 \cup S_1 \cup S_2$, where $S_i \subset N_i$ are totally geodesic manifolds with corners. It is not a manifold near the auxiliary surface with corners $\Sigma = N_0 \cap N_1 \cap N_2$ (represented by a black dot). On the right, the thickening X of N: a 4-manifold with corners, neighbourhood of S in M, tessellated by some copies of Q^4 (represented by 10 gray pentagons)

The surface S cannot be contained in an orientable 3-manifold in M, otherwise $S \cdot S = 0$. Similarly to [MRS20], it will instead be contained in a "locally Y-shaped piece" N obtained by gluing three 3-manifolds with corners N_0, N_1 and N_2 (also) along an isometric facet Σ (see Figure 5.1–left). The intersection $\Theta = \Sigma \cap S = \gamma_0 \cup \gamma_1 \cup \gamma_2$ is a theta-graph that trisects S in three pieces S_0, S_1 and S_2, with S_i properly embedded in N_i and $\gamma_i = \Sigma \cap S_i$ a boundary component of S_i (see Figure 5.3). The 4-manifold with corners X will be a thickening of N (see Figure 5.1–right), and will contain S with $S \cdot S = \pm 1$ by construction (see Figure 5.10).

All Θ, Σ, S and N will be contained in the skeleta of the tessellation of X in copies of Q^4. The auxiliary surface Σ is totally geodesic, while S is pleated. Moreover, Σ and S are tessellated by Q^2's and N by Q^3's. Each N_i is totally geodesic in X, and $N_0 \perp N_1, N_2$. The thickenings $S \subset N \subset X$ are built via the sequence $Q^2 \subset Q^3 \subset Q^4$.

5.2 The polytope

We introduce here Kerckhoff and Storm's right-angled hyperbolic 4-polytope Q^4 [KS16]. Let us identify the hyperbolic 4-space $\mathbb{H}^4$ with the upper sheet of the hyperboloid $\langle x, x \rangle = -1$ in the Minkowski 5-space $\mathbb{R}^{1,4}$. Here $\langle x, y \rangle = -x_0 y_0 + x_1 y_1 + \ldots + x_4 y_4$ for $x = (x_0, \ldots, x_4), y = (y_0, \ldots, y_4) \in \mathbb{R}^{1,4}$. Given a spacelike vector $v \in \mathbb{R}^{1,4}$, the inequality $\langle x, v \rangle \leq 0$ defines a half-space of $\mathbb{H}^4$. Let[1] $Q^4 \subset \mathbb{H}^4$ be the intersection of the 22 half-spaces given by the vectors in Table 5.1. It is an unbounded, right-angled polytope of finite volume [KS16, Proposition 13.1].

Note that the isometry a defined by $a(x_0, x_1, \ldots, x_4) = (x_0, -x_1, \ldots, -x_4)$ is a symmetry of Q^4. Moreover, the notation (taken from [Rio24]) is such that we

[1] In [KS16; MR18], Q^4 is denoted by P_t, where $t = t_4 = \bar{t} = \sqrt{3}/3$.

$$
\begin{aligned}
E_1 &= \big(\sqrt{2}, +1, +1, +1, +\sqrt{3}\big) & H_1 &= \big(\sqrt{2}, -1, -1, -1, +\sqrt{3}/3\big)\\
E_1' &= \big(\sqrt{2}, -1, -1, -1, -\sqrt{3}\big) & H_1' &= \big(\sqrt{2}, +1, +1, +1, -\sqrt{3}/3\big)\\
E_2 &= \big(\sqrt{2}, +1, -1, -1, +\sqrt{3}\big) & H_2 &= \big(\sqrt{2}, -1, +1, +1, +\sqrt{3}/3\big)\\
E_2' &= \big(\sqrt{2}, -1, +1, +1, -\sqrt{3}\big) & H_2' &= \big(\sqrt{2}, +1, -1, -1, -\sqrt{3}/3\big)\\
E_3 &= \big(\sqrt{2}, -1, +1, -1, +\sqrt{3}\big) & H_3 &= \big(\sqrt{2}, +1, -1, +1, +\sqrt{3}/3\big)\\
E_3' &= \big(\sqrt{2}, +1, -1, +1, -\sqrt{3}\big) & H_3' &= \big(\sqrt{2}, -1, +1, -1, -\sqrt{3}/3\big)\\
E_4 &= \big(\sqrt{2}, -1, -1, +1, +\sqrt{3}\big) & H_4 &= \big(\sqrt{2}, +1, +1, -1, +\sqrt{3}/3\big)\\
E_4' &= \big(\sqrt{2}, +1, +1, -1, -\sqrt{3}\big) & H_4' &= \big(\sqrt{2}, -1, -1, +1, -\sqrt{3}/3\big)\\
C_{12} &= \big(1, +\sqrt{2}, 0, 0, 0\big) & C_{34} &= \big(1, -\sqrt{2}, 0, 0, 0\big)\\
C_{13} &= \big(1, 0, +\sqrt{2}, 0, 0\big) & C_{24} &= \big(1, 0, -\sqrt{2}, 0, 0\big)\\
C_{14} &= \big(1, 0, 0, +\sqrt{2}, 0\big) & C_{23} &= \big(1, 0, 0, -\sqrt{2}, 0\big)
\end{aligned}
$$

Table 5.1: The spacelike vectors of $\mathbb{R}^{1,4}$ that define the polytope $Q^4 \subset \mathbb{H}^4$.

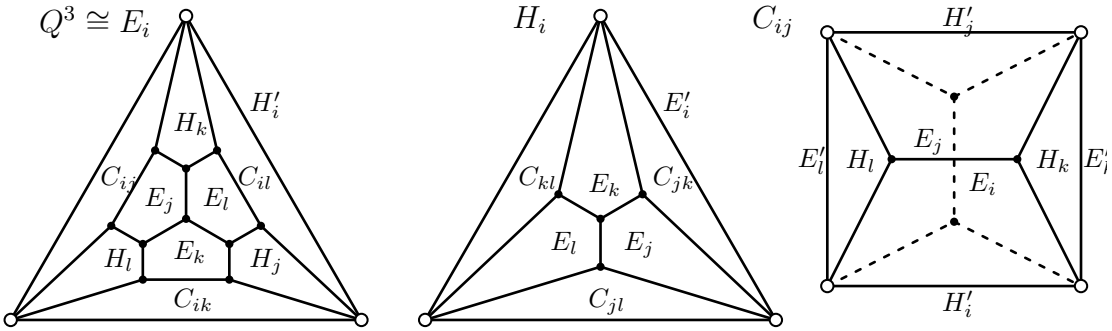

Figure 5.2: The extremal, half-height and central facets $E_i \cong Q^3$, H_i and C_{ij} of Q^4, where $\{i, j, k, l\} = \{1, 2, 3, 4\}$. The ideal vertices are in white. Note the compact pentagon $E_i \cap E_j \cong Q^2$.

have $E_i' = a(E_i)$, $H_i' = a(H_i)$, and $C_{ij} = a(C_{kl})$ for all distinct i, j, k, l. The combinatorics of Q^4 has been studied in detail in [MR18, Proposition 3.16]. Each vector in Table 5.1 corresponds to a facet of Q^4, denoted with the same symbol. The 22 facets, depicted in Figure 5.2, are partitioned up to symmetry into three sets:[2]

1. the *extremal facets* $E_1, E_2, E_3, E_4, E_1', E_2', E_3', E_4'$,
2. the *half-height facets* $H_1, H_2, H_3, H_4, H_1', H_2', H_3', H_4'$,
3. the *central facets* $C_{12}, C_{13}, C_{14}, C_{23}, C_{24}, C_{34}$.

Lemma 5.2.1. *Every combinatorial automorphism of Q^4 is realized by an isometry of Q^4, and every hyperbolic orbifold O tessellated by finitely-many copies of Q^4 is commensurable with $\mathbb{H}^4/\mathrm{PO}(1,4;\mathbb{Z})$.*

Proof. The poof of the first statement (relying on [RS19, Proposition 2.4] and [MR18, Lemma 4.15]) is the same of [Rio24, Lemma 1.2] by [MR18, Section 3.2 and Proposition 3.16]. In particular (see Figure 5.2), every isometry between two facets of Q^4 is the restriction of an isometry of Q^4. Since, by hypothesis, O can be obtained by gluing the facets of some copies Q^4 in pairs via isometries, O covers the orbifold $Q^4/\mathrm{Isom}(Q^4)$, and so it is commensurable with $Q^4 = \mathbb{H}^4/\Gamma$. The reflection group $\Gamma < \mathrm{PO}(1,n)$ of Q^4 is arithmetic [KS16, Theorem 13.2] and commensurable with $\mathrm{PO}(1,4;\mathbb{Z})$ [MR18, Proposition 4.25]. □

Note from Figure 5.2 that the compact 2-faces of Q^4 are 12 isometric pentagons $E_i \cap E_j$, $E_i' \cap E_j'$, $i \neq j$. Defining

$$Q^2 = E_1 \cap E_2 \text{ and } Q^3 = E_1,$$

we have a sequence of right-angled polytopes:

$$Q^2 \subset Q^3 \subset Q^4.$$

We shall think of Q^{n+1} as sitting above its *bottom facet* Q^n, and call the remaining facets *vertical facets* and *top facets*, depending on whether they are adjacent to Q^n or not, respectively. For example, Q^3 has 5 vertical facets and 4 top facets, while Q^4 has 10 vertical facets and 11 top facets.

[2] In [KS16; MR18], these are called: the "positive walls", the "negative walls", and the "letter walls", respectively.

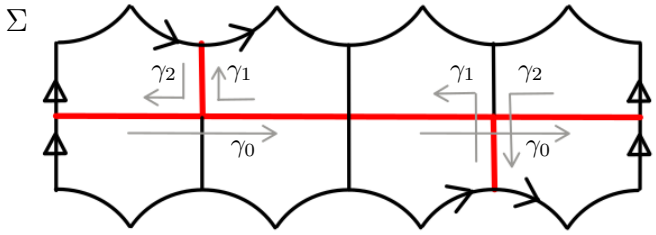

Figure 5.3: The surface Σ with corners obtained by gluing 8 copies of the right-angled pentagon Q^2 (four edges of the big dodecagon are glued in pairs as indicated by the black arrows). It is a holed torus, and deformation retracts onto the red theta-graph $\Theta = \gamma_0 \cup \gamma_1 \cup \gamma_2$. The three red oriented curves γ_0, γ_1 and γ_2 go as indicated by the gray arrows.

5.3 The construction

In this section, we prove Theorem 5.1.1. We first build the auxiliary surface with corners Σ, and thicken it to a 3-manifold with corners Σ^{thick} homeomorphic to $\Sigma \times [0,1]$. Then, we build the 3-manifolds with corners N_0, N_1 and N_2 by gluing some of the top facets of Σ^{thick} in three different ways, and the 3-manifold with corners N_{12} by gluing together N_1 and N_2. After that, we glue the 3-manifolds with corners N_0 and N_{12} and thicken the resulting "locally Y-shaped piece" N to a 4-manifold with corners X. Then we study X, and finally build the 4-manifold M.

5.3.1 The surface with corners Σ and its thickening Σ^{thick}

Let Σ be the surface with corners obtained by gluing in pairs some edges of 8 copies of Q^2 via the identity map, as indicated in Figure 5.3. Topologically, Σ is a once-holed torus. Consider the three oriented curves γ_0, γ_1 and γ_2 in the 1-skeleton of Σ as in Figure 5.3. The surface Σ is a thickening of the theta-graph $\Theta = \gamma_0 \cup \gamma_1 \cup \gamma_2$.

We now place a copy of Q^3 "above" each Q^2 in Σ, to get a 3-manifold with corners Σ^{thick} homeomorphic to $\Sigma \times [0,1]$: the vertical faces of the Q^3's containing the paired edges of the Q^2's in Σ are glued correspondingly via the identity map. So Σ^{thick} has three types of facets: the *bottom facet* Σ, and the *vertical* and *top facets* tessellated by the facets of Q^3 of the corresponding type. The top facets are 8 ideal triangles, 4 ideal rectangles and 3 ideal hexagons, pleated with right angles along the pattern showed in Figure 5.4.

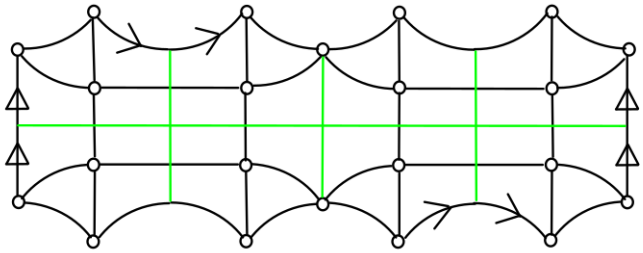

Figure 5.4: The top of the 3-manifold with corners Σ^{thick}. The green lines indicate its tessellation into 8 copies of Q^3. As usual, the ideal vertices are in white.

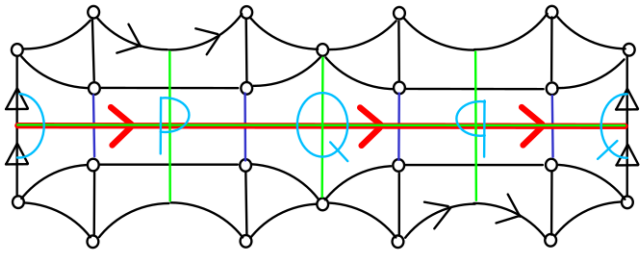

Figure 5.5: The 3-manifold with corners N_0 is built by gluing some top facets of Σ^{thick} as indicated by the blue letters P and Q. It has 5 top facets. The four vertical blue edges are glued making an angle of 2π.

5.3.2 The 3-manifolds with corners N_0, N_1, N_2 and N_{12}

Let N_0, N_1 and N_2 be obtained by gluing some top facets of Σ^{thick} in pairs via the identity map, as indicated by Figures 5.5, 5.6 and 5.7, respectively.

Figure 5.5 helps to verify that N_0 is a 3-manifold with corners and embedded facets: the four glued corners are cyclically glued together in the interior of N_0, and each of the remaining corners is right-angled and belongs to two distinct facets. Moreover, the 8 copies of Q^3 in N_0 that are adjacent to Σ are distinct. The check for N_1 and N_2 is even simpler, and is left to the reader.

For $i = 0, 1, 2$, consider the surface with corners $S_i' \cong \gamma_i \times [0, 1]$ in the 2-skeleton of Σ^{thick}, tessellated by the vertical pentagons that have an edge in $\gamma_i \subset \Sigma \subset \Sigma^{\text{thick}}$. The red line in Figures 5.5, 5.6 and 5.7 is the top of S_i'. We call S_i the surface in N_i obtained from S_i' after the gluing. Both N_i and S_i are orientable, since the gluings reverse the orientation of both the glued polygons and the red curve.

We conclude by gluing together N_1 and N_2 as follows: we glue their two bottom facets (copies of Σ) via the identity map, and some of their top facets as in Figure 5.8. We call N_{12} the resulting 3-manifold with corners. Again, it is easy to check

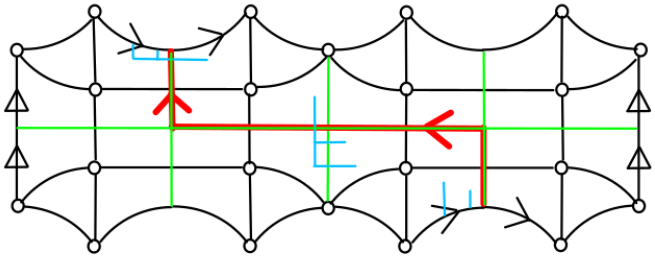

Figure 5.6: The top of the 3-manifold with corners N_1.

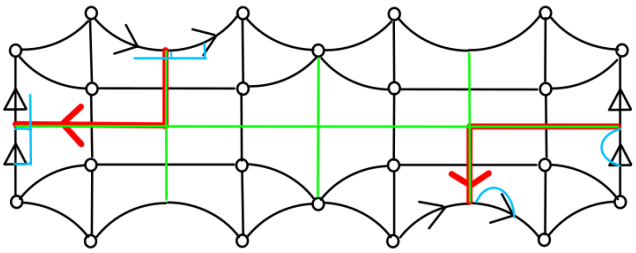

Figure 5.7: The top of the 3-manifold with corners N_2.

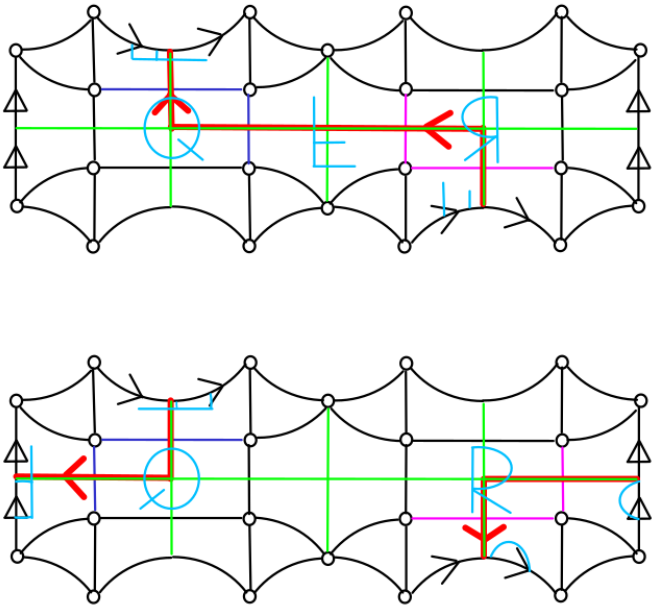

Figure 5.8: The top of the 3-manifold with corners N_{12}, obtained by pairing some top facets of N_1 (top) and N_2 (bottom) as indicated by the symbols P, Q, R and F, and the two bottom facets. It has 15 top facets. The four blue (resp. pink) edges are glued making an angle of 2π.

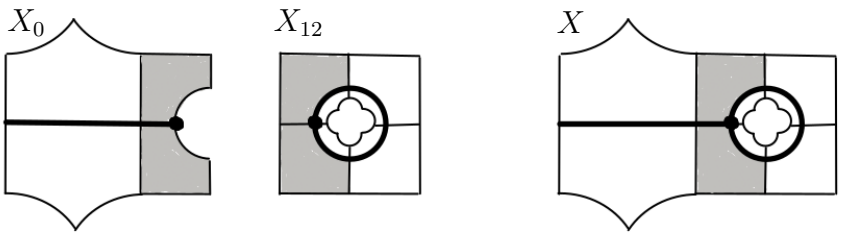

Figure 5.9: A schematic picture of X (right), obtained by gluing the thickenings X_0 and X_{12} of N_0 and N_{12} (left). The pentagons, thick segment, circle and dot represent the copies of Q^4, the 3-manifolds N_0 and N_{12}, and the surface Σ, respectively.

that N_{12} is an orientable 3-manifold with corners and embedded facets, that the 16 copies of Q^3 in N_{12} incident to $\Sigma \subset N_{12}$ are distinct, and that $S_{12} = S_1 \cup S_2$ is an orientable surface embedded in N_{12} with $\partial S_{12} = \gamma_1 \sqcup \gamma_2$.

5.3.3 The spine N and its thickening X

Let N be obtained by gluing N_0 and N_{12} via the identity map along their two isometric copies of Σ: the bottom facet of N_0 and the properly embedded surface in N_{12} obtained by identifying the two bottom facets of N_1 and N_2. It is not a manifold (see Figure 5.1–left).

We now want to thicken N to a 4-manifold with corners X in which N_0 and N_{12} are totally geodesic and orthogonal. Similarly to [MRS20; MRS21], this can be done in two steps.

We first thicken N_0 and N_{12} separately: we place two copies of Q^4 on every copy of Q^3, one "below" and the other "above", and get two 4-manifolds with corners X_0 and X_{12}; see Figure 5.9–left. These are obtained by pairing some vertical facets of some copies of Q^4 with the identity as gluing maps.

Then, we identify in pairs the copies of Q^4 in X_0 incident to Σ with the copies of Q^4 in X_{12} incident to Σ from below, as in Figure 5.9–right. We can do this since for every pentagonal face F of Q^4, there exists an isometry of Q^4 that exchanges the two facets (isometric to Q^3) that share F. The resulting complex X contains N as desired.

5.3.4 The 4-manifold with corners X

By construction, X is a complete and orientable hyperbolic 4-manifold with boundary. Since it is tessellated by copies of Q^4, which is right angled, a priori the angles at the corners are multiples of $\pi/2$. Our aim is now to show that the angles are

$\pi/2$ and the facets are embedded.

Proposition 5.3.1. *The thickening X is a hyperbolic manifold with right-angled corners.*

Proof. Every copy of a pentagonal face $F_i \cap F_j \cong Q^2$ of Q^4 contained in ∂X is shared by at most two copies of Q^4 in X. Indeed, as we see from Figure 5.2, if F and F' are two facets of Q^4 such that $F \cap E_i \neq \emptyset$, $F \cap E_j = \emptyset$, $F' \cap E_i = \emptyset$, $F' \cap E_j \neq \emptyset$, then $F \cap F' = \emptyset$. □

We now want to show that X has embedded facets. We begin by showing that X_0 and X_{12} have embedded facets. Let Y be a facet of X_0 or X_{12}. Since the latter are obtained by gluing copies of Q^4 along facets with the identity, Y is a union of copies of a facet F of Q^4. Consider a corner C of X contained in Y. It is not possible that both sides of C are in Y. Indeed, Q^4 is right-angled, hence both sides of C are in the same copy of Q^4 and, of course, there is only one facet F in Q^4.

Proposition 5.3.2. *The facets of X are embedded.*

Proof. We argue similarly to the previous paragraph. Let $i\colon X_0 \to X$ and $j\colon X_{12} \to X$ be the natural inclusion embeddings. Let Y be a facet of X. If Y is entirely contained in $i(X_0)$ or $j(X_{12})$, then we easily conclude as in the previous paragraph. Otherwise, $Y \cap i(X_0)$ is union of copies of the facet F of Q^4 and $Y \cap j(X_{12})$ is union of copies of the facet $f(F)$ of Q^4, where f is the isometry used for the identification in the construction of X starting from X_0 and X_{12}. We conclude as before, since Q^4 has only one facet F and one facet $f(F)$. □

The construction ensures the following.

Proposition 5.3.3. *The surface $S = S_0 \cup S_{12}$ has self-intersection ± 1 in X.*

Proof. We isotope N inside a regular neighbourhood U of N in X as follows. Say that $U = U_0 \cup U_{12}$ for two tubular neighbourhoods U_0 and U_{12} of N_0 and N_{12}. The latter are two-sided. Call U_+ and U_- the two sides of U_{12}, with $U_+ \cup U_- = U_{12}$ and $U_+ \cap U_- = N_{12}$.

We first move N in one direction as in Figure 5.10–left, obtaining an isotopic copy $N' = N'_0 \cup N'_{12}$ of N transverse to it, with $N' \cap N \subset U_{12}$. Then, to remove the intersection with N'_{12}, we "push" $N' \cap U_+$ in the interior of U_- as in Figure 5.10–right, obtaining $N'' = N'_0 \cup N''_{12}$.

Then the surface $\Sigma''' = N \cap N'' = N_{12} \cap N'_0$ is a surface parallel to Σ and Σ''. Moreover, S and its isotopic copy $S'' \subset N''$ intersect transversely at one point, corresponding to the transverse intersection of the simple closed curves $\gamma'''_0 = S_0 \cap \Sigma'''$ and $\gamma'''_2 = S_2 \cap \Sigma'''$ in Σ'''. Therefore $S \cdot S = S \cdot S'' = \pm 1$. □

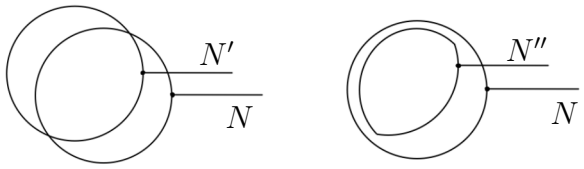

Figure 5.10: On the left, N and its isotopic copy N'. On the right, N and its isotopic copy N'', which transversely intersects N in the point $S \cap S''$, so $S \cdot S = S \cdot S'' = \pm 1$.

5.3.5 The 4-manifold M

Let $Y_1, \ldots, Y_m$ the facets of X. We now double X along Y_1, then double the result along the copies of Y_2, and continue iteratively, until we get a 4-manifold M without boundary tessellated by 2^m copies of X. Since the facets of X are embedded, M is hyperbolic manifold (see e.g. [Mar22, Proposition 6]). Moreover, M is arithmetic by Lemma 5.2.1. To complete the proof of Theorem 5.1.1, it suffices to choose the orientation of M such that $S \cdot S = +1$.

Chapter 6

Tables and Figures

For reasons of space, we collect here the information (I2) on P_n for $n = 0, \ldots, 8$, and the information (I3) on P_n for $n = 2, \ldots, 8$, regarding Chapter 3.

3	1

Table 6.1: Type-3 and type-7 adjacency matrices of P_0.

7	1

3	1

Table 6.2: Type-3 and type-7 adjacency matrices of P_1.

7	1

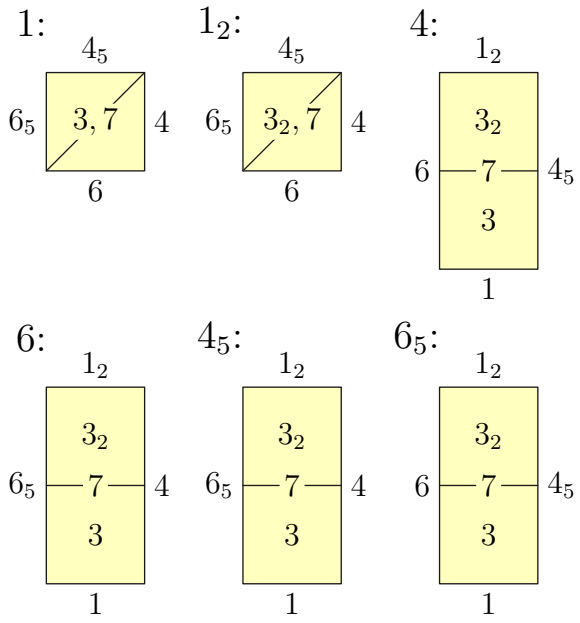

Figure 6.1: The facets of L_2.

3	1	2
3_2	2	1

7	1

Table 6.3: Type-3 and type-7 adjacency matrices of P_2.

3	1	2	3	
3_2	2	1		3
3_{4_5}	3		1	2
$3_{4_5,2}$		3	2	1

7	1

Table 6.4: Type-3 and type-7 adjacency matrices of P_3.

3	1	2	3		3			
3_2	2	1		3		3		
3_{4_5}	3		1	2			3	
$3_{4_5,2}$		3	2	1				3
3_4	3				1	2	3	
$3_{4,2}$		3			2	1		3
$3_{4,4_5}$			3		3		1	2
$3_{4,4_5,2}$				3		3	2	1

7	1

Table 6.5: Type-3 and type-7 adjacency matrices of P_4.

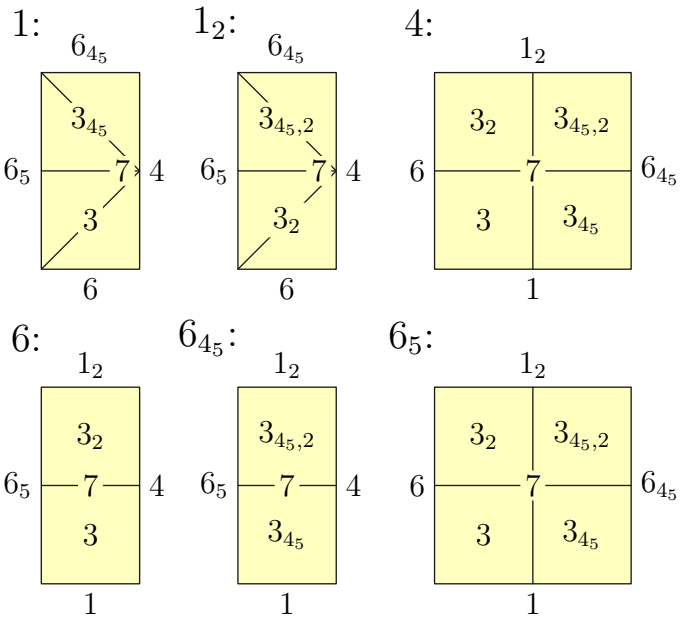

Figure 6.2: The facets of L_3

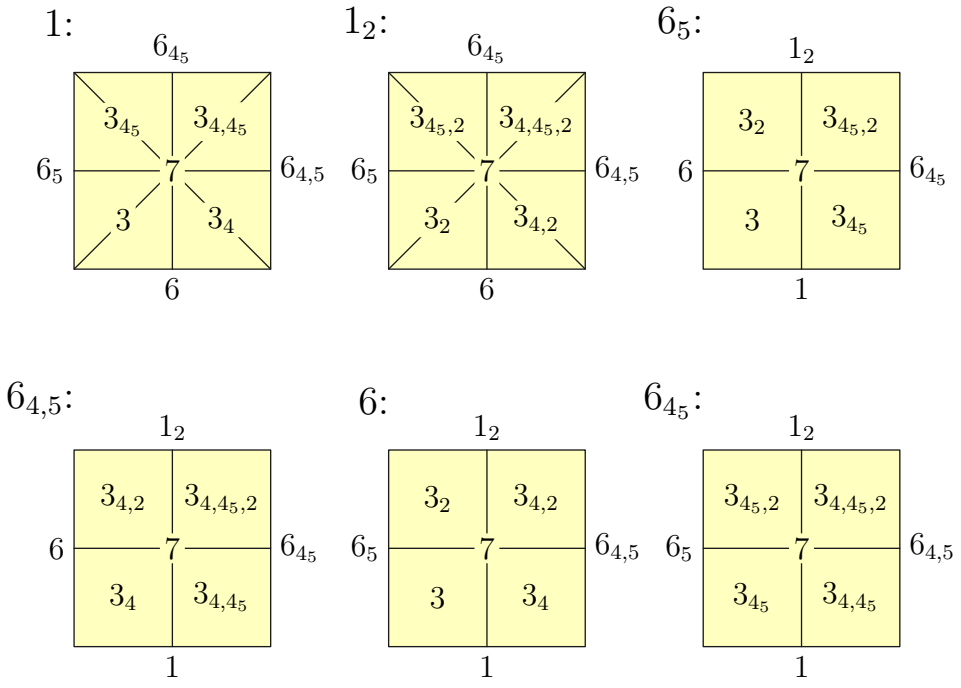

Figure 6.3: The facets of L_4.

3	1	2	3		3				3			
3_2	2	1		3		3						
3_{4_5}	3		1	2			3			3		
$3_{4_5,2}$		3	2	1				3				
3_4	3				1	2	3				2	
$3_{4,2}$		3			2	1		3				
$3_{4,4_5}$			3		3		1	2				2
$3_{4,4_5,2}$				3		3	2	1				
$3_{1,2}$	3								1	3	3	
$3_{1,4_5,2}$			3						3	1		3
$3_{1,4,2}$					2				3		1	3
$3_{1,4,4_5,2}$							2			3	3	1

7	1	2
7_1	2	1

Table 6.6: Type-3 and type-7 adjacency matrices of P_5.

3	1	2	3		3				3				3					
3_2	2	1		3		3								3				
3_{4_5}	3		1	2			3			3								
$3_{4_5,2}$		3	2	1				3										
3_4	3				1	2	3				2				3			
$3_{4,2}$		3			2	1		3								3		
$3_{4,4_5}$			3		3		1	2				2						
$3_{4,4_5,2}$				3		3	2	1										
$3_{1,2}$	3								1	3	3						3	
$3_{1,4_5,2}$			3						3	1		3						
$3_{1,4,2}$					2				3		1	3						3
$3_{1,4,4_5,2}$							2			3	3	1						
$3_{6,4_5}$	3												1	2	3		3	
$3_{6,4_5,2}$		3											2	1		3		
$3_{6,4,4_5}$					3								3		1	2		3
$3_{6,4,4_5,2}$						3								3	2	1		
$3_{6,1,4_5,2}$									3				3				1	3
$3_{6,1,4,4_5,2}$											3				3		3	1

7	1	2	3	
7_1	2	1		3
7_6	3		1	2
$7_{6,1}$		3	2	1

Table 6.7: Type-3 and type-7 adjacency matrices of P_6.

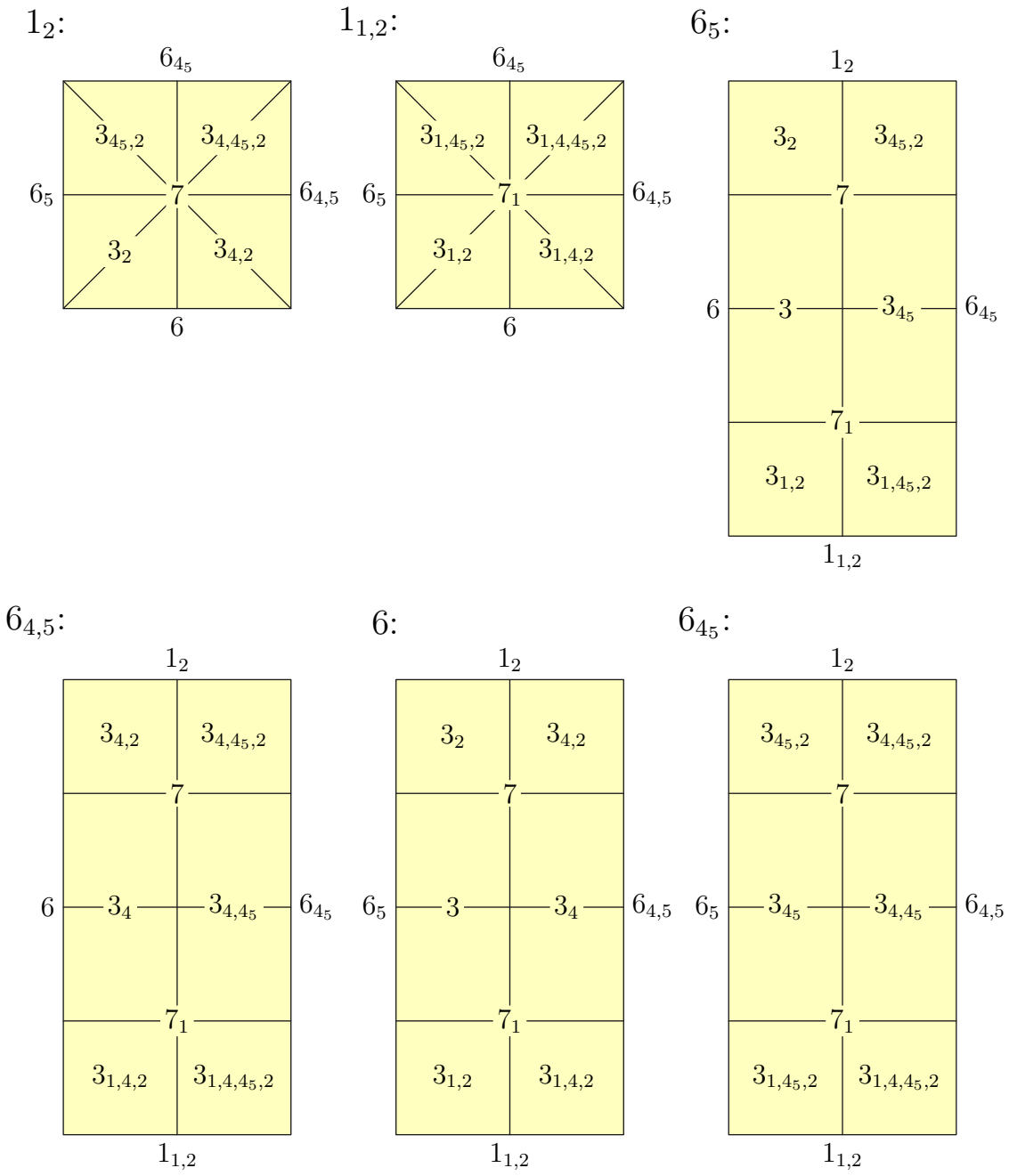

Figure 6.4: The facets of L_5.

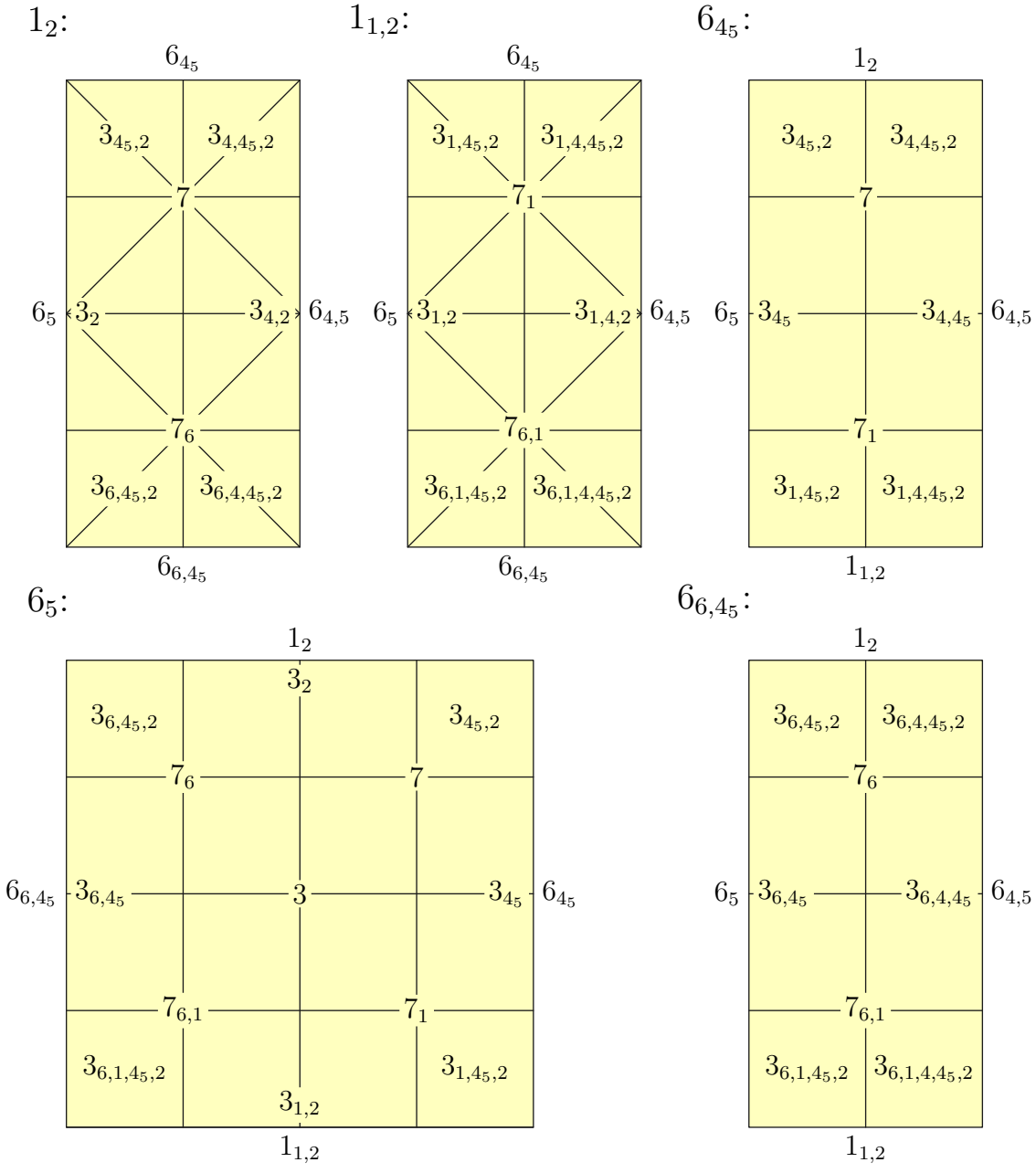

Figure 6.5: Some facets of L_6.

3	1	2	3		3				3				3					3							
3_2	2	1		3		3								3					3						
3_{4_5}	3		1	2			3			3										3					
$3_{4_5,2}$		3	2	1				3													3				
3_4	3				1	2	3				2				3										
$3_{4,2}$		3			2	1		3								3									
$3_{4,4_5}$			3		3		1	2				2													
$3_{4,4_5,2}$				3		3	2	1																	
$3_{1,2}$	3								1	3	3						3					3			
$3_{1,4_5,2}$			3						3	1		3											3		
$3_{1,4,2}$					2				3		1	3						3							
$3_{1,4,4_5,2}$							2			3	3	1													
$3_{6,4_5}$	3												1	2	3		3						3		
$3_{6,4_5,2}$		3											2	1		3								3	
$3_{6,4,4_5}$					3								3		1	2		3							
$3_{6,4,4_5,2}$						3								3	2	1									
$3_{6,1,4_5,2}$									3				3				1	3							3
$3_{6,1,4,4_5,2}$											3				3		3	1							
$3_{6_5,4}$	3																		1	2	3		2		3		
$3_{6_5,4,2}$		3																	2	1		3				3	
$3_{6_5,4,4_5}$			3																3		1	2		2			
$3_{6_5,4,4_5,2}$				3																3	2	1					
$3_{6_5,1,4,2}$									3										2				1	3			3
$3_{6_5,1,4,4_5,2}$										3											2		3	1			
$3_{6_5,6,4,4_5}$													3						3						1	2	3
$3_{6_5,6,4,4_5,2}$														3						3					2	1	
$3_{6_5,6,1,4,4_5,2}$																	3						3		3		1

7	1	2	3		3			
7_1	2	1		3		3		
7_6	3		1	2			3	
$7_{6,1}$		3	2	1				3
7_{6_5}	3				1	2	3	
$7_{6_5,1}$		3			2	1		3
$7_{6_5,6}$			3		3		1	2
$7_{6_5,6,1}$				3		3	2	1

Table 6.8: Type-3 and type-7 adjacency matrices of P_7.

3	1	2	3		3				3				3						3																										
3_2	2	1		3		3								3						3								2																	
3_{4_5}	3		1	2			3			3											3																								
$3_{4_5,2}$		3	2	1				3														3							2																
3_4	3				1	2	3				2				3																														
$3_{4,2}$		3			2	1		3								3														2															
$3_{4,4_5}$			3		3		1	2				2																																	
$3_{4,4_5,2}$				3		3	2	1																							2														
$3_{1,2}$	3								1	3	3						3						3																						
$3_{1,4_5,2}$			3						3	1		3												3																					
$3_{1,4,2}$					2				3		1	3						3																											
$3_{1,4,4_5,2}$							2			3	3	1																																	
$3_{6,4_5}$	3												1	2	3		3								3																				
$3_{6,4_5,2}$		3											2	1		3										3										2									
$3_{6,4,4_5}$					3								3		1	2		3																											
$3_{6,4,4_5,2}$						3								3	2	1																					2								
$3_{6,1,4_5,2}$									3				3				1	3									3																		
$3_{6,1,4,4_5,2}$											3				3		3	1																											
$3_{6_5,4}$	3																		1	2	3		2		3																				
$3_{6_5,4,2}$		3																	2	1		3				3																2			
$3_{6_5,4,4_5}$			3																3		1	2		2																					
$3_{6_5,4,4_5,2}$				3																3	2	1																			2				
$3_{6_5,1,4,2}$									3										2				1	3			3																		
$3_{6_5,1,4,4_5,2}$										3											2		3	1																					
$3_{6_5,6,4,4_5}$													3						3						1	2	3																		
$3_{6_5,6,4,4_5,2}$														3						3					2	1																		2	
$3_{6_5,6,1,4,4_5,2}$																	3						3		3		1																		
3_{1_2}		2																										1	3	3		3				3				3					
$3_{1_2,4_5}$				2																								3	1		3		3								3				
$3_{1_2,4}$						2																						3		1	3			2			3								
$3_{1_2,4,4_5}$								2																					3	3	1				2										
$3_{1_2,1,2}$																												3				1	3	3				3				3			
$3_{1_2,1,4_5,2}$																													3			3	1		3								3		
$3_{1_2,1,4,2}$																														2		3		1	3				3						
$3_{1_2,1,4,4_5,2}$																															2		3	3	1										
$3_{1_2,6,4_5}$														2														3								1	3	3						3	
$3_{1_2,6,4,4_5}$																2														3						3	1		3						
$3_{1_2,6,1,4_5,2}$																																3				3		1	3						3
$3_{1_2,6,1,4,4_5,2}$																																		3			3	3	1						
$3_{1_2,6_5,4}$																				2								3												1	3	2		3	
$3_{1_2,6_5,4,4_5}$																						2							3											3	1		2		
$3_{1_2,6_5,1,4,2}$																																3								2		1	3		3
$3_{1_2,6_5,1,4,4_5,2}$																																	3								2	3	1		
$3_{1_2,6_5,6,4,4_5}$																										2										3				3				1	3
$3_{1_2,6_5,6,1,4,4_5,2}$																																						3				3		3	1

7	1	2	3		3				2							
7_1	2	1		3		3										
7_6	3		1	2			3				2					
$7_{6,1}$		3	2	1				3								
7_{6_5}	3				1	2	3						2			
$7_{6_5,1}$		3			2	1		3								
$7_{6_5,6}$			3		3		1	2							2	
$7_{6_5,6,1}$				3		3	2	1								
7_{1_2}	2								1	2	3		3			
$7_{1_2,1}$									2	1		3		3		
$7_{1_2,6}$			2						3		1	2			3	
$7_{1_2,6,1}$										3	2	1				3
$7_{1_2,6_5}$					2				3				1	2	3	
$7_{1_2,6_5,1}$										3			2	1		3
$7_{1_2,6_5,6}$							2				3		3		1	2
$7_{1_2,6_5,6,1}$												3		3	2	1

Table 6.9: Type-3 and type-7 adjacency matrices of P_8.

$6_{4,5}$:

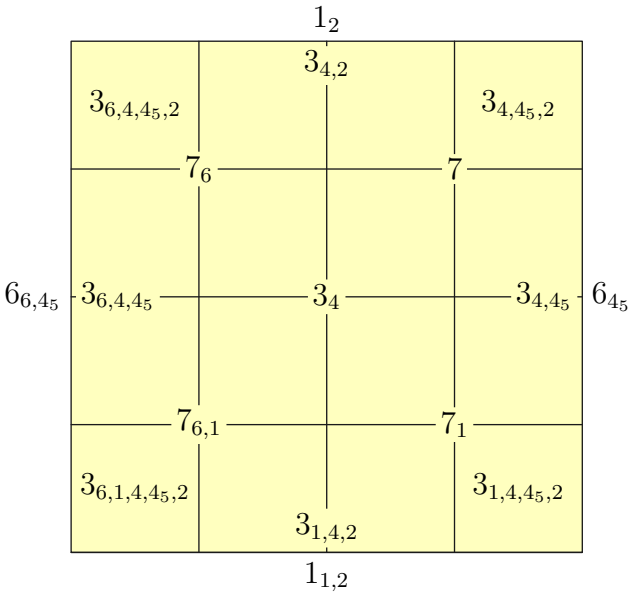

Figure 6.6: A facet of L_6.

1_2:

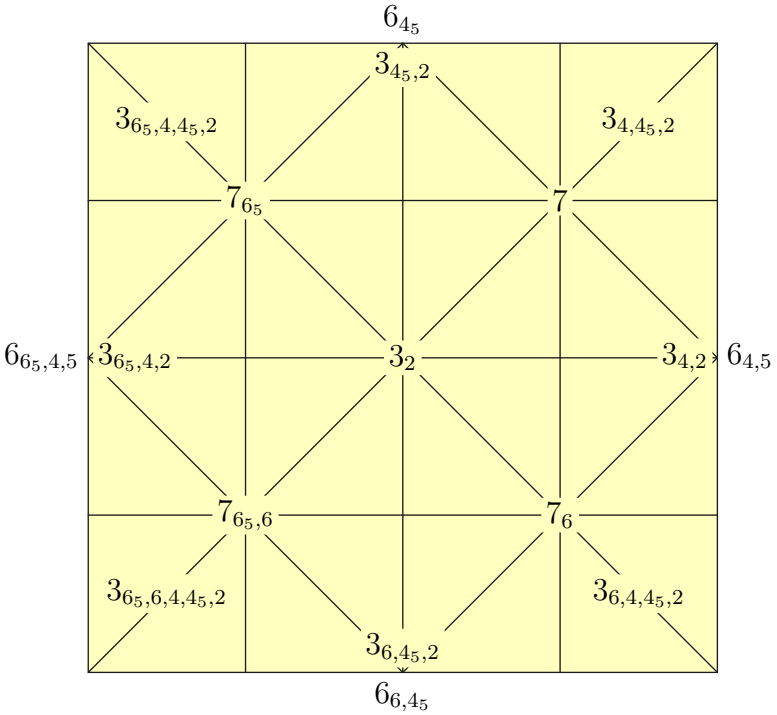

$1_{1,2}$:

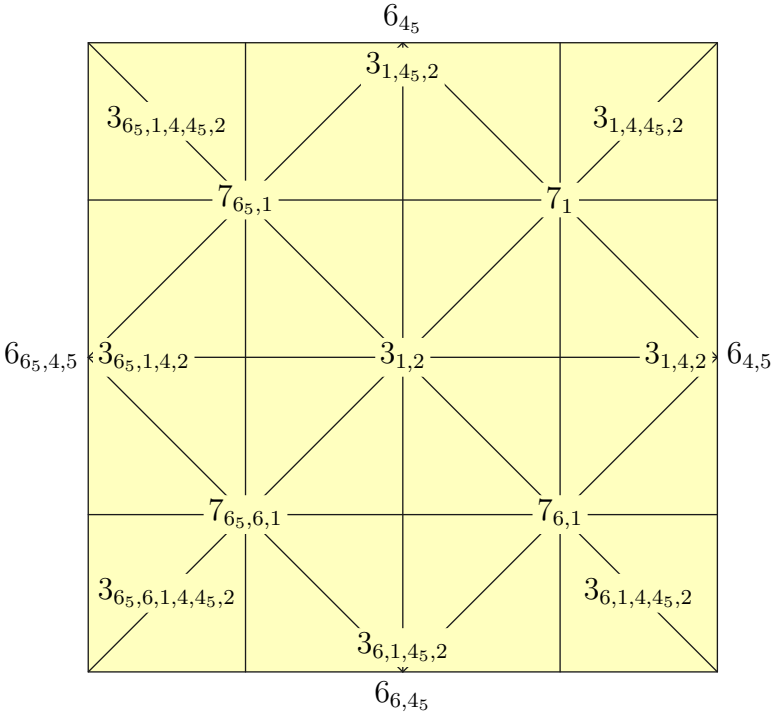

Figure 6.7: Some facets of L_7.

$6_{4,5}$:

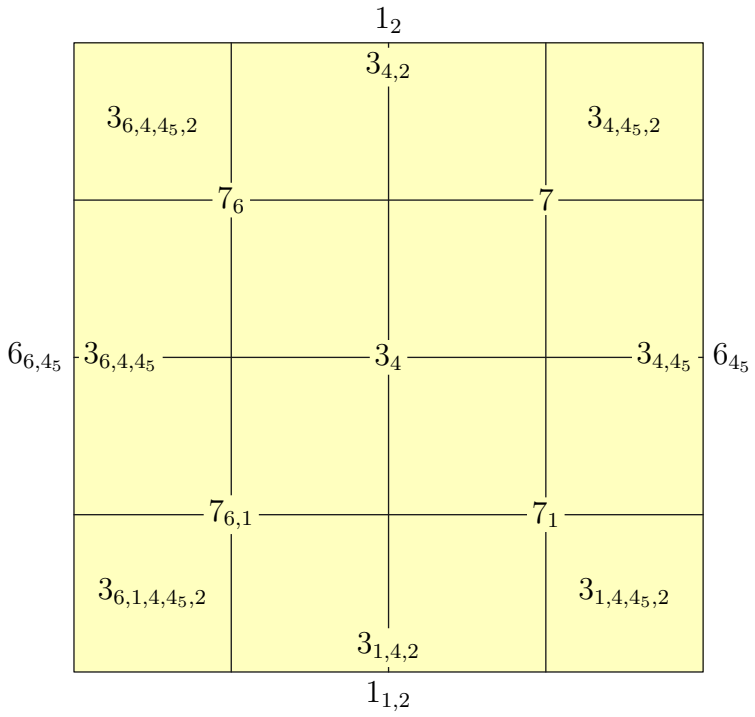

$6_{6_5,4,5}$:

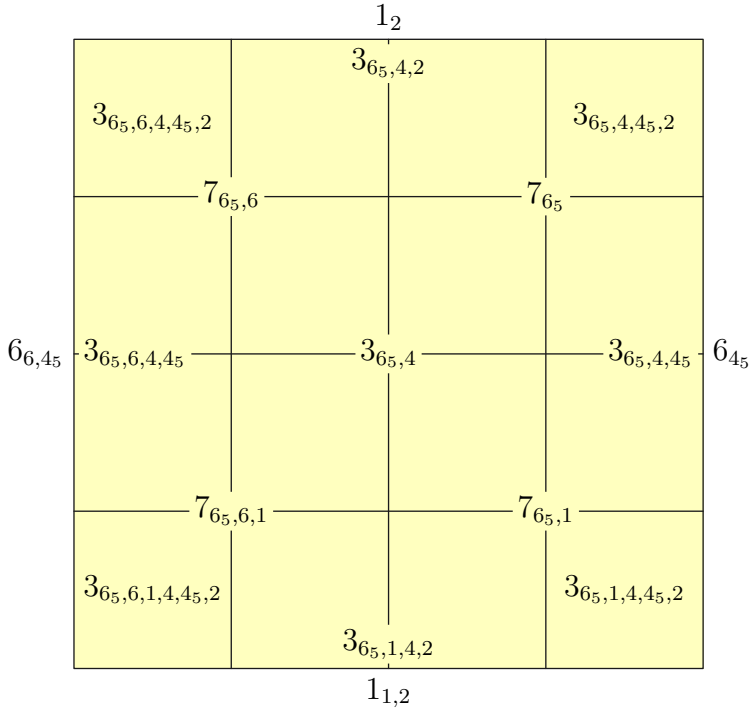

Figure 6.8: Some facets of L_7.

6_{4_5}:

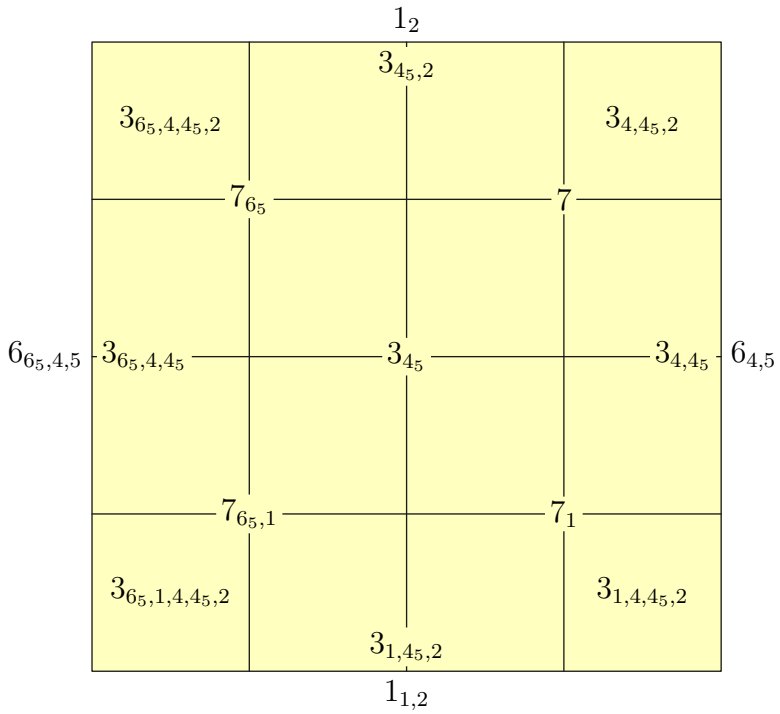

$6_{6,4_5}$:

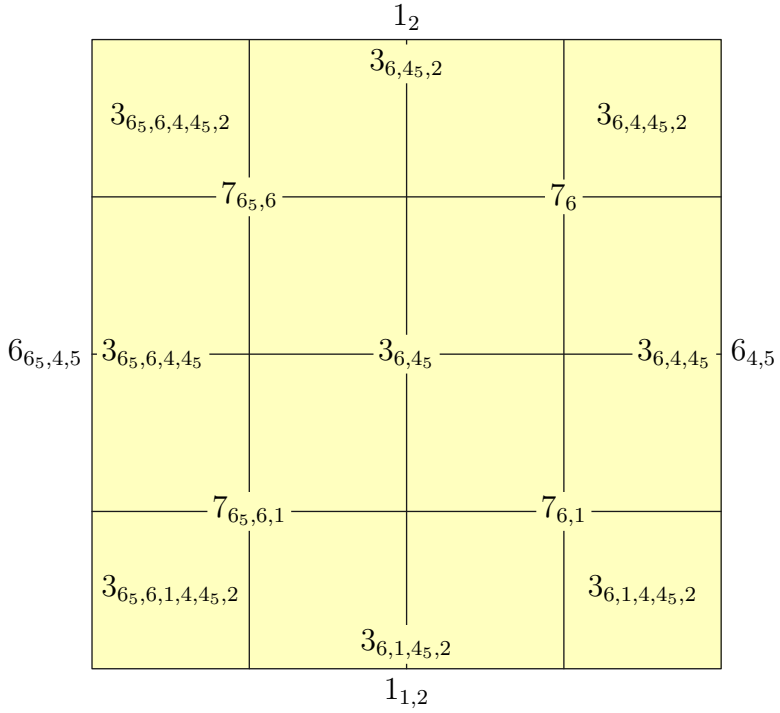

Figure 6.9: Some facets of L_7.

$1_{1_2,1,2}$:

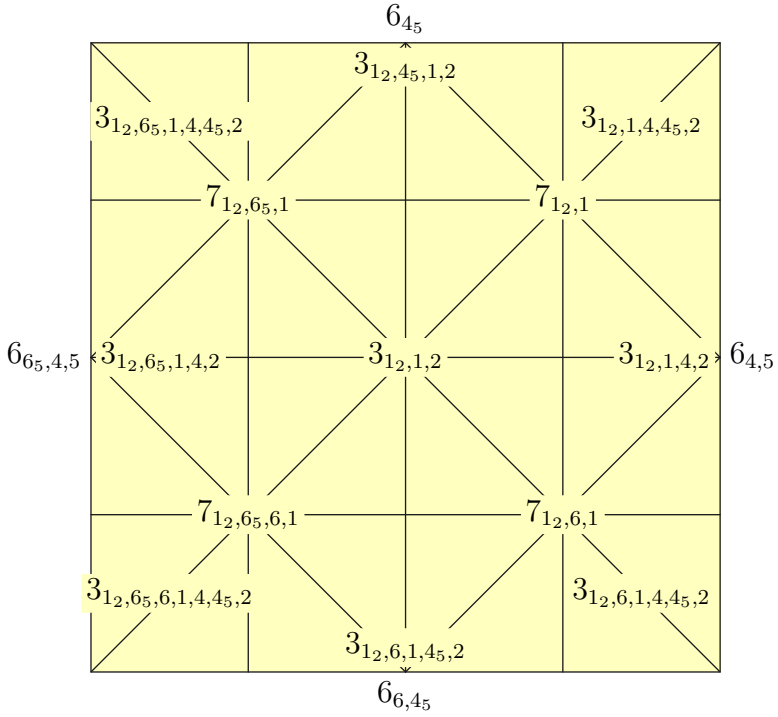

$1_{1,2}$:

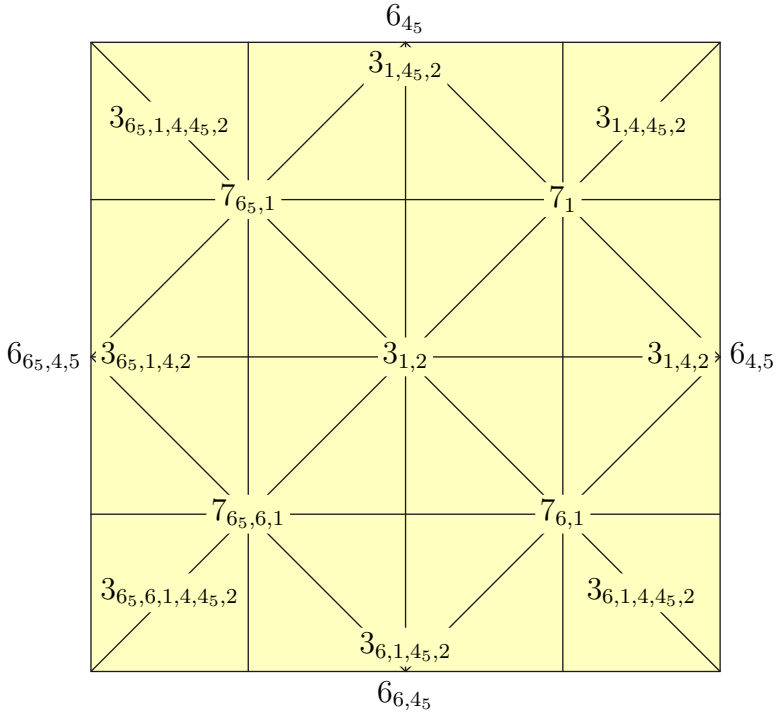

Figure 6.10: Some facets of L_8.

$6_{4,5}$:

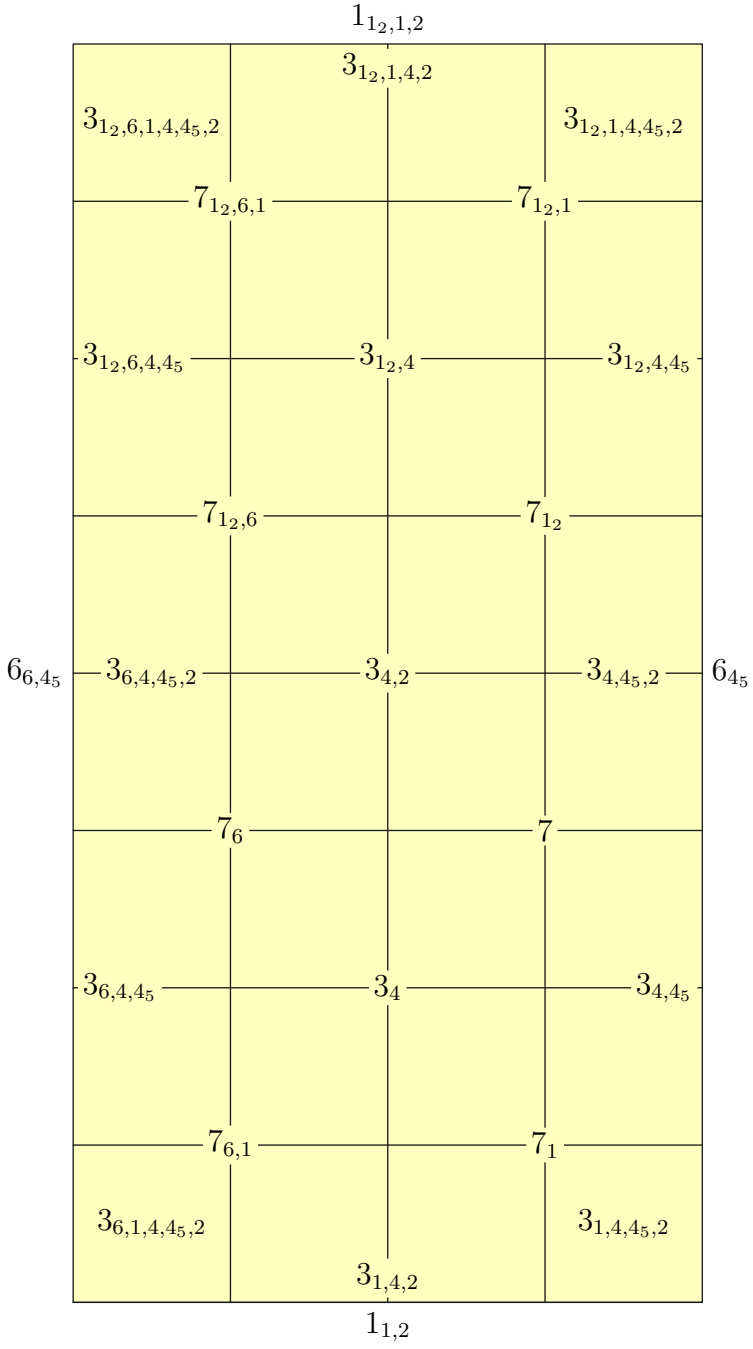

Figure 6.11: A facet of L_8.

$6_{6_5,4,5}$:

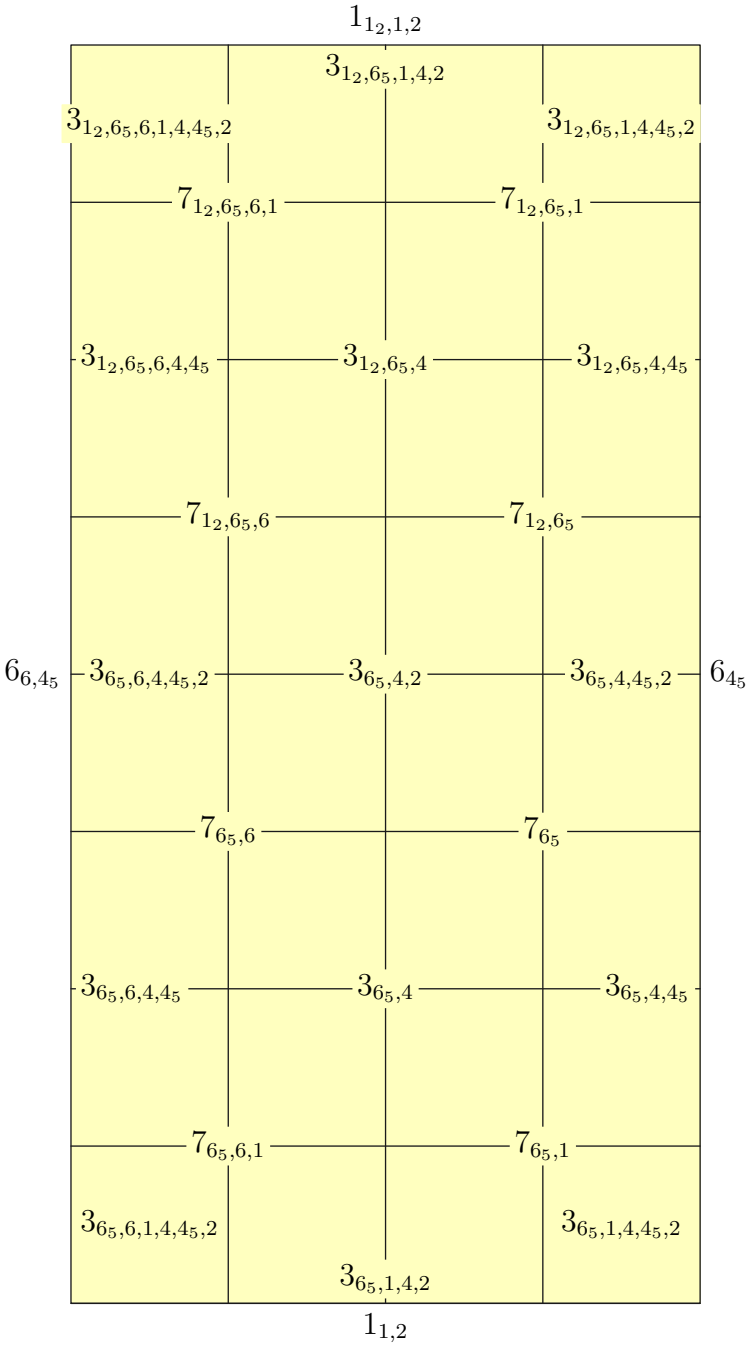

Figure 6.12: A facet of L_8.

6_{4_5}:

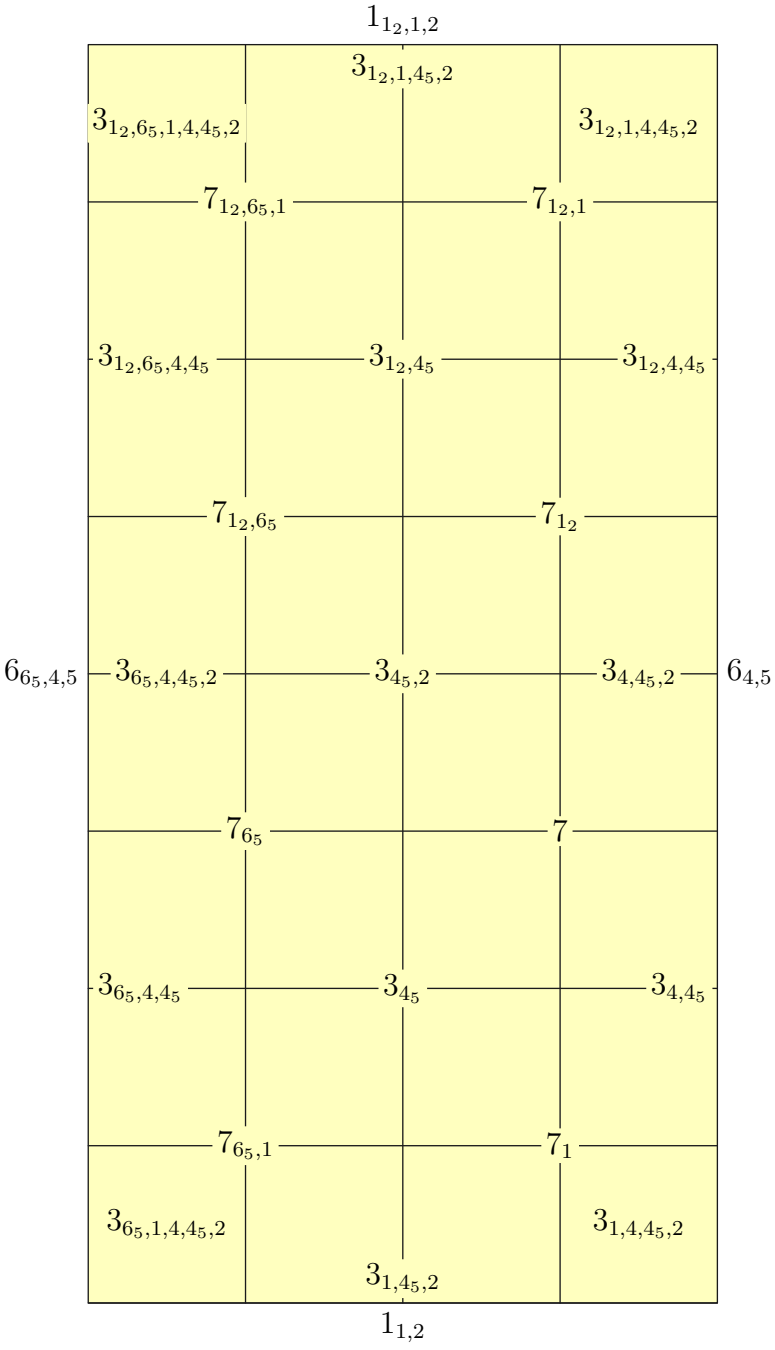

Figure 6.13: A facet of L_8.

$6_{6,4_5}$:

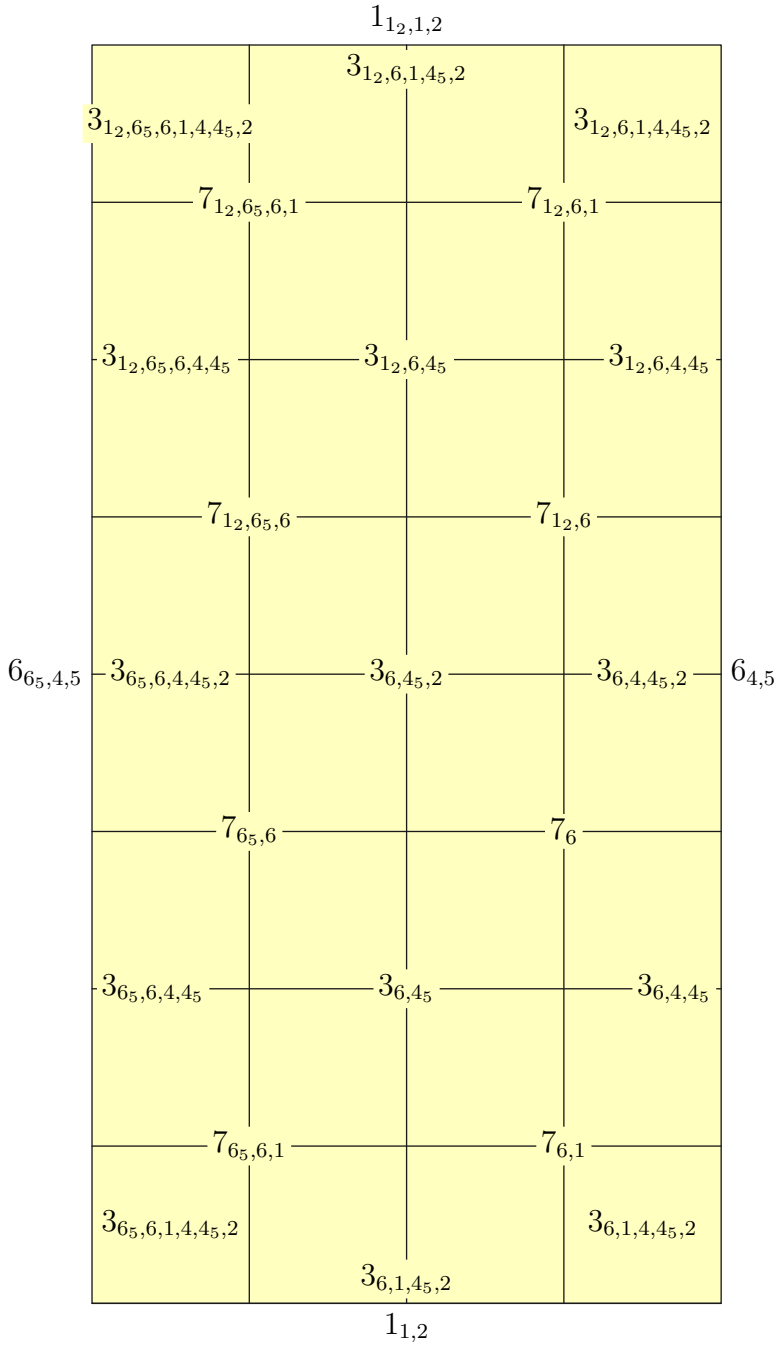

Figure 6.14: A facet of L_8.

References

[BFS24] L. Battista, L. Ferrari, and D. Santoro. "Dodecahedral L-spaces and hyperbolic 4-manifolds". In: *Commun. Anal. Geom.* 32.8 (2024), pp. 2095–2134.

[BM22] L. Battista and B. Martelli. "Hyperbolic 4-manifolds with perfect circle-valued Morse functions". In: *Trans. Amer. Math. Soc.* 375 (2022).

[Bel+10] M. Belolipetsky, T. Gelander, A. Lubotzky, and A. Shalev. "Counting arithmetic lattices and surfaces". In: *Ann. of Math. (2)* 172.3 (2010), pp. 2197–2221.

[Bor87] R. Borcherds. "Automorphism groups of Lorentzian lattices". In: *Journal of Algebra* 111.1 (Nov. 1987), pp. 133–153.

[Bur+02] M. Burger, T. Gelander, A. Lubotzky, and S. Mozes. "Counting hyperbolic manifolds". In: *Geom. Funct. Anal.* 12.6 (2002), pp. 1161–1173.

[CD95] R. M. Charney and M. W. Davis. "Strict hyperbolization". In: *Topology* 34.2 (1995), pp. 329–350.

[Che69] M. Chein. "Recherche des graphes des matrices de Coxeter hyperboliques d'ordre $\leqslant 10$". fre. In: *ESAIM: Mathematical Modelling and Numerical Analysis - Modélisation Mathématique et Analyse Numérique* 3.R3 (1969), pp. 3–16.

[Che25a] J. G. Chen. *Closed hyperbolic manifolds without spin^c structures*. 2025. arXiv: `2501.07796 [math.GT]`.

[Che25b] J. G. Chen. *Non-cobordant hyperbolic manifolds*. 2025. arXiv: `2501.11610 [math.GT]`.

[Che25c] J. G. Chen. *Some closed hyperbolic 5-manifolds*. To appear in Algebr. Geom. Topol. 2025. arXiv: `2502.19225 [math.GT]`.

[CR] J. G. Chen and E. Rizzi. *Cusp-transitive 4-manifolds with every cusp section*. To appear in Algebr. Geom. Topol. arXiv: `2408.05080 [math.GT]`.

[CR21] M. Chu and A. W. Reid. "Embedding closed hyperbolic 3-manifolds in small volume hyperbolic 4-manifolds". In: *Algebr. Geom. Topol.* 21 (2021), pp. 2627–2647.

[CM05] M. Conder and C. Maclachlan. "Small volume compact hyperbolic 4-manifolds". In: *Proc. Amer. Math. Soc.* 133 (2005), pp. 2469–2476.

[CR03] J. H. Conway and J. P. Rossetti. *Describing the platycosms*. 2003. arXiv: `math/0311476 [math.DG]`.

[Dav85] M. Davis. “A hyperbolic 4-manifold”. In: *Proc. Amer. Math. Soc.* 93 (1985), pp. 325–328.

[Dav12] M. W. Davis. *The Geometry and Topology of Coxeter Groups*. London Mathematical Society Monographs, volume 32. Princeton University Press, 2012.

[DS75] P. Deligne and D. Sullivan. “Fibrés vectoriels complexes à groupe structural discret”. In: *C. R. Acad. Sci., Paris, Sér. A* 281 (1975), pp. 1081–1083.

[FT] A. Felikson and P. Tumarkin. *Hyperbolic Coxeter polytopes*. `https://www.maths.dur.ac.uk/users/anna.felikson/Polytopes/polytopes.html`.

[FKS21] L. Ferrari, A. Kolpakov, and L. Slavich. “Cusps of hyperbolic 4-manifolds and rational homology spheres”. In: *Proc. Lond. Math. Soc.* 6.3 (2021), pp. 636–648.

[Gug15] R. Guglielmetti. “CoxIter – Computing invariants of hyperbolic Coxeter groups”. In: *LMS Journal of Computation and Mathematics* 18.1 (2015), pp. 754–773.

[Gug] R. Guglielmetti. *CoxIter*. Version 1.3. `https://rgugliel.github.io/CoxIter/index.html`.

[Hal49] M. Hall. “Subgroups of Finite Index in Free Groups”. In: *Canadian Journal of Mathematics* 1.2 (1949), pp. 187–190.

[IH90] H.-C. Im Hof. “Napier cycles and hyperbolic Coxeter groups”. In: *Bull. Soc. Math. Belg. Sér. A* 42.3 (1990), pp. 523–545.

[IMM22] G. Italiano, B. Martelli, and M. Migliorini. “Hyperbolic 5-manifolds that fiber over S^1”. In: *Inventiones mathematicae* 231.1 (July 2022), pp. 1–38.

[KS10] S. Kerckhoff and P. Storm. “From the hyperbolic 24–cell to the cuboctahedron”. In: *Geometry & Topology - GEOM TOPOL* 14 (June 2010), pp. 1383–1477.

[KM13] A. Kolpakov and B. Martelli. “Hyperbolic four-manifolds with one cusp”. In: *Geom. Funct. Anal.* 23.6 (2013), pp. 1903–1933.

[KRS18] A. Kolpakov, A. W. Reid, and L. Slavich. “Embedding arithmetic hyperbolic manifolds”. In: *Math. Res. Lett.* 25 (2018), pp. 1305–1328.

[KS15] A. Kolpakov and L. Slavich. “Symmetries of Hyperbolic 4-Manifolds”. In: *International Mathematics Research Notices* 2016.9 (July 2015), pp. 2677–2716.

[KS16] A. Kolpakov and L. Slavich. “Hyperbolic 4-manifolds, colourings and mutations”. In: *Proc. Lond. Math. Soc.* 113.2 (2016), pp. 163–184.

[Lon08] C. Long. “Small volume closed hyperbolic 4-manifolds”. In: *Bull. London Math. Soc.* 40 (2008), pp. 913–916.

[LR00] D. D. Long and A. W. Reid. “On the geometric boundaries of hyperbolic 4-manifolds”. In: *Geom. Topol.* 4.1 (2000), pp. 171–178.

[LR02] D. D. Long and A. W. Reid. “All flat manifolds are cusps of hyperbolic orbifolds”. In: *Algebr. Geom. Topol.* 2.1 (2002), pp. 285–296.

[LR20] D. D. Long and A. W. Reid. “Virtually spinning hyperbolic manifolds”. In: *Proc. Edinb. Math. Soc.* 63 (2020), pp. 305–313.

[MZ23] J. Ma and F. Zheng. “Geometrically bounding 3–manifolds, volume and Betti numbers”. In: *Algebr. Geom. Topol.* 23 (June 2023), pp. 1055–1096.

[Mar91] G. A. Margulis. *Discrete subgroups of semisimple Lie groups*. Vol. 17. Ergebnisse der Mathematik und ihrer Grenzgebiete (3) [Results in Mathematics and Related Areas (3)]. Springer-Verlag, Berlin, 1991, pp. x+388.

[MV00] G. A. Margulis and É. B. Vinberg. “Some linear groups virtually having a free quotient”. In: *J. Lie Theory* 10.1 (2000), pp. 171–180.

[Mar18] B. Martelli. “Hyperbolic four-manifolds”. In: *Handbook of group actions. Vol. III*. Vol. 40. Adv. Lect. Math. (ALM). Int. Press, Somerville, MA, 2018, pp. 37–58.

[Mar22] B. Martelli. *Hyperbolic three-manifolds that embed geodesically*. 2022. arXiv: `1510.06325 [math.GT]`.

[Mar23] B. Martelli. *An introduction to Geometric Topology*. Version 3. CreateSpace Independent Publishing Platform, 2023.

[MR18] B. Martelli and S. Riolo. “Hyperbolic Dehn filling in dimension four”. In: *Geom. Topol.* 22 (2018), pp. 1647–1716.

[MRS20] B. Martelli, S. Riolo, and L. Slavich. “Compact hyperbolic manifolds without spin structures”. In: *Geom. Topol.* 24 (2020), pp. 2647–2674.

[MRS21] B. Martelli, S. Riolo, and L. Slavich. “Convex plumbings in closed hyperbolic 4-manifolds”. In: *Geom. Dedicata* 212 (2021), pp. 243–259.

[McR04] D. B. McReynolds. “Peripheral separability and cusps of arithmetic hyperbolic orbifolds”. In: *Algebr. Geom. Topol.* 4.2 (2004), pp. 721–755.

[McR09] D. B. McReynolds. “Controlling manifold covers of orbifolds”. In: *Math. Res. Lett.* 16.4 (2009), pp. 651–662.

[MS74] J.W. Milnor and J.D. Stasheff. *Characteristic Classes*. Annals of mathematics studies. Princeton University Press, 1974.

[Nim98] B. E. Nimershiem. "All flat three-manifolds appear as cusps of hyperbolic four-manifolds". In: *Topology and its Appl.* 90 (1998), pp. 109–133.

[Pro86] M. N. Prokhorov. "Absence of discrete groups of reflections with a noncompact fundamental polyhedron of finite volume in a Lobachevskiĭ space of high dimension". In: *Izv. Akad. Nauk SSSR Ser. Mat.* 50.2 (1986), pp. 413–424.

[Pro87] M. N. Prokhorov. "The absence of discrete reflection groups with non-compact fundamental polyhedron of finite volume in Lobachevsky space of large dimension". In: *Mathematics of the USSR-Izvestiya* 28.2 (Apr. 1987), pp. 401–411.

[Rat19] J. G. Ratcliffe. *Foundations of Hyperbolic Manifolds*. Springer Cham, 2019.

[RT21] J. G. Ratcliffe and S. T. Tschantz. "Hyperbolic 24-cell 4-manifolds with one cusp". In: *Experiment. Math.* (2021).

[RT23] J. G. Ratcliffe and S. T. Tschantz. "Hyperbolic 24-Cell 4-Manifolds With One Cusp". In: *Experimental Mathematics* 32.2 (2023), pp. 269–279.

[RT00] J. G. Ratcliffe and S.+ T. Tschantz. "The Volume Spectrum of Hyperbolic 4-Manifolds". In: *Experimental Mathematics* 9.1 (Jan. 2000), pp. 101–125.

[RS] A. W. Reid and C. Sell. *Hyperbolic manifolds without spin$^{\mathbb{C}}$ structures and non-vanishing higher order Stiefel-Whitney classes*. To appear in Proc. Amer. Math. Soc. arXiv: `2302.08060 [math.GT]`.

[Rio24] S. Riolo. "A small cusped hyperbolic 4-manifold". In: *Bull. Lond. Math. Soc.* 56 (2024), pp. 176–187.

[RR25] S. Riolo and E. Rizzi. *A cusped hyperbolic 4-manifold without spin structures*. 2025. arXiv: `2510.12657 [math.GT]`.

[RS22a] S. Riolo and A. Seppi. "Character varieties of a transitioning Coxeter 4-orbifold". In: *Groups Geom. Dyn.* 16 (2022), pp. 779–842.

[RS22b] S. Riolo and A. Seppi. "Geometric transition from hyperbolic to anti-de Sitter structures in dimension four". In: *Ann. Sc. Norm. Super. Pisa Cl. Sci.* 23 (2022), pp. 115–176.

[RS19] S. Riolo and L. Slavich. "New hyperbolic 4-manifolds of low volume". In: *Algebr. Geom. Topol.* 19 (2019), pp. 2653–2676.

[Riz25] E. Rizzi. “Some cusp-transitive hyperbolic 4-manifolds”. In: *Geometriae Dedicata* 219.4 (June 2025), p. 61.

[Sco05] A. Scorpan. *The Wild World of 4-Manifolds*. American Mathematical Society, 2005.

[Sto13] M. Stover. “On the number of ends of rank one locally symmetric spaces”. In: *Geom. Topol.* 17.2 (2013), pp. 905–924.

[Sul79] D. Sullivan. “Hyperbolic geometry and homeomorphisms”. In: *Geometric topology Proc. Conf., Athens/Ga. 1977* (1979), pp. 543–555.

[Vin72] È. B. Vinberg. “On groups of unit elements of certain quadratic forms”. In: *Mathematics of the USSR-Sbornik* 16.1 (Feb. 1972), p. 17.

[Vin81] È. B. Vinberg. “Absence of crystallographic groups of reflections in Lobachevskii spaces of large dimension”. In: *Functional Analysis and Its Applications* 15.2 (1981), pp. 128–130.

[Vin85] È. B. Vinberg. “Hyperbolic reflection groups”. In: *Uspekhi Mat. Nauk* 40.1(241) (1985), pp. 29–66, 255.